UNIVERSITY OF CALIFORNIA SAN DIEGO

Cellular and molecular characterization of intrinsic foot muscle loss in the lesser Egyptian jerboa (*Jaculus jaculus*)

A dissertation submitted in partial satisfaction of the requirements for the degree of Doctor of Philosophy

in

Biology

by

Mai Phuong Tran

Committee in charge:

Professor Kimberly L. Cooper, Chair
Professor Stephan Lange
Professor Samuel R. Ward
Professor James E. Wilhelm
Professor Deborah Yelon

2019

The Dissertation of Mai Phuong Tran is approved, and it is acceptable in quality and form for publication on microfilm and electronically:

Chair

University of California San Diego

2019

DEDICATION

I would like to dedicate this dissertation to my family for their unlimited support throughout my education and life. I am who I am because of their unconditional love and encouragement.

I would also like to dedicate this dissertation to members of the Cooper lab (2014-2019). I am inspired by your resilience, dedication, and excitement for science. Your presence and support made every day a joy. And to the undergraduate students working with me, thank you for giving me the opportunity to teach and for putting your trust in me.

EPIGRAPH

An understanding of the natural world and what's in it is a source of not only a great curiosity but great fulfilment.

Sir David Attenborough

TABLE OF CONTENTS

LIST OF ABBREVIATIONS

AchRs: Acetylcholine Receptors

ATP: Adenosine Triphosphate

BMP: Bone Morphogenic Protein

BrdU: Bromodeoxyuridine

BT: Botulinum Toxin

DE: Differential Expressed

EBD: Evans Blue Dye

FAPs: Fibro-Adipogenic Progenitors

FDS: Flexor Digitorum Superficialis

FL: Forelimb

HL: Hindlimb

LCM: Laser Capture Microdissection

MuSC: Satellite Cells

MyHC: Myosin Heavy Chain

NMJ: Neuromuscular Junction

NO: Nitric oxide

ORO: Oil Red O

SHH: Sonic Hedgehog

TEM: Transmission Electron Microscopy

UPS: Ubiquitin Proteasome System

LIST OF FIGURES

LIST OF TABLES

ACKNOWLEDGEMENTS

I would like to acknowledge my advisor Dr. Kimberly Cooper, as the chair of my committee, for her support and guidance throughout my training. I additionally thank all members of the Cooper lab with whom I have worked over these last few years (2014-2019), especially Dr. Aditya Saxena, Dr. Rio Tsutsumi, Haydee Guitierrez, Hannah Grunwald, Michelle Flores, and Joel Erberich. Lastly, I would like to thank the remainder of my thesis committee: Dr. Stephan Lange, Dr. Samuel Ward, Dr. James Wilhelm, and Dr. Deborah Yelon for their scientific guidance and support.

I would like to acknowledge the Cellular and Molecular Genetics Training Grant for funding and support.

Chapter 2, in full, has been submitted for publication of the material. Tran, Mai P., Tsutsumi, Rio, Erberich, Joel M., Chen, Kevin D., Flores, Michelle D., and Cooper, Kimberly L. (2019). Evolutionary loss of foot muscle during development with characteristics of atrophy and no evidence of cell death. *Submitted.* The dissertation author was the primary investigator and author of this material.

Chapter 3, in full, is currently being prepared for submission for publication of the material. Tran, Mai P., Saxena, Aditya, and Cooper, Kimberly L. (2019) The dissertation author was the primary investigator and first author of this material.

VITA

2013 Bachelor of Science, University of California Los Angeles

2019 Doctor of Philosophy, University of California San Diego

PUBLICATIONS

Tstutsumi, R., Tran, M.P., and Cooper, K.L. (2017). Changing While Staying the Same: Preservation of Structural Continuity During Limb Evolution by Developmental Integration. Review. *Integrative and Comparative Biology*. **57(6)**: 1269-1280.

Tran M.P., Tsutsumi, R., Erberich, J.M., Chen, K.D., Flores, M.D., and Cooper, K.L. (2019). Evolutionary loss of foot muscle during development with characteristics of atrophy and no evidence of cell death. *Submitted*.

ABSTRACT OF THE DISSERTATION

Cellular and molecular characterization of intrinsic foot muscle loss in the lesser Egyptian jerboa (*Jaculus jaculus*)

by

Mai Phuong Tran

Doctor of Philosophy in Biology

University of California San Diego, 2019

Professor Kimberly L. Cooper, Chair

Many species that run or leap across sparsely vegetated habitats, including hooved animals like horses and deer, evolved the severe reduction or complete loss of foot muscles as skeletal elements elongated and digits were lost. Although entire groups of muscles were lost repeatedly throughout vertebrate evolution, the developmental mechanisms remain unknown. Here, we investigate the cellular and molecular mechanisms underlying the natural loss of intrinsic foot muscles in a small bipedal rodent, the lesser Egyptian jerboa (*Jaculus jaculus*). Although adults have no muscles in their feet, myoblast migration and fusion proceed normally to form multinucleated myofibers in newborn animals that rapidly disappear soon after birth. We were therefore surprised to find no evidence of apoptotic or necrotic cell death and no

stimulation of a local immune response during stages of peak myofiber loss, countering well-supported assumptions of developmental tissue remodeling. We instead see hallmarks of muscle atrophy, including an ordered disassembly of the sarcomere apparatus associated with upregulation of the E3 ubiquitin ligases, *MuRF1* and *Atrogin-1*. In addition to identifying putative regulators of jerboa foot muscle loss, transcriptome profiling of newborn jerboa and mouse foot and forearm muscle showed differentially expressed genes significant overlap with two clinical models of muscle loss, cancer-induced cachexia and botulinum-toxin-induced muscle loss. We propose that the natural loss of muscle, which remodeled foot anatomy during evolution and development, involves cellular mechanisms that are typically associated with disease or injury.

CHAPTER 1. Research Background

Movement – the defining factor that governs our day-to-day living. From the simple action of walking or scratching your nose to the more complicated task of playing a musical instrument, movement requires precise use of the most abundant tissue in our body – the skeletal muscle. Any failure during its development or maturation and growth resulted in debilitating musculoskeletal disorders. Research into the biological processes underlying muscle development and diversity, together with investigations of the mechanisms of muscle loss in diseases, has led to a better understanding of muscle biology and physiology. While we have achieved great leaps over a century of muscle research, from the early work of A. V. Hill to understand force generation to the latest success of using NF-κB inhibitor to slow down Duchene Muscular Dystrophy [1,2], we have yet to discover the cure for many muscle diseases.

The natural diversity of muscle anatomy and physiology provide a great resource revealing not only mechanisms of muscle development but also species locomotor evolutionary history. Having or not having a muscle group means gain or loss of a specific motion; a seemingly efficient way to adapt various body parts – head, jaws, neck, limbs, etc. - to well suit the living requirements of specific species. From fish to human, the origin and developmental mechanism underlying muscle formation are the same yet specific muscle is lost or gained, or the composition of individual muscle is altered. This suggests both existence of a conserve network of development and of modular components that can be modified to achieve diversity. A deeper understanding of how muscle diversity is achieved will add to the current knowledge of muscle development and disease.

The vertebrate limb is a great system to study muscle development, its interaction with other tissues, and its response to injury or disease, because it is one of the most amenable systems for experimental manipulation without severely affecting the remaining body development. Understanding the mechanisms of muscle development and adaptation will help unravel the molecular basis of skeletal muscle diseases. In this introductory chapter, I will briefly describe the origin and development of skeletal muscle as well as its interaction with other tissues with a focus on muscles of the limb. Next, I will elaborate on how the muscle contractile machinery is assembled highlighting key proteins. I will then discuss the cellular and molecular mechanisms involved in skeletal muscle loss with a focus on muscular atrophy. Finally, I will introduce the lesser Egyptian jerboa as a model of muscle loss in the context of the diversification of limb muscle anatomy. The search for cellular and molecular mechanisms of muscle loss in the jerboa was informed by what was previously known about muscle cell biology, and our findings have reciprocally added to a deeper understanding of the fundamental mechanisms of muscle development and disease.

1.1 Muscle development: origin, differentiation, growth, and repair

1.1.1 Muscle origin, differentiation, and formation

During embryogenesis, a series of cell movement, a process called gastrulation, forms the three germ layers: the innermost layer is endoderm, the middle layer is mesoderm, and the outermost layer is ectoderm. The mesoderm is further segmented into the chordamesoderm, paraxial mesoderm, intermediate mesoderm, and lateral plate mesoderm giving rise to different tissues in the body (Figure 1.1A). The paraxial

mesoderm, which lies between the neural tube and intermediate mesoderm, is then further segmented to form an anterior structure that gives rise to the head musculature and a posterior structure that gives rise to the somites from which all axial and limb skeletal muscles are derived [3–5] (Figure 1.1A). The developmental and evolutionary history of head muscles is different from the rest of the body and will not be discuss here.

Somites contain multipotent cells whose specification depends on their location within the somite and on factors from the neighboring neural tube, notochord, and epidermis. Somites can be divided into two main compartments: the ventral region called the sclerotome, which gives rise to vertebrae and rib cartilage; the remaining portion called dermamyotome, which gives rise to all skeletal muscles, brown fat, as well as the dermis of the back [6] (Figure 1.1A). Fate mapping experiments revealed that the dermomyotome is arranged into three regions: cells of the central region, the central dermamyotome (i.e. dermatome), form the back dermis and brown fat; cells of the lateral portion closest to the neural tube, the primaxial dermamyotome (i.e. epaxial dermamyotome), form musculature of the back, ribcage, and ventral body wall; and cells of the lateral portion farthest from the neural tube, the abaxial dermomyotome (i.e. hypaxial dermamyotome), form abaxial muscles of body wall, limbs and tongue [7–10] (Figure 1.1B).

Limb muscle progenitors are specified from cells at the abaxial dermomyotome lip (i.e. ventrolateral edge of the dermomyotome), which originates from somites aligned with the prospective limb. These cells delaminate and migrate into the limb bud where they proliferate and initiate a myoblast specification program forming the dorsal and

ventral muscle masses [11–14]. The muscle masses are then subdivided into individual muscle groups in response to cues from the developing muscle connective tissue, which is derived from limb field lateral plate mesoderm [13,15–17]. This is evident in experiments in which transplantation of non-limb level somite, such as cervical and interlimb somite, to the limb level give rise to normal limb muscles [4,18].

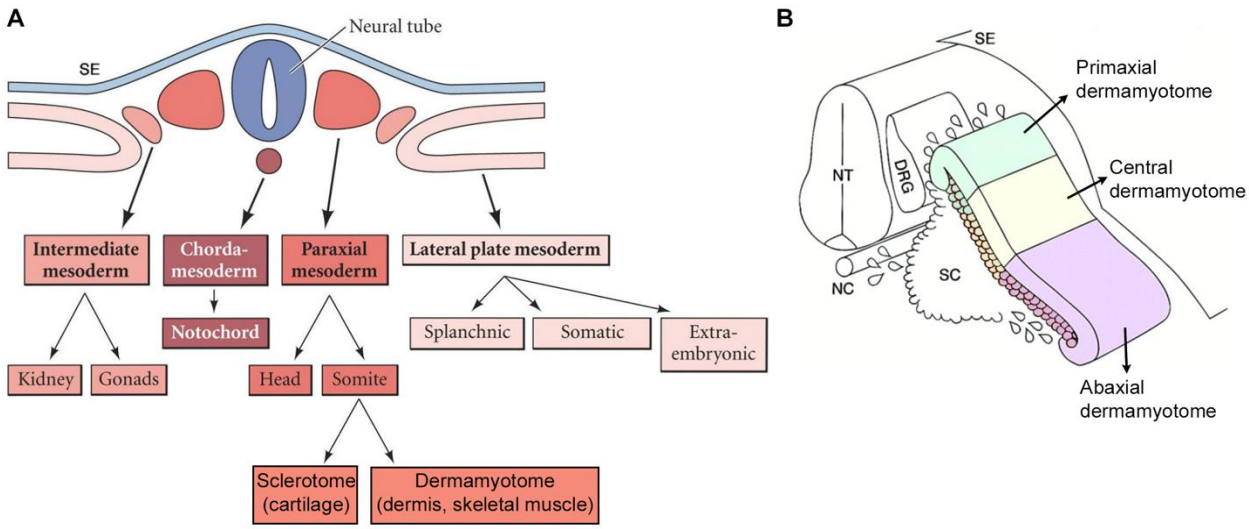

Figure 1.1 – Overview of amniote mesoderm compartments
(A) Major lineages of mesoderm. Image adapted from Gilbert [6, Figure 12.1].
(B) Alternate view showing detail compartments of the dermamyotome. Image adapted from Tajbkhsh and Spörle [19].
DRG: dorsal root ganglia, NC: notochord, NT: neural tube, SC: sclerotome, SE: surface ectoderm.

Specification of the myotome is induced by two distinct programs. The primaxial myotome is specified by factors from the neural tube, mainly Wnt1, Wnt3a, and low level of Sonic Hedgehog (SHH) [20–22]. Further away from the neural tube, the abaxial myotome, receives Wnt signal from the ectoderm and bone morphogenic protein (BMP) from the lateral plate mesoderm for proper specification [6,23]. Cells of the myotome are Paired-box 3 (*Pax3*) positive, and *Pax3* is required for delamination and migration of muscle precursors. The Splotch (*Pax3* loss-of-function) mutant embryos lack limb and diaphragm muscles, muscles that each require a population of migratory precursors [24,25]. With respect to limb muscles in mouse, the absence of autopod (i.e. distal limb) muscles was seen in the muscle-specific Smoothened knockout mouse, a mutant where muscle cells fail to receive SHH signaling [26]. This work showed that SHH signal, which originates in the zone of polarizing activity (ZPA) at the posterior limb region, directs muscle progenitors' migration through the limb bud to form autopod muscles.

From the pool of *Pax3* positive somitic cells, further commitment to the muscle lineage, the making of myoblasts or muscle progenitors, involves activation of a suite of basic helix-loop-helix transcription factors called myogenic regulatory factors (MRFs) [6,27,23]. This family of transcription factors includes *MyoD, Myf5*, *Mrf4*, and Myogenin [23,27,28]. *Mrf4* is genetically linked to *Myf5* and also plays a role in muscle lineage specification [29,30]. Genetic deletion of either *MyoD* or *Myf5* alone does not significantly affect muscle development [31,32], suggesting both genes are functionally redundant. However, deletion of both *MyoD* and *Myf5* - with linked deletion of *Mrf4* - resulted in mice born with a complete lack of skeletal muscle [33]. When the expression and function of *Mrf4* is preserved in *Myod:Myf5* double mutants, embryonic skeletal

muscle was present when previous *Myod:Myf5:Myf4* mutant did not form muscle; these muscles rapidly degenerate during fetal development leading to complete lack of muscle at birth [29]. *MyoD* serves as one of the earliest markers of myogenic commitment and is considered a master regulator of skeletal myogenesis, due to its ability to convert non-muscle cells, such as fibroblasts, to a myogenic fate [33–35]. Myogenin acts genetically downstream of *MyoD* and *Myf5* to induce myoblast cell cycle exit and differentiation to become a myocyte and thus serves as a marker for skeletal muscle terminal differentiation [36,37]. Mice with Myogenin deletion have myoblasts correctly specified and positioned, but they fail to differentiate leading to neonatal death [36,37].

Myocytes align and fuse to form a single large cell with multiple nuclei, called the myofiber. A myofiber is made up of several myofibrils organized in parallel, and many myofibers are bundled together via connective tissue to form the muscle tissue (Figure 1.2). Adult muscle is composed of a heterogenous population of myofibers consisting of fast-twitch and slow-twitch myofibers, so named because of their myosin ATPase activity and subsequent contractile force and velocity [38]. Fiber type is first established during embryonic development and later modulated by neuronal and hormonal factors [39]. Specification of fiber type is controlled by the transcription factors *Six* and *Eya*, which promote fast myofiber development; forced expression can reprogram slow myofiber to become fast fiber type [40,41].

Vertebrate skeletal myogenesis happens in successive, distinct but overlapping waves of myoblast proliferation and differentiation. Each wave involves different cell population with different gene expression [42,43,27]. In mouse, early embryonic or

primary myogenesis occurs between embryonic day (E)10.5-12.5 and the later fetal or secondary myogenesis happens around E14.5-17.5 [44,45]. During primary myogenesis, *Pax3*+ muscle progenitors fuse to form primary myotubes, providing a template on which secondary myogenesis occurs [46]. During secondary myogenesis, a subset of *Pax3*+ cells starts to express *Pax7* while downregulating *Pax3*. These *Pax7*+ precursors fuse to each other to form secondary myofibers, initially smaller and surrounding primary myofibers, or to primary myofibers [46]. A subset of the *Pax7*+ progenitors forms the pool of adult muscle stem cells – muscle satellite cells [47–49]. At the end of secondary myogenesis, a basal lamina surrounds each myofiber, and satellite cells can be seen wedged between the basal lamina and the myofiber plasma membrane [50].

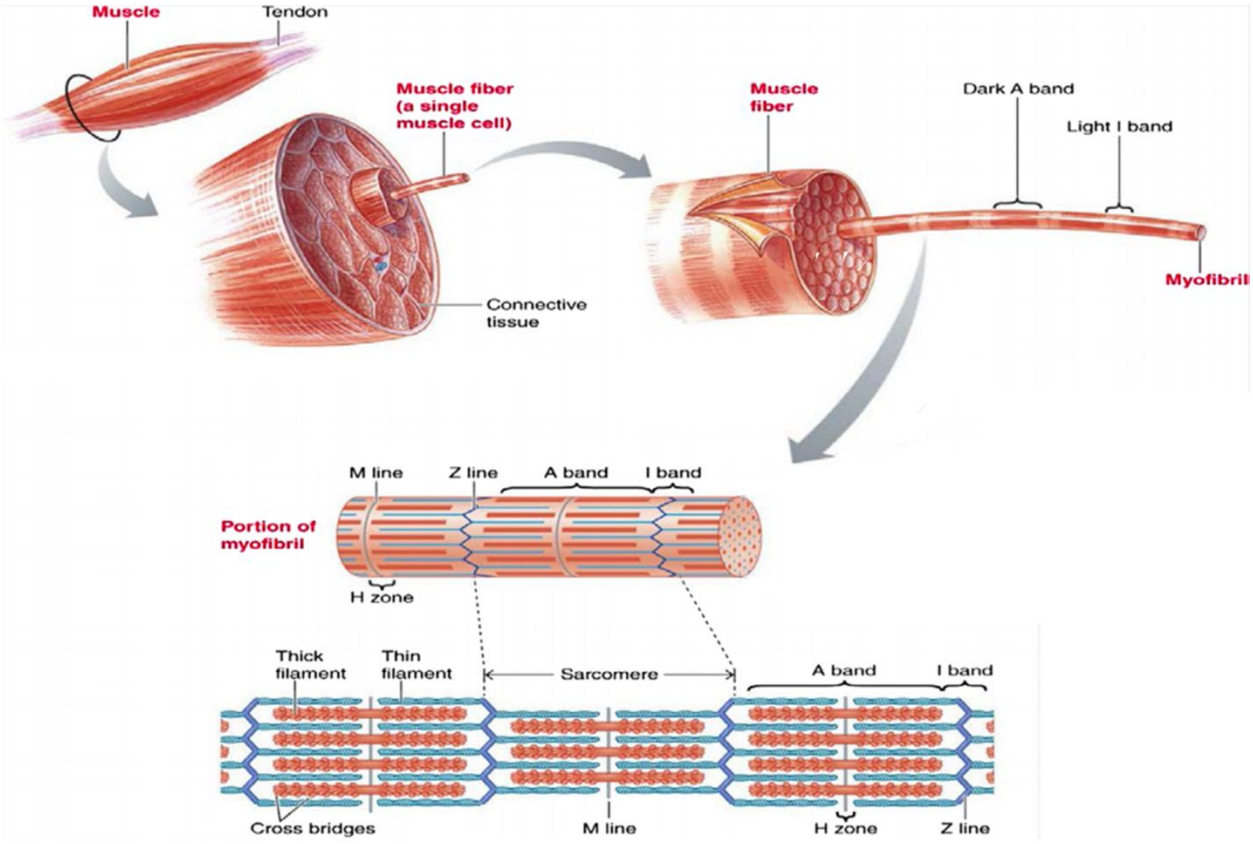

Figure 1.2 – Overview of muscle structure
Image adapted from Frontera and Ochala [51].

1.1.2 Muscle growth and repair

Muscle satellite cells (MuSCs) are a heterogenous population of muscle progenitors possessing the capability to self-renew, expand, and/or undergo myogenic differentiation and are therefore crucial for muscle growth and repair. Muscle satellite cells are identified as *Pax7*+, mononucleated cell that reside inside the basal lamina but outside the muscle plasma membrane [47,50]. MuSCs have been shown to express additional markers such as cell adhesion protein M-cadherin, tyrosine receptor kinase c-Met, cell surface attachment receptor α7-integrin, cluster of differentiation protein CD34, transmembrane heparan sulfate proteoglycans syndecan-3 and syndecan-4 [52–56]. During secondary myogenesis, muscle grows via fusion of SCs to existing myotubes, thus increasing myofiber length and myonuclei numbers [57]. Muscle satellite cells are also responsible for the increase in myofiber number (hyperplasia) in the first week after birth [58–60]. In fetal and perinatal stages, the pool of satellite cells can reach up to 30% of the mononucleated cells in muscles [61,62]. However, in the adult, the pool of satellite cells is greatly reduced to only a few percentage [40,41]. Recently, a population of muscle progenitors, marked by *Twist2* and distinct from *Pax7*+ MuSCs, has been shown to be a fiber-type specific stem cell due to its ability to form only fast myofibers [64]. Twist2 muscle progenitors are important for postnatal growth and regeneration since its ablation causes wasting of type IIB myofibers [64].

In contrast to hyperplasia, later postnatal growth involves an increase in myofiber size (hypertrophy) via addition of novel contractile apparatus (sarcomeres), in series or in parallel within a myofiber [58–60]. Autoradiography of 3H-leucine labeling showed newly synthesized proteins being incorporated at the periphery of muscle cell

cytoplasm, where nascent myofibrils are formed [65]. This suggests that as muscle grows in diameter, it is filled with myofibrils from the periphery inward. The *Akt/mTOR* pathway is crucial to promote muscle skeletal muscle hypertrophy by increasing protein synthesis [66]. Genetic activation of *Akt* in normal mouse significantly increased muscle fiber cross sectional area and protected animals from loss of muscle mass in a mouse model of muscle atrophy [66]. The *Akt* signaling pathway is activated by insulin growth factor 1 (IGF-1), which is secreted by the liver or produced locally in various tissues, including muscle [67]. In contrast, Myostatin (*Gdf8*) – a member of the transforming growth factor-beta (TGFβ) superfamily – acts as negative regulator of muscle hypertrophy. Mutants lacking Myostatin showed a striking hypertrophic phenotype [68,69]. *IGF-1* and Myostatin, together, represent the two most well-known factors that regulate muscle growth by balancing protein synthesis versus protein catabolism. In addition, because these are circulating ligands whose levels are tuned by nutritional state, these provide a means for which muscle interacts with other tissues in the body and responds to environmental factors such as diet and nutrition.

Muscle is a highly adaptable tissue, capable of repair and regeneration following injury; though its regenerative property is limited in mammals. Satellite cells in the adult muscle are maintained in a quiescent state and upon activation due to injury, they proliferate and fuse with each other or to damaged myotubes to form or repair myofibers [70,71]. Maintenance of satellite cells in a quiescence state requires Notch signaling, as inhibition or disruption of Notch leads to early differentiation and fusion [72–74]. Nitric oxide (NO), often produced by injured muscle, is important for satellite cell activation and Wnt signaling drives MuSC differentiation following proliferation [75,76]. During

regeneration, MuSC activity can be modulated by cells in the local environment. For example, muscle connective tissue fibroblasts have been shown to prevent early differentiation of myoblasts by creating a transitional niche [77]. Pro-inflammatory cytokines, such as tumor necrosis factor α (TNFα), secreted by macrophages can induce myoblast entry into terminal differentiation [78]. The genetic hierarchy involved in the process of muscle repair and regeneration is largely the same as in embryonic myogenesis [70,71].

While all mammals employ muscle satellite cells as a mode of muscle repair, studies of muscle regeneration in non-mammals reveal unexpected muscle capabilities: dedifferentiation and reversal of a multinucleate state to mononucleate cells. Newt and salamander are capable of regenerating the whole limb, in contrast with mammals where injury often lead to fibrosis and reduced or lost muscle function [79–81]. In newts, muscle can regenerate, without using muscle satellite cell, via a process of myofiber dedifferentiation and redifferentiation. The multinucleate injured myofiber dedifferentiate and fragment into mononucleate cells that regain their myoblast identity [82–84]. These cells proliferate and re-differentiate to form new myofibers [82–84].

In addition to muscle's ability to dedifferentiate and re-differentiate to similar muscle fate, muscles can transform to become a different cell identity in some species. The electric organ of fish species that can produce an electric field (e.g. knifefish and elephant fish) is thought to be derived from skeletal muscle. Electrocytes of *Sternopygus macrurus* express muscle proteins such as Desmin, Actin, and α-Actinin, and electrocytes of *Paramormyrops kingsleyae* retain sarcomeres that are disarrayed and non-contractile [85,86]. Upon denervation of the electric organ in *S. macrurus*,

electrocytes form nascent sarcomeres, T-tubules, and sarcoplasmic reticulum, which further strengthens the hypothesis that muscle transdifferentiates to become the electric organ [86]. The luminescent tissue of deep sea fish also seems to be derived from skeletal muscle; the luminescent cells contain remnants of disorganized myofibrils with no contractility and are instead filled with bioluminescent vesicles [87]. These examples showcase the diversity of muscle regenerative capacity and the plasticity of muscle fate.

1.2 Muscle innervation and interactions with other tissues

Proper muscle development and function requires innervation. In experimentally denervated duck embryos, muscle is composed of largely mononucleated cells with few to no multinucleated myotubes and a high amount of cell death [88]. In the less severe condition where muscles were paralyzed, myoblast differentiation and fusion were retarded and numerous myotubes formed but with disorganized myofibrils [88]. In contrast, in aneural and paralyzed mouse embryos, myogenesis proceeded normally with modest decrease in the number of primary myotubes but with a significant change in secondary myotube formation – reduced in denervation and increased in the hyperinnervation condition [89,90]. These experiments suggest that innervation, while dispensable for primary myogenesis in mammals, is required for secondary myotube formation.

During development, all muscles are innervated by at least two axons. However, this pattern of polyneuronal innervation is transient, and all but one axon retracts soon after birth. This is a result of competition between the axons; when one of the neurons is active, it suppresses the synapses of other neurons [91,92]. Thus, the less active

synapses are eliminated while the active axon terminal further develops, forming a focal and highly specialized synaptic site on the myofiber – the neuromuscular junction (NMJ) [91,92]. Expression of acetylcholine receptors (AChRs) at the NMJ allows for muscle to respond to acetylcholine neurotransmitter released upon neuronal activation. In the mouse, AChR clusters are present in a broad domain of fetal muscle prior to innervation and are refined to nerve terminals in response to chemical synapse activity before birth [93]. In addition to its role in restricting the localization of AChR clusters, innervation contributes to the establishment of muscle fiber type. In experiments in which the motor nerves to fast and slow-twitch muscles were switched, muscles adapt and the resulting fiber type follows the property of the new neuron [94,95]. While the contractile property of muscle is completely changed after cross-reinnervation, myosin of fast and slow-type coexist in individual fibers [96].

Integration with the nervous system allows muscles to voluntarily contract but movement is produced as a result of muscles, via tendon connections, pulling on the skeletal elements. The limb is an integrated structure made up several tissues such as bone, tendon, muscle, etc. that are arranged and integrated in an orderly fashion. It is no surprise that muscles can influence the development of other tissues and vice versa to enable the integration of these tissues. Among these musculoskeletal tissues, muscle seems to be the most reliant on extrinsic cues for its development. While primary and secondary myogenesis occur autonomously, the spatial pattern of adult limb muscle anatomy is not specified by the myoblast population itself but is instead entirely dependent upon the surrounding limb mesoderm [4,97,98]. This allows muscle to

accommodate evolutionary changes that occur in other tissues by the addition or loss of individual muscles or by changing their connections to the skeleton.

In addition to muscle connective tissue, muscles develop in proximity with tendon such that their positioning and growth are integrated to allow for proper function of the muscle-tendon unit. During juvenile development, muscle and tendon growth continues to be accommodative such that the length of muscle contraction will optimally produce the full range of motion about the joint. Surgical release of the tibialis anterior tendon by clipping the crural ligament in young rabbits changes the effective tendon angle and increases the distance over which the muscle must contract to exact a full range of joint motion [99]. Over the subsequent year, the muscle elongates and the tendon shortens to increase the length of muscle contraction to recover the full range of motion [99].

Altogether, these interactions illustrate that both muscle development as a single unit and its integration with other tissue are both required to maintain functional integrity of the limb. The information in this section is a vignette account of muscle interactions with muscle connective tissue and tendon. Please refer to Tsutsumi et al., 2018 [100] for a thorough discussion of the development and integration of different tissues in the vertebrate limb including interactions between muscle and muscle connective tissue, tendon, and bone.

1.3 The sarcomere: its assembly and maturation

1.3.1 Myofibrillogenesis:

A single multinucleated myofiber is composed of several myofibrils bundled together; each myofibril consists of a series of sarcomeres, which are highly ordered

interdigitated actin and myosin filaments (Figure 1.2). Force is generated in individual sarcomeres that act in concert across the length of the myofibril, thus amplifying that force across the myofibril and ultimately through the myofiber and the entire muscle bundle. Modulated by actin and myosin overlap, the force of a muscle can be described as a function of its sarcomere length, known as the force-length relationship [101]. It is characterized by: a positive slope at short length, where force increases proportionally to length; a zero slope (plateau) at intermediate length; a negative slope at long muscle length, where force decreases with increasing length [101–103]. Most muscles operate within a stereotypical sarcomere length range; vertebrate skeletal and cardiac sarcomeres have resting length of 2.5 microns [104]. Remarkably, sarcomere length is tightly regulated, as muscles immobilized for weeks at length far from optimal add or remove sarcomeres to restore sarcomere length [105]. This demonstrates that sarcomere number is highly plastic and yet tightly regulated.

Sarcomere assembly and maturation follow an orderly process. Figure 1.3 diagrams the sarcomere structure and some associated proteins during sarcomere assembly. In early skeletal muscle formation, primordial Z-bodies, actin filaments, and non-muscle Myosin assemble into a premyofibril [106–109]. At this stage, Desmin, muscle-specific α-Actinin, and the Z-body portion of Titin are also expressed and assemble on the premyofibril [108,110]. Subsequent increasing Z-body spacing along with expression and integration of skeletal muscle Myosin into sarcomeres result in formation of nascent myofibrils [109,111]. At this stage, the C-terminal epitopes of Titin are not resolved suggesting that Titin is coiled [112]. Later, Titin uncoils exposing its M-band epitope, and this coincides with assembly of Myomesin in the M-band [112].

Subsequent maturation of the nascent myofibril into a mature myofibril involves alignment of the actin-myosin complex and incorporation of additional proteins that are important for sarcomere structure and function and Titin uncoiling [111,113]. The following details the major proteins associated with the sarcomere structure and their roles in sarcomere formation and muscle function.

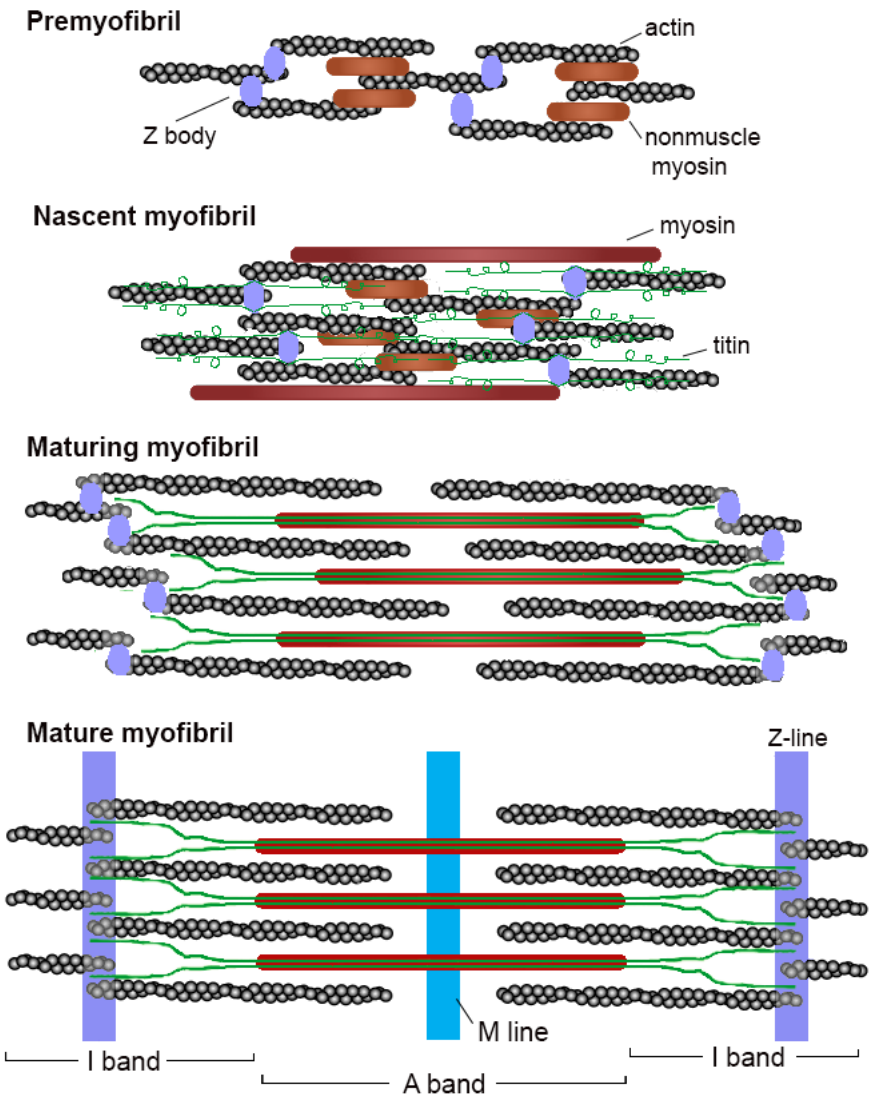

Figure 1.3 – Overview of sarcomere maturation
Sarcomere maturation involves progressively aligned sarcomere components. Image adapted from Ono [114].

1.3.2 Actin and Myosin

Interdigitated actin-myosin filaments are the contractile engine of muscle: Actin is the thin filament and Myosin is the thick filament. Actin and Myosin are amongst the early expressed proteins of differentiated muscle that appear even before myocyte fusion. The myosin filaments have projections or cross-bridges on their surfaces that form links with actin filaments in the region of overlap [115]. Such an arrangement allows for Myosin and Actin to slide across each other as Myosin attaches and then detaches from Actin, thus generating force via shortening and lengthening of the cross-bridges [115].

Before the addition of non-muscle Myosin during early myofibril assembly, actin filaments are associated with components of I- and Z-bands forming structures termed I-Z-I bodies that are believed to be precursors of mature I-Z-I bands [116,117]. Once assembled within the sarcomere, actin filaments are oriented in opposite direction with the barbed (+) end anchored to the Z-line. Both pointed and barbed ends of Actin filament are capped by capping proteins. The barbed end (Z-line) is capped by CAPZ and the pointed end is capped by Tropomodulin (TMOD) [118,119]. Capping of each actin filament contributes to regulation of its length. Overexpression of *Tmod* shortens thin filaments, whereas knockdown or inhibition of its activity elongates thin filaments [120]. Though thin filaments are capped on both ends and they are always maintained at a similar length, there is dynamic exchange of actin subunits within the filament suggesting that actin filament has dynamic caps [114]. Actin dynamics within the sarcomere are regulated by Actin-binding proteins such as Cofilin, which disassembles actin filaments thus enhancing Actin turn over. Injection of high concentration of Cofilin

leads to formation of Actin-Cofilin rods and subsequent disruption of sarcomeres [121]. In addition, mutation in the human *COFILIN-2* gene causes nemaline myopathy, which is characterized by formation and accumulation of nemaline rods (rods containing Actin and Z-proteins [122]. In mature myofibril, Actin is a very stable structure with a half-life reported on the order of days [123]. Mutation in skeletal muscle Actin itself or in Actin associated proteins lead to nemaline myopathies [124–126].

The Myosin molecule is a hexamer consisting of two heavy chains and two pairs of light chains. Myosin is both a structural protein and an enzyme, capable of hydrolyzing ATP as it changes conformation and slides along actin filaments. The speed of Myosin turn over in the adult muscle is on the order of days, with Myosin heavy chain having a faster rate of turn-over than Actin and Myosin light chain [123]. Early in myofibrillogenesis, non-muscle Myosin is first assembled into the premyofibril to form a scaffold where muscle-specific Myosin will replace non-muscle Myosin to form the nascent myofibril [127]. There are multiple Myosin isoforms in mammals, referred by their heavy chain (MyHC) isoforms and the expression of each marks a different stage of muscle development from embryonic to neonatal to adult [128]. Since regeneration involves reactivation of embryonic myogenesis, presence of embryonic MyHC serves as a useful marker for immature, recently regenerated myofibers in adult muscles. In addition, MyHCs are categorized into either slow (type I, oxidative) or fast (type IIA, B & X, oxidative and/or glycolytic) reflecting their myosin ATPase activity.

Specialized fiber types are present in muscles of all mammals but the proportion of fiber types varies greatly in the same muscle between species [39]. This reflects the evolutionary adaptation of muscles to meet species-specific functional demands. Body

size also varies greatly between animals. How then do muscles adapt to such differences to achieve speed during locomotion independent of body size? One proposed adaptation is utilizing different proportion of fast- and slow-type myofibers [129]. Small animals like mice have predominantly type IIB and IIX myofibers with abundant oxidative enzyme [39]. In contrast, muscles in larger mammals, like humans, are composed mainly of type I and type IIA with lower level of oxidative enzyme [39]. An additional means to achieve locomotion speed independent of body size is having higher maximum velocity of shortening and tension in smaller animals [39]. For example, slow fibers from mouse muscles are faster than slow fibers from human muscles [130]. While each case has been observed, the relationships between body size and fiber type composition or body size and maximum velocity and tension are not absolute [39]. This suggests that much more complicated interactions, not solely based on body size, underlie muscle evolution to accommodate the functional demand of the animal.

1.3.3 Tropomyosin

Tropomyosin (TPM1) is one of the best-characterized Actin-binding proteins. Different isoforms of Tropomyosin exist in skeletal, cardiac, and smooth muscles [131]. Mutation in the Tropomyosin gene has been linked to human diseases. For example, mutation in *TPM1* causes familial hypertrophic cardiomyopathy, in which cardiac muscles have increased mass with myocyte and myofibrillar disarray [132]. *In vitro*, Tropomyosin itself can bind to and stabilize actin filaments by inhibiting spontaneous Actin polymerization and depolymerization [133]. Tropomyosin, along with another Actin binding protein, Troponin, also makes the actin filament stronger and less likely to bend

or break [134]. *In vivo* knockdown of Tropomyosin expression in *C. elegans* led to disorganization of muscle actin filaments [135]. This suggests that Tropomyosin plays a similar role in stabilizing actin filaments *in vitro* and *in vivo*. Tropomyosin forms a complex with the Ca^{2+} sensitive Troponin to regulate actin-myosin interaction, and hence muscle contraction [131,136].

1.3.4 Alpha-Actinin (α-Actinin)

α-Actinin is one of the first proteins expressed in myocyte and assemble in premyofibril, forming the I-Z-I structures proposed to be the precursor to I-band and Z-band [106,107,111]. α-Actinin functions to anchor and cross link actin filaments at the Z-disk [113]. In mammals, there are two *α-Actinin (ACTN)* isoforms: *ACTN2* is the constitutive α-Actinin present in all muscles where as *ACTN3* is restricted to fast fibers [137]. Interestingly, a high percentage of human population, approximately 18%, lacks ACTN3 due to a mutation resulted in premature stop codon [138]. Research shows that lack of ACTN3 correlates with higher endurance and population analysis suggests there is positive selection for the mutant *ACTN3* [138,139]. While no *ACTN2* knockdown/knockout data exist in mammals, *α-actinin 2* knockout in fish resulted in sarcomeric defects and expression of *α-actinin 3* cannot rescue this phenotype suggesting a functional difference between the two isoforms [140].

1.3.5 Titin

Titin acts as a molecular spring, establishing muscle resting tension and maintaining myofibril integrity when sarcomeres are stretched beyond actin-myosin overlap [141]. In early myofibrillogenesis, Titin colocalizes with α-Actinin in the Z bodies of each premyofibril and is thought to not only anchor α-Actinin but to also establish

spacing. It has been observed that spacing between presumptive Z-bands was one micron though the I-Z-I structures do not yet contain Myosin [142–144]. Initially, only the N-terminus at the Z-disk is accessible to antibody binding. Later in sarcomere maturation, Titin stretches to expose the C-terminus at the M-band, and mature sarcomeres achieve 2.5 microns in length [145,146]. The stretching of Titin possibly exposes important protein binding sites to facilitate incorporation of additional myofibrillar proteins in the sarcomeres. Notably, exposure of Titin M-band epitope coincides with assembly of Myomesin in the M-band [145,146]. Titin is a giant protein, the largest known protein, with a transcript of over 80,000 bp. Sarcomere assembly is coupled in a cotranslational mechanism where nascent (not yet complete) peptides first associate with the sarcomere, and translation completes in conjunction with cytoskeletal assembly [147]. This explains the observation that only the N-terminus of such a large protein like Titin was initially detectable. Since it is so large, only partially deletions have been made: mutation in the N2B region severely affects early myofibrillogenesis resulted in complete lack of sarcomeres [148]; deletion of Titin's M-band region resulted in initial sarcomere assembly but with eventual disassembly [149,150]. These partial knockout models of Titin suggest that Titin is indispensable for myofibrillogenesis.

1.3.6 Myomesin

Myomesin resides in the M-band of the sarcomere, and each of multiple isoforms is expressed in a different fiber type: Myomesin-1 is expressed in all muscles, Myomesin-2 is expressed in cardiac and fast skeletal fibers, and Myomesin-3 is found in intermediate skeletal fibers [151,152]. Myomesin N-terminus binds to Myosin and its central region interacts with the C-terminus of Titin, acting as an important link between

Titin and the thick filament [153]. By linking neighboring filaments to each other, the M-band stabilizes and aligns the actin-myosin filament lattice. Myomesin also plays a role in regulating sarcomere assembly and turn over. Phosphorylation of specific serine residues on Myomesin inhibits its binding to Titin, and knockdown of Myomesin-1 leads to myofibril disorganization, though initial sarcomere assembly occurs normally [154,155].

1.3.7 Desmin

In addition to Actin and non-muscle Myosin, Desmin is also one of the first cytoskeletal proteins expressed in myocytes, and it is the first observed in sarcomere assembly along with Actin and non-muscle Myosin, followed by α-Actinin and Titin [110]. Desmin forms a network of intermediate filaments that connects parallel sarcomeres to one another and coordinates myofibril contraction within cells and between neighboring cells [156–158]. Desmin knockout animals are viable and assemble normal sarcomeres, though sarcomere maintenance is compromised, and animals suffer from cardiomyopathy [159,160]. Loss of Desmin leads to severe muscle structural disorganization: loss of lateral myofibril alignment, disruption of the myofibril anchorage to the sarcolemma, and perturbation of muscle nucleus shape and position [159,160]. Desmin interacts with many other structural proteins and serves an integral role in maintaining sarcomere structure. Thus, mutation in Desmin resulted in skeletal/cardiac myopathies called desminopathies. Mutations in Desmin often render the protein assembly-incompetent, and mutant Desmin exerts a dominant-negative effect by disrupting pre-existing filamentous network [161–163]. This partially explains

the hallmark characteristic of desminopathy – the accumulation of intracellular aggregates of mixed sarcomeric proteins including Desmin.

1.4 Cellular and molecular pathways involved in muscle atrophy

Muscle development and growth require coordinated participation of multiple proteins. Various pathological (disease mutation) and physiological conditions (denervation, disuse, aging) can lead to muscle loss. Muscle loss can be broadly categorized into two categories: loss of myofibers via cell death or loss of muscle mass due to shrinkage. In the case of losing muscle mass via decrease in muscle cross sectional area, i.e. muscle atrophy, often the final fate of the muscle cell and its nuclei are ambiguous. In this section, I will summarize the current knowledge of the cellular and molecular pathways that have been implicated in muscle loss reported in human skeletal muscle diseases or in animal models.

1.4.1 Cell death in muscular atrophy

If muscle cells die, i.e. loss of muscle nuclei, the underlying causes and pathway(s) are not often simple to understand. There are two main pathways to cell death: apoptosis and necrosis. Apoptosis is considered “programmed cell death” due to its role in the genetically determined elimination of cells. We now know that apoptosis happens under genetic regulation (in development), or in response to environmental or pathological stimuli [164,165]. Apoptosis occurs in three stages, each with distinct molecular characteristics: activation of initiation Caspases (Caspase 8), activation of effector Caspases (mainly Caspase 3), and phagocytosis of apoptotic bodies [164,165].

In muscle, apoptosis is triggered by activation of tumor necrosis factor receptor (TNF-R), accumulation of reactive oxygen species (ROS), and/or imbalanced calcium regulation [164,165]. Activation of apoptosis leads to activation of Caspase 8, which in turn activates downstream effector Caspases, mainly Caspase 3. Caspase 3 is responsible for the process of cell death: chromatin condensation, DNA fragmentation, breakdown of the nuclear envelope and finally cells disintegrate into apoptotic bodies containing intact organelles [165,166]. The final stage of apoptosis is clearance of apoptotic bodies via phagocytosis by neighboring cells or macrophages without triggering an inflammatory response [165,166]. Muscle is a multinucleated cell and the loss of some but not all myonuclei and its associated sarcoplasm via apoptosis leads to myofiber atrophy (reduced size) rather than death of the whole cell [167].

In contrast to apoptosis, which does not release cellular contents into the surrounding interstitial tissues, necrosis is cell death accompanied by inflammatory activation due to leakage of cellular content. Muscle necrosis has characteristic sequential events: at its initiation, the plasma membrane becomes permeable; there is formation of cytoplasmic vacuoles, followed by swelling of organelles and cells, rupture of the plasma membrane, and release of the intracellular contents [168]. Apoptosis and necrosis processes are distinguishable via light or electron microscopy and have different downstream signaling cascades [165,166]. However, there is overlap in which an ongoing apoptotic process can become necrotic due to decreased in Caspases and intracellular ATP [169]. In addition, a failure of apoptotic body clearance can trigger an inflammatory response, a process termed secondary necrosis. Thus, while apoptosis

and necrosis are morphologically distinguishable, the molecular signaling involved and the tissue response to the two cell death processes are not as exclusive.

1.4.2 Molecular mechanism of muscle atrophy

Muscular atrophy is the loss of muscle mass as a result of disease-causing mutations, injury, fasting, aging, or cancer. While the morphological phenotype is similar, our understanding of muscle loss causes and progression is limited. In recent years, we have, however, gained a deeper understanding in the molecular mechanisms underlying muscle atrophy. First the discovery of protein degradation via the ubiquitin proteasome system (UPS) demonstrates the essential role of UPS in facilitating muscle atrophy by favoring catabolism. In UPS, proteins targeted for degradation are marked with ubiquitin. The final step of the ubiquitination cascade is catalyzed by the E3 enzyme, a ubiquitin ligase. In mammals, there is a diverse population of E3 ligases with some acting in a tissue-specific manner. In muscle, two muscle-specific E3 ligases are highly upregulated in atrophy: the Cullin-1 linked substrate adaptor Atrogin-1/MAFbx (muscle atrophy F-box, Fbxo32) and MuRF1 (muscle RING finger 1, Trim63) [170,171]. Mice lacking *Atrogin-1* and *MuRF-1* are resistant to denervation induced atrophy, and knockdown of *Atrogin-1* prevents muscle loss during fasting [172,173]. Atrogin-1 has been shown to target the key muscle transcription factor (MyoD) and an important activator of protein synthesis (eIF3-f) for degradation [174,175]. MuRF1 has been shown to target various sarcomeric proteins including Myosin, Actin, Troponin I, α-Actinin, Titin, and Desmin [170,176]. Together, Atrogin-1 acts to primarily to inhibit new muscle protein synthesis while MuRF1 promotes protein degradation to facilitate muscle atrophy. Another E3 ubiquitin ligase – TRAF6 – was shown to play a role in muscle

atrophy though its expression is not restricted to muscle [177]. Animals with muscle-specific ablation of TRAF6 are resistant to muscle loss induced by starvation, denervation, or cancer [177,178].

The diversity of E3 ligases identified suggests that these factors are involved in different atrophy-inducing conditions. What are the upstream regulators activating UPS in muscle atrophy? Several factors have been identified including the transcription factors FoxO3 and NF-κB [170,178,179]. FoxO3 reduces total protein synthesis in adult and was shown to not only regulate UPS but also autophagy [180–182]. Akt phoshorylates all members of the FoxO family including FoxO3, promoting their export from nucleus to cytoplasm [181]. In conditions of atrophy, reduced activity of Akt both reduces protein synthesis via Akt signaling and leads to accumulation of FoxO in the nucleus furthering FoxO activation of atrogenes [181]. The crosstalk between the nutrient-responsive muscle growth pathway (IGF1-Akt-mTOR) and atrogene activation provides a way for muscle to respond to environmental stimuli.

In addition to UPS, another form of protein degradation, autophagy, is involved in muscle mass maintenance and in muscular atrophy. Autophagy is a process of bulk degradation of proteins and organelles, which is important for maintaining homeostasis and cellular survival during starvation [183]. However, insufficient or excessive autophagy can lead to muscle degeneration [184]. A recent study showed that autophagy was induced in cancer cachexia leading to pathologic muscle wasting [185]. Autophagy occurs in three steps: initiation, autophagosome formation enclosing protein aggregate and organelles, and the final protein/organelle degradation via fusion of autophagosome to lysosome [183]. Activation and execution of autophagy involve a

suite of conserved autophagy related genes (*ATGs*) [164,186]. Autophagy is regulated in response to nutrient levels and is activated in fasting condition via the IGF-1 signaling pathway [164,186]. Thus, autophagy facilitates muscle adaption to its current nutrient environment. Recent studies suggest that there is cross-talk, via the FoxO3 transcription factor, between the UPS and autophagy in skeletal muscles [187,188]. Different disease conditions may depend on either the UPS or autophagy or both. It remains unclear how these pathways are regulated in normal versus diseased muscles. It is important to note that autophagy-related cell death is a result of accumulation of autophagic vesicles due to unregulated autophagy [189–191]. It remains controversial as to whether unregulated autophagy is a 'mechanism' of cell death or a sign of cellular stress.

The third molecular mechanism that has been implicated in muscular atrophy involves the NF-κB family of transcription factor, known to regulate a variety of cellular responses. There are five members in the NF-κB family: RelA (p65), RelB, c-Rel, NF-κB1 (p50) and NF-κB2 (p52) proteins, all acting as homo- or hetero-dimers. NF-κB is sequestered in the cytoplasm by IκB kinase (IKK) and upon activation, NF-κB is released and exported into the nucleus to activate downstream genes. When muscle is injured, an inflammatory response is important for healthy muscle recovery but uncheck inflammation often lead to pathological muscle loss. NF-κB is an important mediator of the immune/inflammatory response; thus, its inhibition in various muscle diseases leads to improved muscle recovery following injury [192].

NF-κB has also been shown to regulate muscle mass in atrophic muscle disease and muscle inactivity [192,193]. In models of atrophy induced by hindlimb unloading,

NF-κB is dramatically increased in the unloaded limb compared to control, and NF-κB1 knockout mice are resistant to atrophy [194,195]. Recent research shows that both isoforms of IKK (IKKα and IKKβ) are necessary and sufficient for muscle atrophy [196,197]. Discoveries of downstream effectors of NF-κB signaling in muscle atrophy are in the early stages but there is evidence for NF-κB function as an upstream regulator of the ubiquitin proteasome system in skeletal muscle. Muscle-specific transgenic activation of NF-κB causes severe muscle atrophy and increases *MuRF1* expression [193,197]. This suggests that there is complex crosstalk between different pathways that regulate muscle mass in physiological as well as pathological conditions.

1.5 Muscle loss in limb adaptation

The organization of the musculoskeletal system differs substantially in different parts of the body (e.g., head and limb) and anatomy is morphologically diverse between orthologous locations of different species to achieve adaptive feeding and locomotory diversity. Studies of muscle evolution, including the increase or loss of specific muscle or muscle groups, provide insights into the evolution of the limb as well as inferences of the consequent effects on locomotion. For example, we can trace the evolutionary history of the majority of the pectoral and forelimb muscles of the tetrapod to be derived from the adductor and abductor of basal fish [198].

Comparative studies of muscles of humans and other mammals suggests that more muscles were lost in the evolution of the human lineage than in species such as opossums (marsupials) or rats (rodents). Modern humans have fewer number of muscles of the hand than many other tetrapods: 20 intrinsic muscles of the hand in

contrast to more than 35 in lizards [199]. Intrinsic muscles are fully contained within the limb segment that they control (e.g. *interossei* of foot) in contrast to extrinsic muscles that arise outside of, but act on, the structure under consideration (e.g. *tibialis anterior*). While we lost most of the muscles related to the movement of each of the four digits, muscles associated with the thumb evolve to become more robust and mobile [200]. Similar to the loss of multiple forelimb muscles during the evolutionary transitions leading to mammals, the number of muscles in the foot decreased from salamander (28) to lizard (25), to rat (22), and to modern human (21) [201]. The evolution of muscles also involves many splitting events that led to the subdivision of the ancestral muscle rather than making an entirely new muscle, suggesting a deep conservation of muscle groups across different taxa [198].

In rodents, osteological and myological studies show that intrinsic muscle loss, often associated with reduced digit number and elongated skeletal elements, correlates with bipedalism. Intrinsic foot muscles are those situated in the foot that are partly responsible for movement of the digits. Dipodidea – commonly known as jerboas – is a family of bipedal desert rodents with members having diverse limb morphology and gait. Within Dipodidea, the lesser Egyptian jerboa (*Jaculus jaculus)*, among the most derived subfamily of jerboa is bipedal, has 3 digits, and has lost all 19 of the intrinsic foot muscles that are present in more basally derived rodent species [202]. In contrast, its relative, the woodland jumping mouse (*Napaeozapus insignis*), is quadrupedal and has 5 digits and retained most ancestral intrinsic foot muscles (16 out of 19) [202]. Presumably, adaptation toward bipedalism allows the jerboa to run or leap at high speeds across great distances and to change direction rapidly to avoid predation in an

open desert environment [202,203]. In addition, perhaps the development of robust tendon, in place of muscle, aid to resist hyperextension across the ankle in species that land with greater force when running or leaping on elongated feet.

Muscles were also lost multiple times independently in the evolution of birds, reptiles, ungulates, bipedal rodents, and humans [204–211]. In species in which muscle loss occurs after its formation and maturation, is there any observed relationship between the natural process of muscle loss and that observed in pathological context? Indeed, anatomical and histological studies of muscle loss in ungulates – horses, deer, and camels – shows striking similarities to characteristics observed in pathological muscle dystrophies [212]. The suspensory ligament in the foot of the horse is formed by a fibrous transformation of the intrinsic muscle of the third digit [212]. Similarly, in the feet of ox and deer, as muscle tissue degenerates, fat cells accumulate and the connective tissue proliferates to fill the space an increase the size of connective tissues [212]. Such morphological transformation mirrors fatty and fibrous tissue accumulation observed in various skeletal muscle dystrophies and atrophies in human [213].

1.6 Summary and questions:

Muscle development occurs in multiple stages and requires participation and coordination of diverse proteins. Thus, failure at any point during muscle development and maturation will compromise muscle function and manifest as disease. Numerous mutations of different components of the sarcomere have been reported and the associated pathology well described. Animal models have contributed to our

understanding on the progression and potential cause of various myopathies, though the detailed step-wise mechanism of muscle degeneration remains unclear.

Our current understanding of muscle loss is often from a pathological context, yet muscles have been lost several times during evolution as the limb adapts for optimal function. It is not well known what the cellular and molecular similarities and differences between muscle loss are in pathological versus natural contexts. Studying a natural developmental process of distal hindlimb muscle loss will shed light on evolutionarily conserved aspects of muscle development, muscle maturation, maintenance, and plasticity of muscle cell fate. The work described here has uncovered cellular and molecular aspects of natural muscle loss, their implication in muscle disease and evolution, and has opened new avenues to discover novel aspects of muscle development and plasticity.

CHAPTER 2. Cellular characterization of muscle loss in the jerboa foot

2.1 Introduction

Muscles in the feet of birds, reptiles, and mammals were lost multiple times in the course of limb evolution, usually coinciding with the loss of associated digits and elongation of remaining skeletal elements [204–211]. Despite its frequent occurrence, the developmental mechanisms that lead to the natural absence of adult limb muscle are not known. I focus here on a representative example of distal limb muscle loss in the bipedal three-toed jerboa, a small laboratory rodent model for evolutionary developmental biology, to determine if evolutionary muscle loss conforms to expectations based on what was previously known about muscle cell biology.

The hindlimb architecture of the adult jerboa is strikingly similar to the larger and more familiar hooved animals, like horses, including the disproportionately elongated foot that lacks all intrinsic muscle [209,210]. The tendons were retained and expanded in each of the anatomical positions where flexor muscles are absent and serve to resist hyperextension when the terminal phalanx contacts the ground during locomotion [214,215]. The evolutionary origin of jerboa intrinsic foot muscle loss lies deep in the phylogenetic tree of Dipodoid rodents. Compared to the ancestral state, the number of intrinsic foot muscles are reduced from sixteen to six in pygmy jerboas [216] which diverged from the three-toed jerboa lineage more than 20 million years ago [217,218].

The mechanisms of limb muscle development have been extensively studied in traditional model systems, and its degeneration has been studied after injury and during disease. Briefly, muscle progenitors delaminate and migrate from the somite into the limb bud where they proliferate and initiate a myoblast differentiation program [11–14].

Following differentiation, muscle progenitors fuse to form aligned multinucleated myofibers [219,220]. Each differentiated myofiber produces an assemblage sarcomeric proteins, organized to form myofibrils; the myofibrils themselves also undergo a process of maturation resulted in aligned sarcomeres to produce contractions in unison [106–109]. Failure at any point of myoblast specification, migration, myofiber differentiation, or myofibril maturation compromises muscle function and manifests as muscle degenerative disease in humans [124–126].

The mouse foot has three layers of tendon and intrinsic muscle with the *flexor digitorum superficialis* being the most superficial (Figure 2.1A). The deeper layer is the *flexor digitorum profundus* (Figure 2.1B) and the deepest layer is the *interoseous* (Figure 2.1C). Where there are muscles in the mouse foot, the jerboa foot has robust and long tendons (Figure 2.1, 2.3A,B). The absence of intrinsic foot muscle in the adult jerboa shares striking similarity to the muscle-specific *Smoothened* knockout mouse in which muscles fail to migrate into the distal limb [26]. It is possible that SHH signaling was disrupted in the jerboa resulted in the lack of foot muscle progenitors in the distal limb. Alternatively, muscles may form early during development and were subsequently eliminated in the fetus or after birth. Results reported in this chapter describe the morphological and cellular characterizations of muscle loss in the jerboa foot.

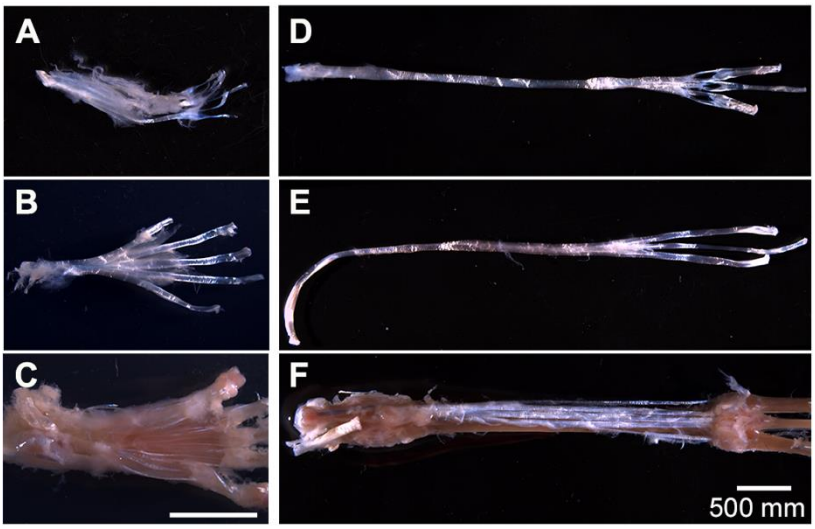

Figure 2.1 – Anatomy of mouse and jerboa foot
(A) In the adult mouse, tendon of the *flexor digitorum superficialis* supports the *m. flexor digitorum brevis* with distal tendon branches that each divide in two before inserting into either side of the base of the middle phalanx of each digit.
(B) Dorsal to this layer, the tendon of the *flexor digitorum longus* splits upon entering the foot and carries the *m. lumbricales.* Each *flexor digitorum longus* tendon emerges distally from between the branches of each *flexor digitorum superficialis* tendon and inserts into the base of each of the terminal phalanges.
(C) The *m. interossei* have a common tendon that originates in the tarsus, branches into each of the interosseus muscles, and inserts distally into the base of each of the proximal phalanges.
(D-F) The adult jerboa retained the tendons of (D) the *flexor digitorum superficialis*, (E) the *flexor digitorum longus*, and (F) the *interossei*, but all are devoid of muscle.

2.2 Results

2.2.1 Timing and rate of myofiber loss

The absence of intrinsic foot muscle in the adult jerboa could be due to a failure of early myoblasts to migrate into and/or to differentiate in the distal limb. To test this hypothesis, we performed whole-mount *in situ* hybridization in approximately stage-matched embryos to detect mRNA expression of the myogenic transcription factor, *MyoD*, in muscle progenitor cells. The presence of *MyoD*-positive cells in the jerboa hindfoot indicates that, similar to the mouse, myoblast migration and muscle patterning proceed normally in the jerboa hindlimb (Figure 2.2A,B).

Alternatively, embryonic muscles may form but not persist through development to the adult. In transverse sections of newborn mouse feet, immunofluorescent detection of skeletal muscle myosin heavy chain reveals each intrinsic muscle group (Figure 2.2C). In newborn jerboas, we observed two of the three groups of flexor muscles. While the *m. lumbricales* never form, the jerboa has a single *m. flexor digitorum brevis* and three pinnate *m. interossei* that are not present in adults (Figure 2.2C,D).

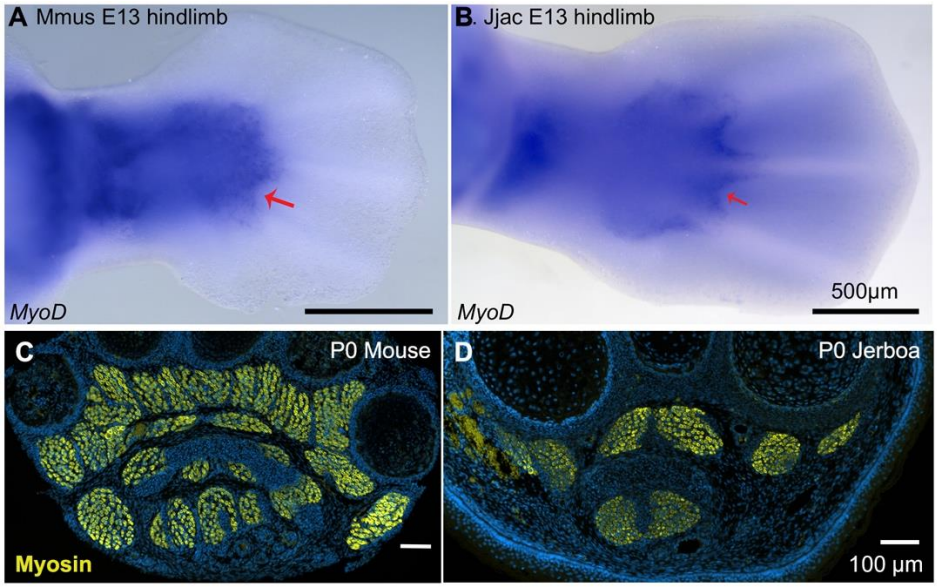

Figure 2.2 - Jerboa foot muscles are formed and pattern properly at birth
MyoD whole mount *in situ* hybridization in developing mouse (A) and jerboa (B) hind limb respectively. Ventral view.
A representative transverse section illustrates the presence of foot muscle in the newborn (C) mouse and (D) jerboa. Top dorsal; bottom ventral.

Postnatal growth of vertebrate skeletal muscle typically involves an increase in myofiber number (hyperplasia) within the first week, followed by an increase in myofiber size (hypertrophy) [58–60]. In order to understand the dynamics of muscle growth and loss, we quantified the rate of myofiber hyperplasia at two-day intervals after birth of the mouse and jerboa, focusing on the representative interosseous muscle that is associated with the third metatarsal (Figure 2.3E,F). As expected in the mouse, we observed a steady increase in the average number of myofibers in cross section from birth to P8 (Figure 2.3C). In contrast, the number of myofibers in the third interosseous of the jerboa foot rapidly declines beginning at approximately P4, and few myofibers remain by P8 (Figure 2.3D).

It is possible that the rate of myofiber loss outpaces a typical rate of new cell addition such that muscles with the potential to grow are instead steadily diminished. Alternatively, myofiber loss may be accelerated by a compromised ability to form new myofibers and to add nuclei to growing myofibers. To distinguish these hypotheses, we analyzed cohorts of animals two days after intraperitoneal BrdU injection at P0, P2, or P4. Since multinucleated jerboa foot myofibers are postmitotic (Figure 2.4), we reasoned that BrdU+ nuclei present within Dystroglycan+ myofiber membrane were added by myocyte fusion during the two-day window after they were labeled as myoblasts or myocytes in S-phase (Figure 2.5A). When normalized to the total number of myofiber nuclei, we found that myocytes fuse to form multinucleated myofibers in jerboa hand muscle at a consistent rate from P0 to P6. However, their incorporation into jerboa foot muscle decreased significantly after P2 (Figure 2.5B). These results suggest that myofiber loss, which begins at P4, is preceded by reduced myogenesis.

The reduced rate of myocyte incorporation could be due to reduced numbers of muscle progenitor cells or to an inability of these cells to mature and fuse. To distinguish these possibilities by quantifying proliferative muscle progenitor cells, we analyzed animals two hours after BrdU injection at P0, P2, and P4 and counted the number of BrdU+ nuclei located between Dystroglycan+ myofiber membrane and the Laminin+ basal lamina (Fig. 2.5C). Normalized to the total number of myofibers, we found that the number of proliferative progenitor cells in jerboa foot muscle significantly decreased from P0 to P4 compared to hand muscles that showed no change over time (Fig. 2.5D). These results suggest that a reduced number of muscle progenitor cells might contribute to the reduced prevalence of myocyte fusion events.

We next tested whether compromised proliferation and differentiation of the jerboa foot muscle progenitors is cell autonomous or non-cell autonomous. We isolated single cells, including myoblasts and myocytes but excluding myofibers, by mechanical trituration and enzymatic digestion of P1 jerboa and mouse lower leg and foot muscles [221]. After 6 days and 9 days of culture, we detected Myogenin+ differentiating myocytes and Myosin+ fully differentiated myofibers in primary cell cultures isolated from each muscle (Fig. 2.5E), and there was no significant decline in the number of cells over time (Figure 2.6). Jerboa foot muscle cell differentiation and survival *in vitro* days after cell number begins to decline *in vivo* suggests that loss of jerboa foot myofibers is non-cell autonomous.

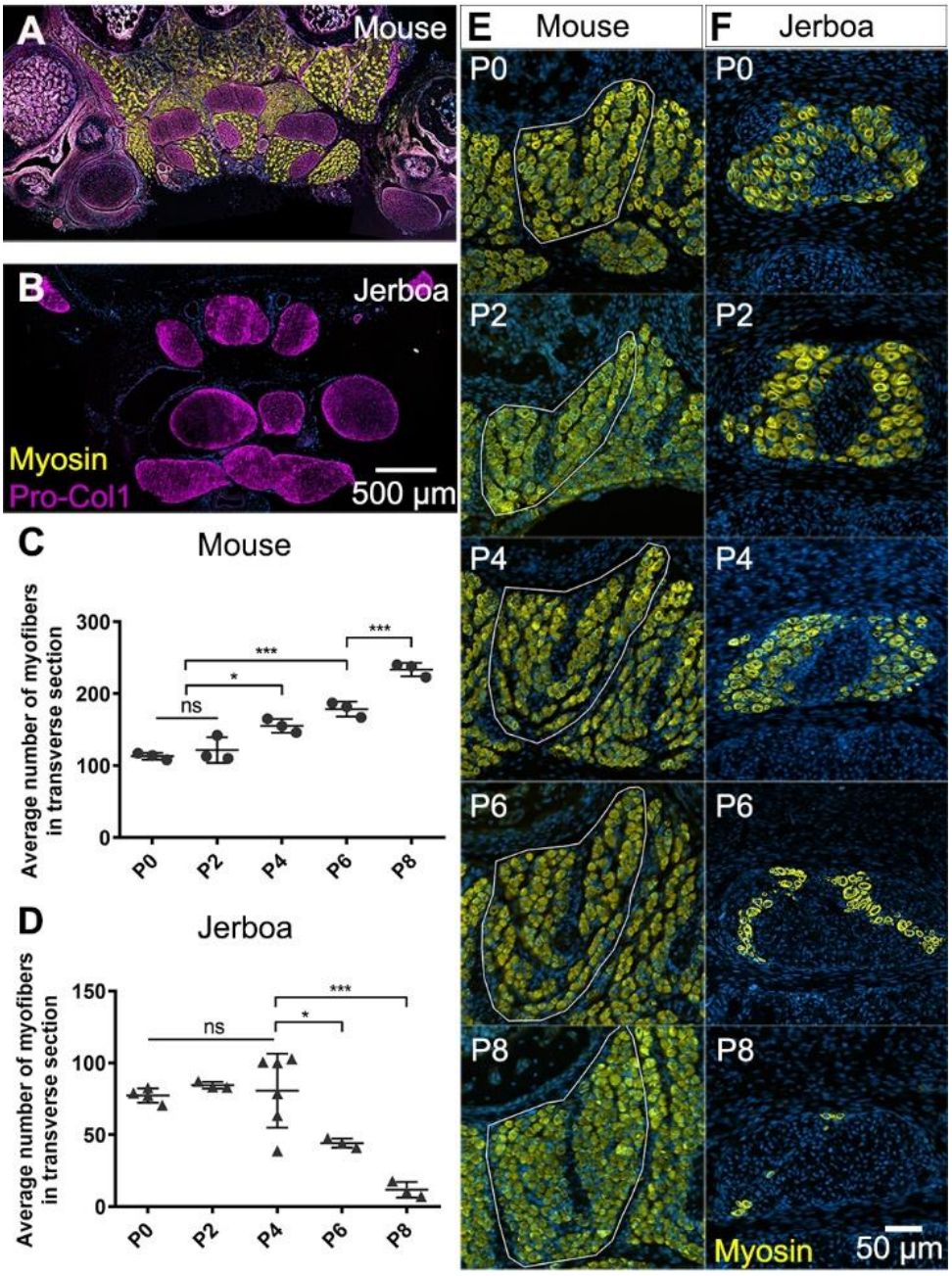

Figure 2.3 - Muscles are rapidly lost in the neonatal jerboa foot
(A and B) Transverse sections of adult (A) mouse and (B) jerboa foot.
(C and D) Mean and standard deviation of the number of myofibers in transverse sections of third digit interosseous muscle at two-day intervals from birth to postnatal day 8. (C) Mouse P0-P8, n=3 animals each. P0-P4 (p=0.0062), P2-P4 (p=0.0262), P0-P6 (p=0.0002), P2-P6 (p=0.0007), P6-P8 (p=0.0009). (D) Jerboa P0, n=4 animals; P2, P6, P8, n=3 animals each; P4, n=6 animals. P4-P6 (p=0.0376), P4-P8 (p=0.0002). (*p<0.05, **p<0.01, ***p<0.001)
(E and F) Representative transverse sections of interosseous muscle of the third digit of (E) mouse and (F) jerboa at each stage. For all: top dorsal; bottom ventral.

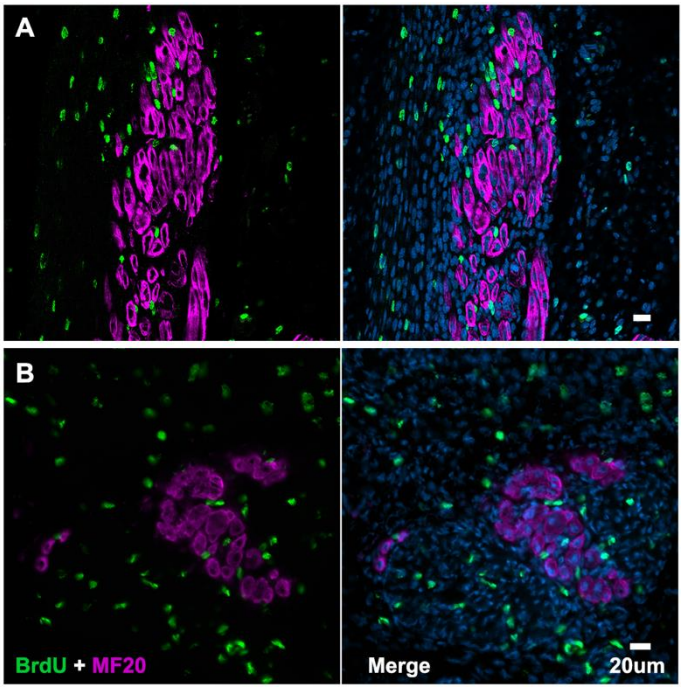

Figure 2.4 - Jerboa foot muscles are postmitotic
Representative image of (A) longitudinal section of P4 (n=1 animal, 156 myofibers) and (B) transverse section of P5 jerboa foot interosseous muscle (n=1 animal, 297 myofibers) illustrating jerboa foot myofibers are postmitotic. BrdU+ nuclei are peripheral to MF20+ myofibers.

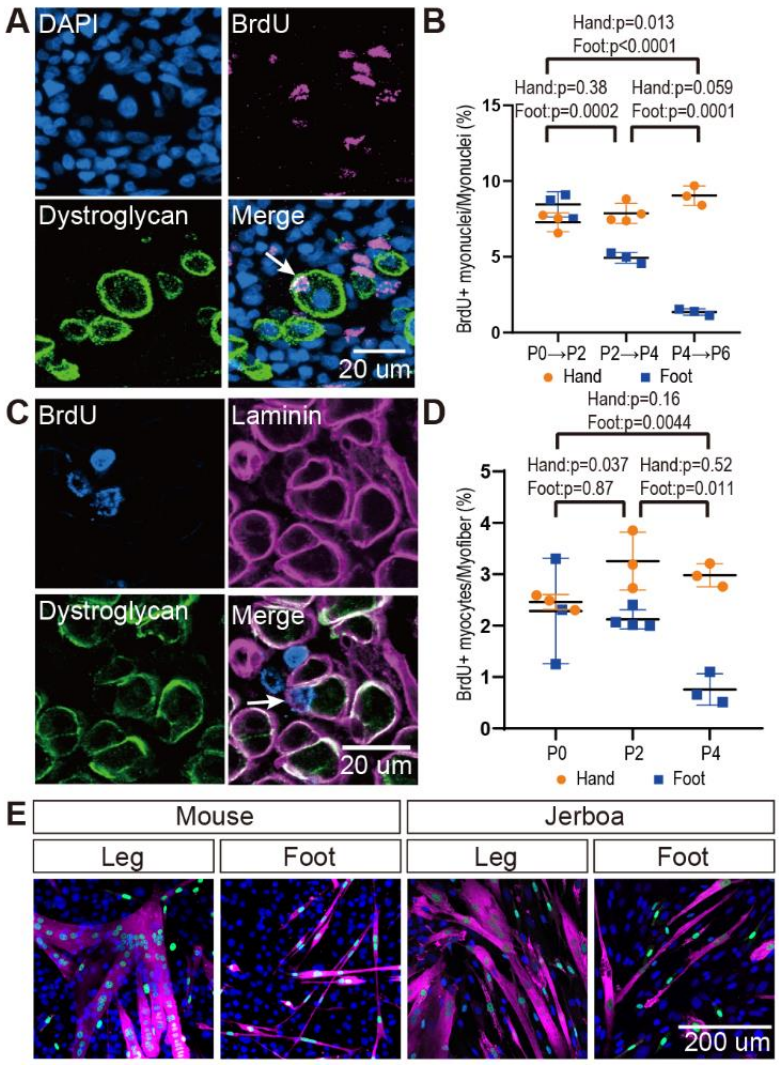

Figure 2.5 - The rate of myocyte fusion is reduced prior to myofiber loss
(A) Newly fused nuclei within Dystroglycan+ myofiber membranes (arrow) can be distinguished two days after labeling with BrdU.
(B) The mean and standard deviation of BrdU+ myonuclei (putative fusion events) normalized to all myofiber nuclei in sections of jerboa hand and foot muscles at intervals from P0 to P6. Foot at P0-P2, P2-P4, P4-P6, Hand at P0-P2, P4-P6, n=3 animals each. Hands at P2-P4, n=4 animals.
(C) Proliferative muscle progenitor cells that are BrdU+ are found outside Dystroglycan+ membrane and inside the Laminin+ basal lamina (Arrow).
(D) The mean and standard deviation of BrdU+ muscle progenitor cells was normalized to the number of myofibers in sections of jerboa hand and foot muscles at P0, P2, and P4. Foot at P0, P4, Hand at P2, P4, n=3 animals each. Foot at P2, Hand at P0, n=4 animals each.
(E) Differentiated myofibers after 6 days of culturing primary muscle progenitor cells isolated from lower leg and foot muscles of mouse and jerboa. Green, Myogenin; Magenta, Myosin.

Mouse Leg MHC+ nuclei		
	Day 6	Day 9
Litter 1	115	264.5
Litter 2	132.6	128.2
Litter 3	53.6	93.8
Litter 4	98.4	486.8

Mouse Foot MHC+ nuclei		
	Day 6	Day 9
Litter 1	156.8	120
Litter 2	43	129.4
Litter 3	69.4	138.2
Litter 4	294.8	199.4

Jerboa Leg MHC+ nuclei		
	Day 6	Day 9
Litter 1	58.2	74.4
Litter 2	117.5	207.4
Litter 3	100.2	405.8

Jerboa Leg MHC+ nuclei		
	Day 6	Day 9
Litter 1	58.2	74.4
Litter 2	117.5	207.4
Litter 3	100.2	405.8

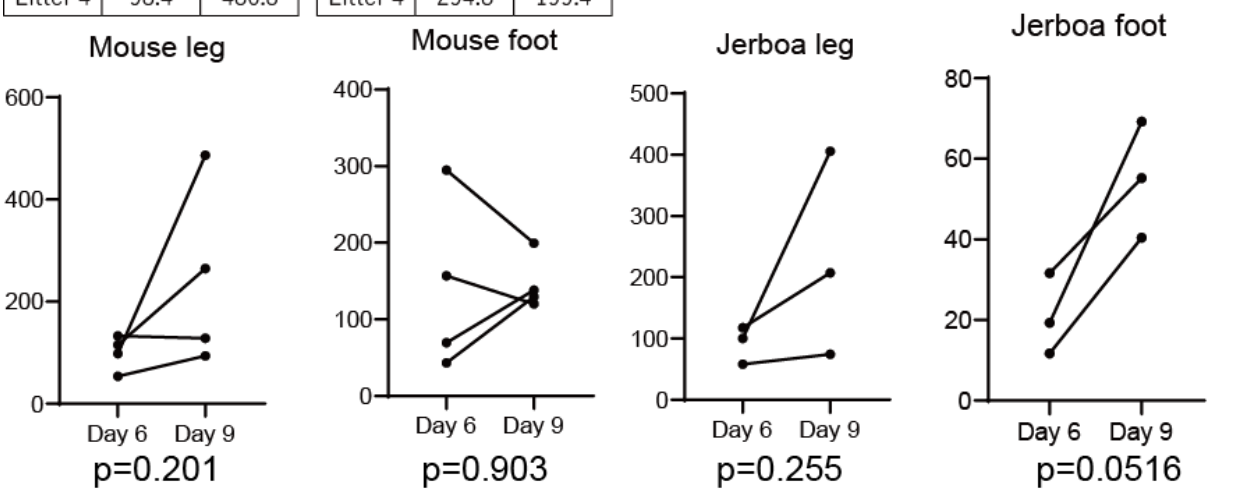

Figure 2.6 – Persistence of differentiated muscle cells in culture after loss *in vivo*
Myoblasts and myocytes were isolated from leg and foot muscles of P1 mouse and jerboa and differentiated in culture for 6 days and 9 days. The number of nuclei within MHC positive cells found in 10 microscopic fields of replica-plated cultures were averaged and represented in graphs and tables. P-values were calculated using paired t-test for replicated wells. None of the experimental groups showed a statistically significant difference in the number of nuclei in Myosin positive cells between Day 6 and Day 9 of culture.

2.2.2 Testing for muscle cell death

The rapid and almost complete loss of differentiated myofibers from P4 to P8 suggested these cells die, since individual cells or groups of cells are commonly eliminated by apoptosis during development [222,223]. We therefore tested the hypothesis that neonatal intrinsic foot muscles undergo apoptosis by implementing the TUNEL assay to detect DNA fragmentation and by immunofluorescent detection of cleaved Caspase-3, a key protein in the apoptotic program [224]. Each revealed keratinocyte apoptosis in hair follicles, which are known to undergo programmed cell death, as a positive control in the same tissue sections [225]. However, TUNEL or cleaved Caspase-3 positive jerboa foot myofibers or cells in their vicinity were an extreme rarity (0.25% of myofibers) in animals ranging from P0 to P8 and comparable to mouse myofibers suggesting muscle is not eliminated by apoptosis (Figure 2.7A,B, 2.8).

Alternatively, myofiber loss may occur through a cell death mechanism that is first characterized by plasma membrane permeability, such as necrosis [168]. To test this hypothesis, we injected Evans blue dye (EBD), a fluorescent molecule that accumulates in cells with compromised plasma membranes [226,227], into the peritoneum of P3 and P4 neonatal jerboas 24 hours before euthanasia. Although we detected EBD in mechanically injured myofibers of the gastrocnemius as a control, we saw no EBD fluorescence in jerboa foot myofibers or in surrounding cells (Figure 2.7C, 2.9). We also saw no Annexin V immunofluorescence on the surface of jerboa foot myofibers, another hallmark of dying cells that flip Annexin V to the outer plasma membrane (Figure 2.7D, 2.9).

Since we observed no direct evidence of cell death, we asked whether there was an immune response that might be an indirect proxy for undetected death. Dying muscle cells frequently recruit phagocytic macrophages that engulf cellular debris [228–230]. We predicted that myofibers that die by any mechanism that produces cellular debris might recruit macrophages that are detectable by expression of the F4/80 glycoprotein. However, consistent with the lack of evidence of cell death in the jerboa foot, no F4/80^{+} macrophages were found among myofibers from birth to P7 (Figure 2.10). Since immune cells other than mature macrophages might be recruited to a site of cell death, we also assessed expression of CD45 and found no evidence of T-cells, B-cells, dendritic cells, natural killer cells, monocytes, or granulocytes near jerboa foot myofibers from P4 to P8 (Figure 2.7E, 2.10).

With no observation of cell death by apoptosis or necrosis, the fate of the myotubes in the jerboa foot remains unknown. To determine the fate of these muscle cells, we attempted to lineage label jerboa foot muscles to track their fate. We engineered an intersectional fate mapping strategy using two different muscle promoters to express the Cre and Flippase (Flp) recombinases. This system uses a reporter that contains LoxP-mCherry-Stop-LoxP-FRT-Stop-FRT-H2bYFP driven by the CAG promoter (Figure 2.11) and has been used successfully to lineage trace specific populations of neurons in the brain [231]. A second plasmid expresses Cre under the promoter for muscle creatine kinase [232] and Flippase under the human skeletal actin promoter [233] (Figure 2.11). Both promoters were previously used successfully to lineage trace dedifferentiated and redifferentiated myofibers in newt and salamanders [234]. A third plasmid that expresses the Tol2 transposase will integrate the reporter

DNA construct into the nuclear genome for long-term stable expression. Despite the requirement for expression of both muscle-specific promoters, analysis of YFP+ cells three days after electroporation showed labeling of non-muscle cells comprising approximately 10% of total labeled cells (Table 2.1). With a relatively low number of labeled myofibers (<10/foot), this hindered our ability to confidently determine the fate of labeled cells at later stages (P14) when almost all muscles are gone.

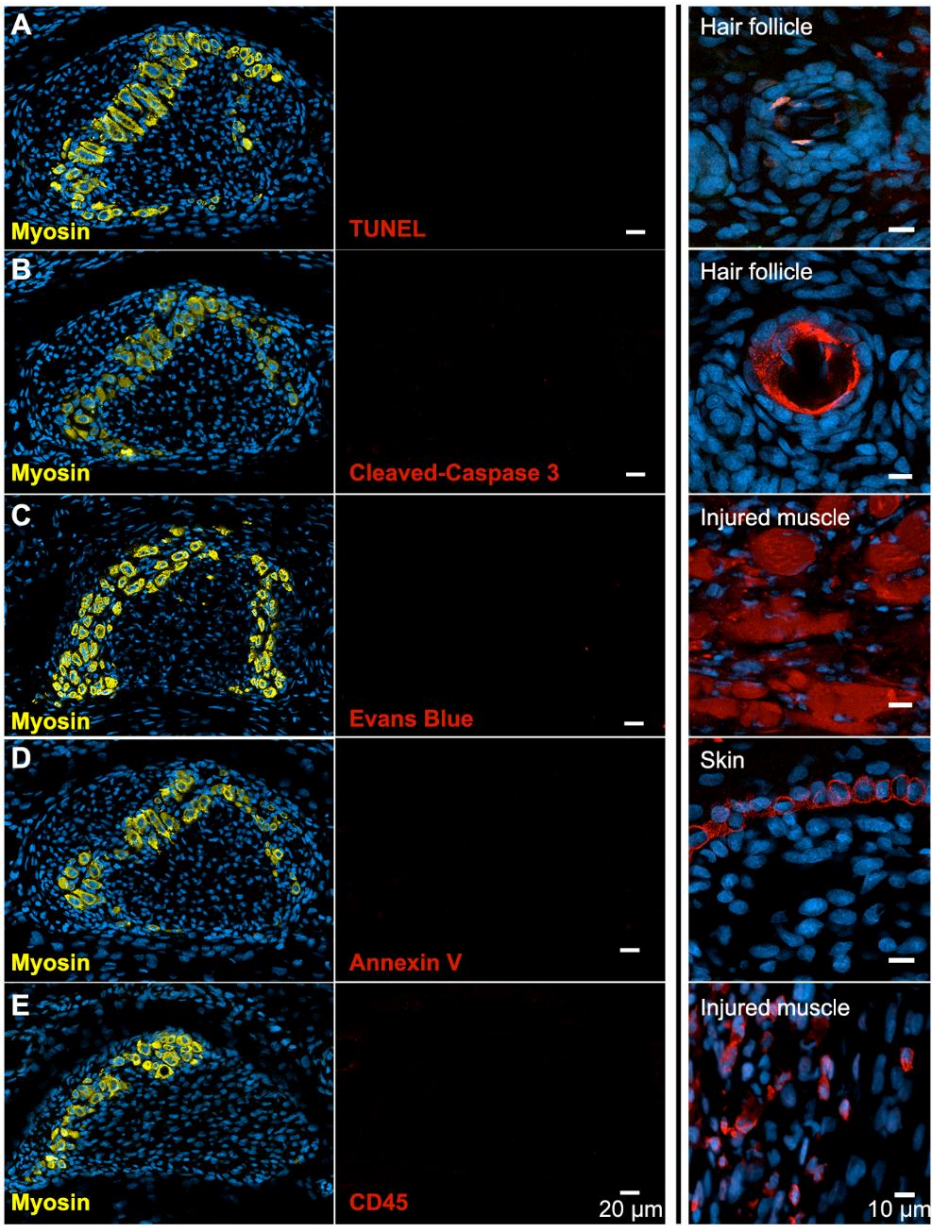

Figure 2.7 - There is no evidence of apoptosis, necrosis, or macrophage infiltration
(A and B) TUNEL and cleaved Caspase-3 staining for apoptotic nuclei in transverse sections of third digit interosseous muscle in the P6 jerboa foot and of positive control (TUNEL, n=3 animals; cleaved Caspase-3, n=2 animals).
(C) EBD detection in transverse section of third digit interosseous muscle in the P5 jerboa foot and of positive control (n=5 animals).
(D) Annexin V immunofluorescence in longitudinal section of third digit interosseous muscle in the P6 jerboa foot and of positive control (n=3 animals).
(E) CD45 immunofluorescence in transverse section of third digit interosseous muscle in the P6 jerboa foot and of positive control (n=3 animals).

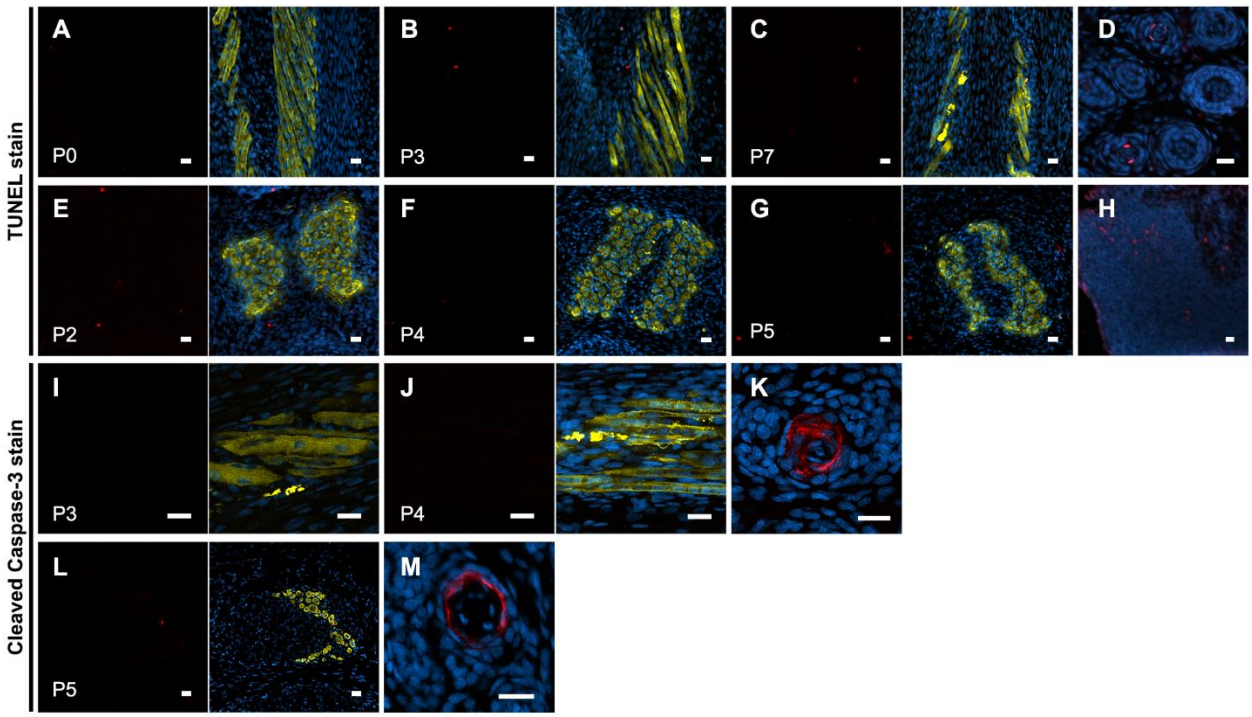

Figure 2.8 - No evidence of jerboa foot muscle apoptosis
TUNEL staining (TUNEL and merge with DAPI and Myosin) for apoptotic nuclei in longitudinal and transverse sections of interosseous muscle in the (A) P0 (n=1 animal), (B) P3 (n=3), (C) P7 (n=1), (E) P2 (n=2), (F) P4 (n=5), and (G) P5 jerboa foot (n=3). (D) Apoptotic keratinocytes as positive control for A-C and (H) apoptotic limb bud cells as positive control for E-G.
Cleaved Caspase-3 staining (Cleaved Caspase-3 and merge with DAPI and Myosin) for apoptotic nuclei in longitudinal and transverse sections of interosseous muscle in the (I) P3 (n=1 animal), (J) P4 (n=5), (L) P5 jerboa foot (n=2). (K) Apoptotic kerotinocytes as positive control for I-J and in (M) for L. Scale bars are each 20 µm.

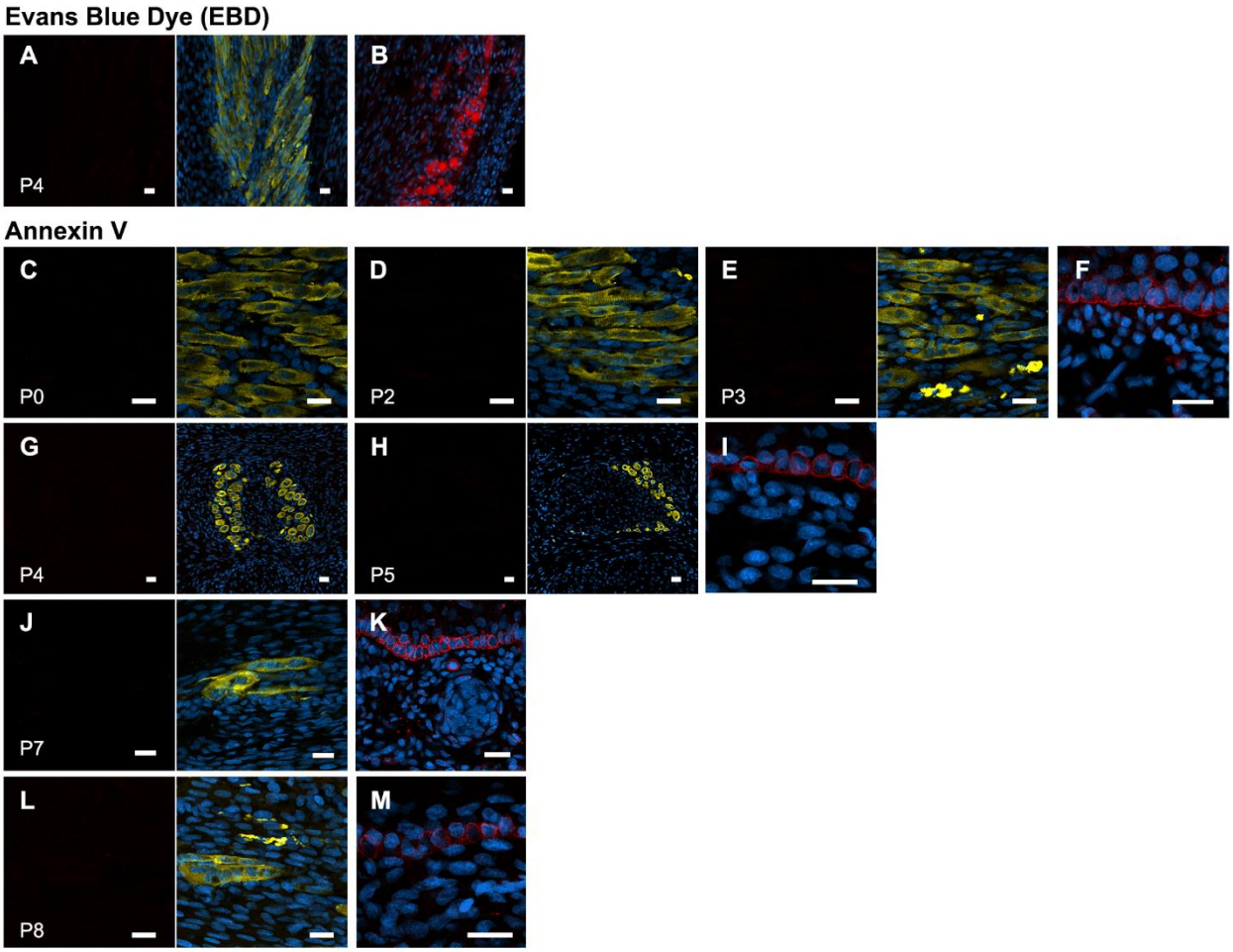

Figure 2.9 – No evidence of jerboa foot muscle necrosis
(A) EBD detection (EBD and merge with DAPI and Myosin) in longitudinal sections of the third digit interosseous muscle in the P4 jerboa foot (n=5 animals) and of (B) positive control mechanically injured gastrocnemius muscle.
Annexin V immunofluorescence (Annexin V and merge with DAPI annd Myosin) in longitudinal and transverse section of interosseous muscle in the (C) P0 (n=1), (D) P2 (n=1), (E) P3 (n=1), (G) P4 (n=2), (H) P5 (n=1), (J) P7 (n=1), (L) P8 jerboa foot (n=1). (F) Cornifying skin keratinocytes as positive control for C-D, (I) for G-H, (K) for J, and (M) for L. Scale bars are each 20 µm.

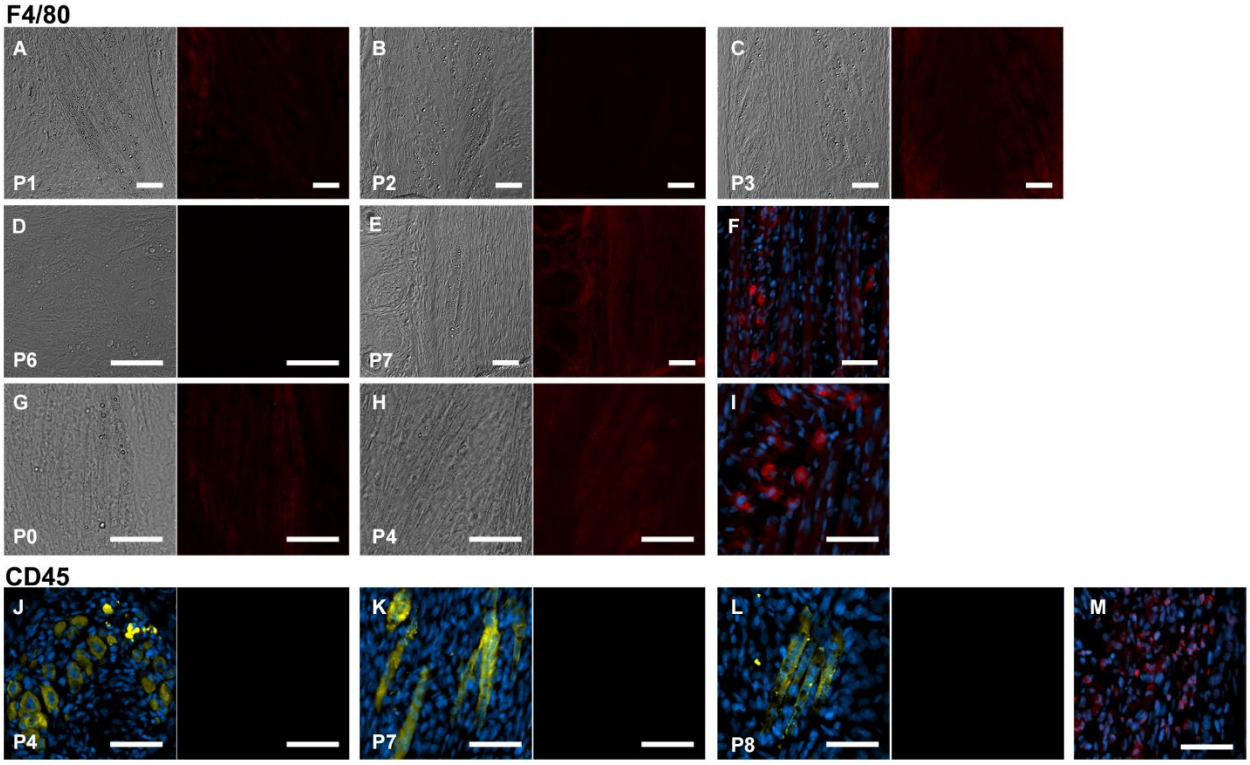

Figure 2.10 – No macrophage infiltration into jerboa foot muscle
Jerboa foot muscles have a distinct morphology and lipid droplets that can be identified by differential interference microscopy in longitudinal sections. F4/80 immunofluorescence in the same longitudinal sections of the third digit interosseous muscle in the (A) P1 (n=2 animals), (B) P2 (n=1), (C) P3 (n=2), (D) P6 (n=2) (E) P7 (n=1), (G) P0 (n=3), and (H) P4 jerboa foot (n=2). Positive control illustrating macrophage presence in mechanically injured jerboa gastrocnemius muscle for A-D in F and for G-H in I.
CD45 immunofluorescence in sections of the third digit interosseous muscle of jerboas. Left panels are a merge of Myosin and DAPI; right panels are CD45 immunofluorescence in (J) P4 (n=3), (K) P7 (n=1), (L) P8 (n=1) animals. Positive control illustrating macrophage presence in mechanically injured jerboa gastrocnemius muscle for J-L in M. Scale bars are each 50 µm.

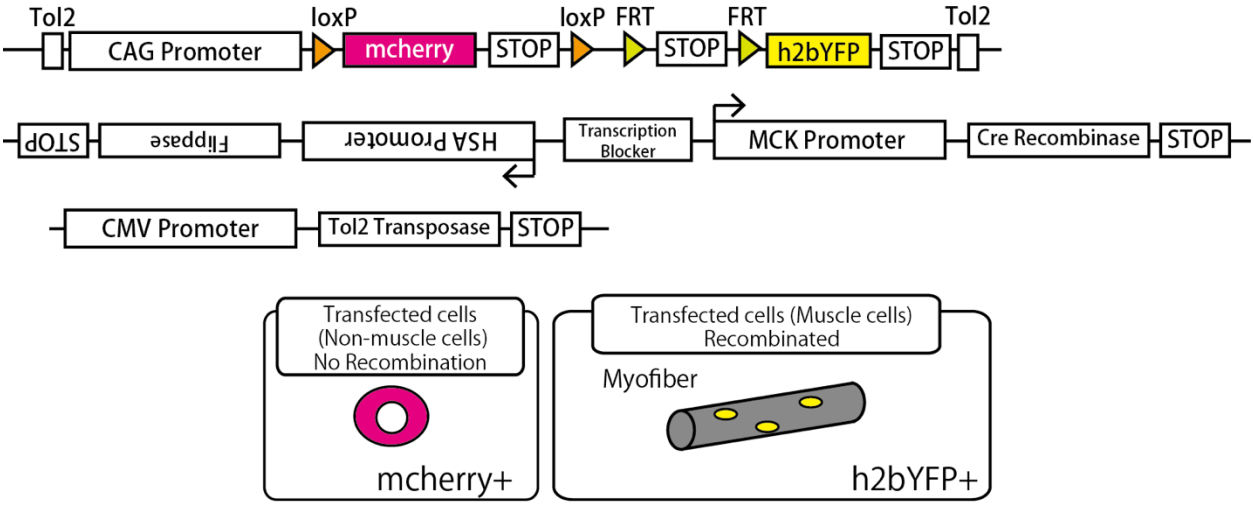

Figure 2.11 – Muscle lineage labeling strategy

Table 2.1 – Count of YFP cells in P3 and P14 jerboa feet

Age	Foot #	YFP muscle	YFP non-muscle	Age	Foot #	YFP muscle	YFP non-muscle
P3	1	10	1	**P14**	1	0	0
	2	0	0		2	0	0
	3	0	0		3	1	18
	4	2	0		4	1	1
	5	0	0		5	0	0
	6	4	0		6	0	2
	7	0	0		7	0	0
	8	1	1		8	2	0
	9	3	1		9	2	0
	10	2	0		10	3	3
	11	1	0		11	0	0
	12	0	0		12	0	0
	13	7	0				
	14	1	0				
	15	0	0				
	16	0	0				
	17	1	1				
	18	0	0				
Total		**32**	**4**	**Total**		**9**	**24**

2.2.3 Jerboa foot muscles fail to mature

The absence of any clear indication of muscle cell death motivated us to re-evaluate muscle maturation at greater resolution in order to capture the earliest detectable signs of muscle cell loss. We collected transmission electron micrographs of jerboa hand and foot muscle at P0, P2, and P4. We identified criteria for three categories of maturation, as described previously [235–237], and two categories of degeneration. Category A cells (nascent) have pre-myofibrils with thick and thin filaments and poorly resolved Z-discs, but the M-lines and I-bands are not yet apparent (Figure 2.12A). In Category B cells (immature), Z-discs of myofibrils are better resolved, and M-lines and I-bands are apparent, but parallel sarcomeres are not in register (Figure 2.12B). The mature myofibrils of Category C cells have Z-lines that are aligned with one another (Figure 2.12C). In Category D cells (early degeneration), some sarcomeres appear similar to Category A, but other areas of the cell contain disorganized filaments (Figure 2.12D). Category E cells (late degeneration) include those in the worst condition where less than half of the cell has any recognizable sarcomeres, and much of the cytoplasm is filled with pools of disorganized filaments and Z-protein aggregates (Figure 2.12E). Additionally, Category D and E cells have membrane-enclosed vacuoles and large lipid droplets (Figure 2.13). However, consistent with a lack of evidence for cell death, none of these cells or their organelles appear swollen, nuclear morphology appears normal, plasma membranes seem to be contiguous, and we do not observe an accumulation of autophagic vesicles that typically characterize cell death associated with unregulated autophagy [189–191].

We then coded and pooled all images of hand and foot myofibers from P0, P2, and P4 jerboas and blindly assigned each cell to one of the five categories. Quantification of the percent of myofibers in each category after unblinding revealed the progressive maturation of jerboa hand myofibers and the progressive degeneration of jerboa foot myofibers (Figure 2.12F). Compared to later stages, there is little difference in the maturation state of hand and foot sarcomeres at birth. Loss of ultrastructural integrity is therefore initiated perinatally, prior to complete myofibril maturation in the jerboa foot.

Our analysis of transmission electron micrographs also revealed the presence of filamentous aggregates that we did not include in our quantifications because they are enucleate, lack all other recognizable organelles, and are not bounded by a plasma membrane. Although these aggregates do not appear to be cellular, they are always closely associated with cells of a fibroblast morphology, and most lie between remaining myofibers in a space we presume was also once occupied by a myofiber (Figures 2.12G,H). To determine if these unusual structures contain muscle protein, we performed immunofluorescence on sections of P4 jerboa foot muscle and found similar aggregates of intensely fluorescent immunoreactivity to skeletal muscle myosin heavy chain. We also found that the surrounding cells, which correlate with the positions of fibroblasts in electron micrographs, express the intracellular pro-peptide of Collagen I (Figure 2.12I), the major component of tendon and other fibrous connective tissues and of fibrotic tissue after injury [238].

Given the apparent deterioration of nascent sarcomeres, we asked whether individual sarcomere proteins are lost from myofibrils in a temporal order or if proteins

disassemble simultaneously. We assessed the organization of sarcomere proteins by multicolor immunofluorescence at P0, P2, and P4. Alpha-Actinin, Desmin, Myomesin, Myosin, Titin, and Tropomyosin are each localized to an ordered series of striations in a subset of myofibers suggesting all are initially incorporated into immature sarcomeres (Figure 2.14A and Tables 2.2-2.6). By assessing all combinations of immunologically compatible primary antibodies, we identified populations of cells where Desmin was no longer present in an ordered array, but each of the other proteins appeared properly localized to the sarcomere (Figure 2.14B and Table 2.3). Although we could not distinguish such clear categories of mislocalization for each protein relative to all others, we inferred a relative timeline whereby Desmin disorganization is followed together by Myosin and Tropomyosin, then Titin, and lastly Myomesin and α-Actinin (Figures 2.14B-F and Tables 2.2-2.6).

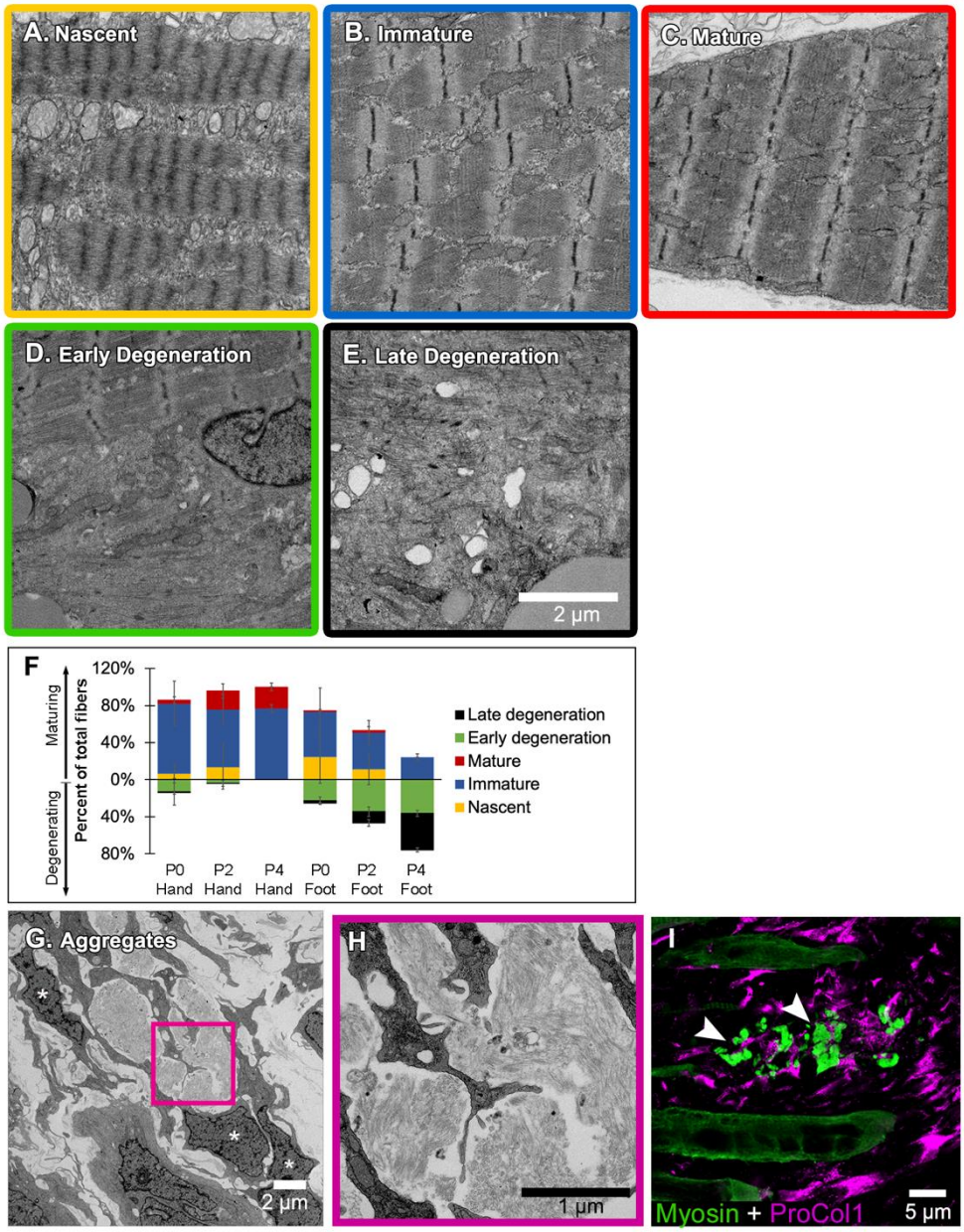

Figure 2.12 - Jerboa foot myofibers degenerate after birth

(A to C) TEM of representative jerboa hand myofibers illustrating categories (A) nascent, (B) immature, and (C) mature. (D and E) TEM of Representative jerboa foot myofibers illustrating categories (D) early degeneration and (E) late degeneration. Scale bar in E is also for A to D.

(F) Mean percentage and standard deviation of myofibers in each category in jerboa P0, P2, P4 hand and foot muscles. Number of myofibers pooled from three animals at each stage: hand – (P0), n=135; (P2), n=195; (P4), n=184 (P4); foot – (P0), n=186; (P2), n=193; (P4), n=186.

(G) TEM of filamentous aggregates and surrounding fibroblast-like cells (asterisks) observed in jerboa feet. (H) Higher magnification image of myofibril aggregates in F. (I) Pro-Collagen I positive cells surround skeletal muscle myosin aggregates (arrowheads) in jerboa feet.

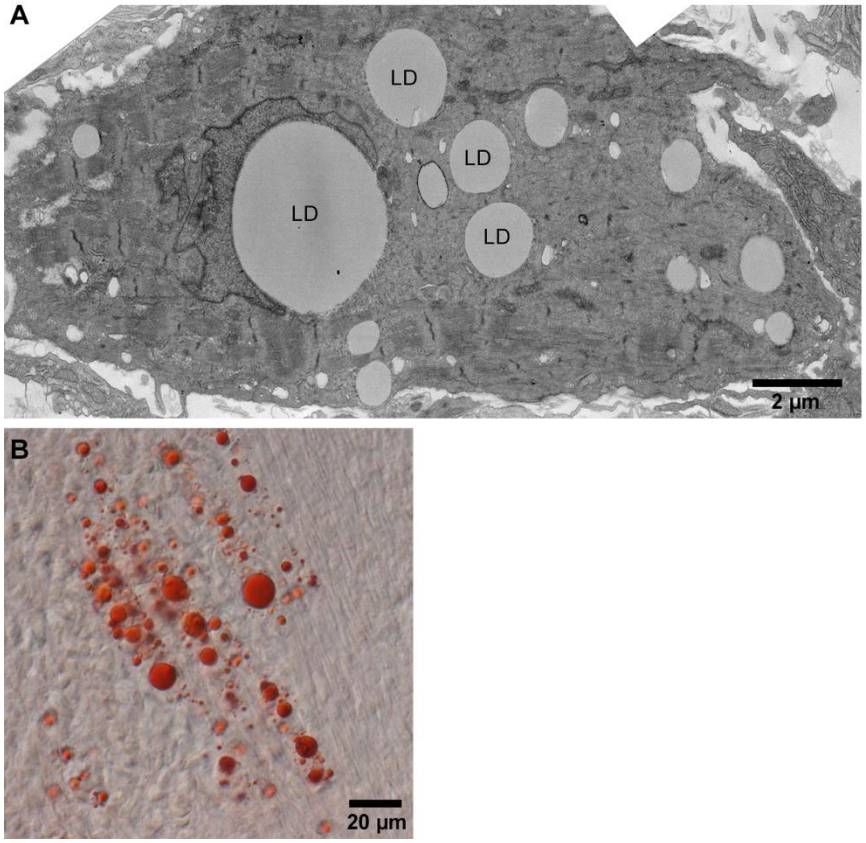

Figure 2.13 – Jerboa foot muscle contains large lipid droplets
(A) TEM and (B) Oil red O stained representative images of P4 jerboa foot muscles confirms presence of large lipid droplets. LD in (A) denotes each lipid droplet.

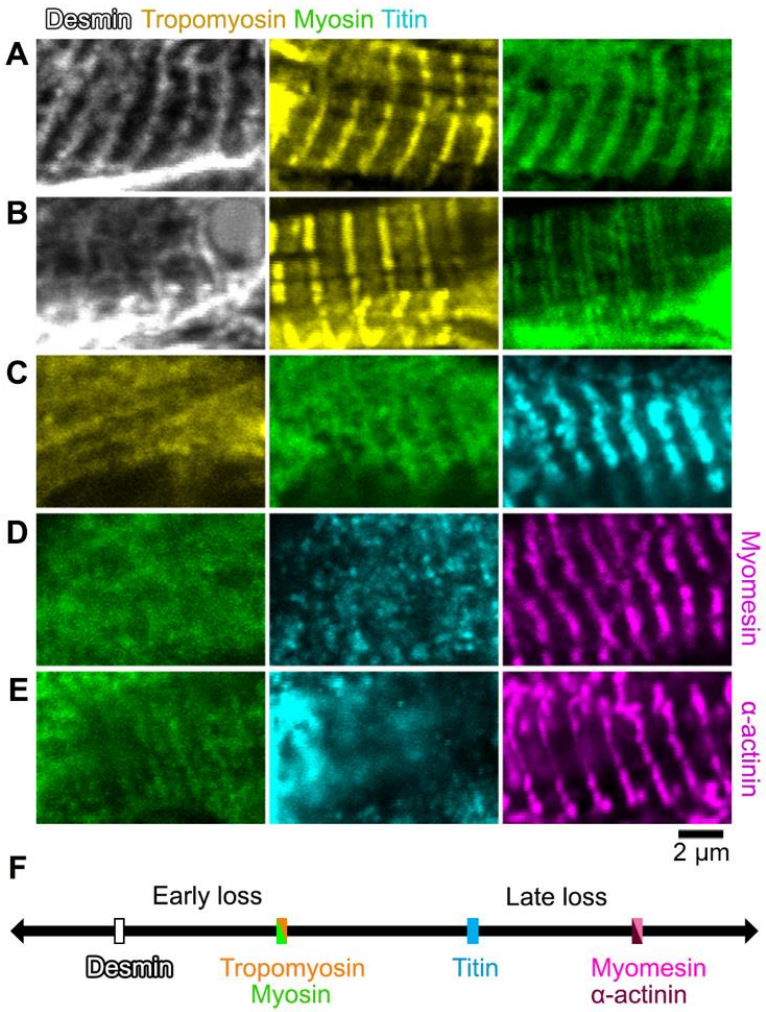

Figure 2.14 - Sarcomere disorganization in jerboa foot muscles
(A to E) Multicolor immunofluorescence images of sarcomere protein organization in P4 jerboa foot muscles (representative of 704 myofibers from seven P4 animals).
(F) Model of the interpreted order of sarcomere protein disorganization derived from Tables S2.2-2.6.

Table 2.2 - Information extracted from multicolor immunofluorescence of individual myofibers to infer the order of sarcomere protein disorganization in jerboa foot muscles

"Good" represents striated localization of each protein to the sarcomere, and "bad" refers to no distinguishable banded pattern of protein expression. In group 1, we saw myofibers with all three proteins properly localized suggesting disorganization follows an initial state of proper localization. When we compared the dRM and Drm categories, we saw loss of Desmin localization when Tropomyosin and Myosin were "good" and almost no myofibers where Desmin was good and the others were bad. This suggests that Desmin is disorganized prior to Tropomyosin and Myosin. In group 2a, there were cells in the rmT category and almost none in the RMt category, suggesting Tropomyosin and Myosin are disorganized prior to Titin. Group 2b illustrates that both categories RmT and rMT appeared at similar frequency, suggesting it is unclear whether Tropomyosin or Myosin become disorganized prior to the other. In group 3, there were cells in the mtA category and none in the MTa category, suggesting Titin becomes disorganized before Alpha-actinin. Similarly, in group 4, there were cells in the mtY category but not in the MTy category suggesting Titin becomes disorganized before Myomesin. Due to shared antibody isotype for Alpha-actinin and Myomesin, the order of disorganization between these two could not be discerned. See Table S2-5 for full details of the percentage of myofibers in each category for each combination of multicolor immunofluorescence.

Key			**Jerboa foot muscles**		
D = Good Desmin			**P0**	**P2**	**P4**
d = Bad Desmin	Group 1	**DRM**	63% ± 26%	23% ± 26%	17% ± 1%
R = Good Tropomyosin		**dRM**	10% ± 2%	5% ± 6%	31% ± 6%
r = Bad Tropomyosin		**Drm**	0	2% ± 3%	0
M = Good Myosin	Group 2a	**rmT**	8% ± 7%	7% ± 7%	23% ± 9%
m = Bad Myosin		**RMt**	1% ± 3%	0	0
T = Good Titin	Group 2b	**RmT**	4% ± 2%	1% ± 3%	17%16%
t = Bad Titin		**rMT**	15% ± 18%	26% ± 11%	12% ± 15%
A = Good α-actinin	Group 3	**mtA**	0	25% ± 21%	25% ± 18%
a = Bad α-actinin		**MTa**	0	0	0
Y = Good Myomesin	Group 4	**mtY**	5% ± 4%	36% ± 18%	27% ± 16%
y = Bad Myomesin		**MTy**	0	0	0

Table 2.3 - Percentage of myofibers in each category for Desmin, Tropomyosin, Myosin, and Titin multicolor immunofluorescence of jerboa hand and foot muscles at three postnatal stages

For the combination of Desmin, Tropomyosin and Myosin: P0 (2 animals) hand n=78 myofibers and foot n=113 myofibers; P2 (2 animals) hand n=56 and foot n=54 myofibers; P4 (2 animals) hand n=69 and foot n=117 myofibers. For the combination of Desmin, Myosin, and Titin: P0 (2 animals) hand n=48 and foot n=96 myofibers; P2 (2 animals) hand n=71 and foot n=77 myofibers; P4 (2 animals) hand n=63 and foot n=92 myofibers.

Key	**Stain: Desmin, Tropomyosin, Myosin**						
D = Good Desmin		**Hand muscles**			**Foot muscles**		
d = Bad Desmin		**P0**	**P2**	**P4**	**P0**	**P2**	**P4**
R = Good Tropomyosin	**DRM**	94% ± 1%	87% ± 2%	96% ± 1%	63% ± 26%	23% ± 26%	17% ± 1%
r = Bad Tropomyosin	**drm**	4% ± 2%	5% ± 7%	0	16% ± 14%	48% ± 15%	36% ± 4%
M = Good Myosin	**dRM**	0	4% ± 5%	4% ± 1%	10% ± 2%	5% ± 6%	31% ± 6%
m = Bad Myosin	**drM**	2% ± 3%	0	0	9% ± 13%	7% ± 10%	7% ± 9%
	dRm	0	4% ± 5%	0	2% ± 0%	6% ± 9%	9% ± 13%
	Drm	0	0	0	0	2% ± 3%	0
	DrM	0	0	0	1% ± 0%	5% ± 6%	0
	DRm	0	0	0	0	5% ± 7%	0
Key	**Stain: Desmin, Myosin, Titin**						
D = Good Desmin		**Hand muscles**			**Foot muscles**		
d = Bad Desmin		**P0**	**P2**	**P4**	**P0**	**P2**	**P4**
M = Good Myosin	**DMT**	90% ± 14%	82% ± 13%	95% ± 4%	32% ± 9%	11% ± 15%	7% ± 5%
m = Bad Myosin	**dmt**	0	7% ± 6%	2% ± 3%	26% ± 13%	47% ± 10%	21% ± 23%
T = Good Titin	**dMT**	2% ± 2%	7% ± 4%	3% ± 1%	33% ± 7%	33% ± 23%	33% ± 18%
t = Bad Titin	**dmT**	8% ± 11%	0	0	10% ± 3%	2% ± 3%	38% ± 1%
	dMt	0	0	0	0	6% ± 8%	0
	Dmt	0	0	0	0	0	0
	DmT	0	1% ± 2%	0	0	0	0
	DMt	0	3% ± 4%	0	0	1% ± 2%	0

Table 2.4 - Percentage of myofibers in each category for Tropomyosin, Myosin, and Titin multicolor immunofluorescence of jerboa hand and foot muscles at three postnatal stages

P0 hand (3 animals; n=125 myofibers) and foot (4 animals; n=225 myofibers); P2 (4 animals) hand n=118 and foot n=183 myofibers; P4 (3 animals) hand n=104 and foot n=172 myofibers.

Key	Stain: Tropomyosin, Myosin, Titin						
R = Good Tropomyosin r = Bad Tropomyosin M = Good Myosin m = Bad Myosin T = Good Titin t = Bad Titin		**Hand muscles**			**Foot muscles**		
		P0	**P2**	**P4**	**P0**	**P2**	**P4**
	RMT	66% ± 30%	72% ± 25%	91% ± 7%	45% ± 33%	15% ± 21%	24% ± 17%
	rmt	6% ± 4%	5% ± 5%	2% ± 4%	18% ± 13%	48% ± 12%	24% ± 5%
	rMT	14% ± 25%	23% ± 27%	3% ± 5%	20% ± 19%	24% ± 11%	12% ± 15%
	rmT	0	0	0	8% ± 7%	7% ± 7%	23% ± 9%
	rMt	4% ± 5%	0	0	1% ± 2%	5% ± 9%	0
	Rmt	3% ± 2%	0	0	2% ± 4%	0	0
	RmT	5% ± 9%	0	4% ± 4%	3% ± 3%	2% ± 4%	17% ± 16%
	RMt	2% ± 4%	0	0	1% ± 3%	0	0

Table 2.5 - Percentage of myofibers in each category for Myosin, Titin, and Alpha-actinin multicolor immunofluorescence of jerboa hand and foot muscles at three postnatal stages

P0 hand (3 animals) n=156 and foot n=182 myofibers; P2 (4 animals) hand n=189 and foot n=203 myofibers; P4 hand (3 animals; n=104 myofibers) and foot (4 animals; n=172 myofibers).

Key	Stain: Myosin, Titin, α-actinin						
M = Good Myosin m = Bad Myosin T = Good Titin t = Bad Titin A = Good α-actinin a = Bad α-actinin		Hand muscles			Foot muscles		
		P0	P2	P4	P0	P2	P4
	MTA	76% ± 1%	84% ± 17%	93% ± 6%	55% ± 23%	27% ± 28%	17% ± 3%
	mta	10% ± 5%	9% ± 13%	2% ± 4%	17% ± 9%	38% ± 32%	34% ± 12%
	mTA	12% ± 6%	3% ± 4%	3% ± 3%	12% ± 6%	6% ± 8%	23% ± 15%
	mtA	1% ± 1%	3% ± 3%	2% ± 3%	0	25% ± 21%	25% ± 18%
	mTa	0	0	0	0	0	0
	Mta	0	0	0	0	0	0
	MtA	1% ± 1%	1% ± 2%	0	16% ± 13%	4% ± 3%	1% ± 2%
	MTa	0	0	0	0	0	0

Table 2.6 - Percentage of myofibers in each category for Myosin, Titin, Myomesin multicolor immunofluorescence of jerboa hand and foot muscles at three postnatal stages

P0 (3 animals) hand n=130 and foot n=159 myofibers; P2 (3 animals) hand n=126 and foot n=142 myofibers; P4 hand (3 animals; n=98 myofibers) and foot (4 animals; n=164 myofibers).

Key	Stain: Myosin, Titin, Myomesin						
M = Good Myosin m = Bad Myosin T = Good Titin t = Bad Titin Y = Good Myomesin y = Bad Myomesin		Hand muscles			Foot muscles		
		P0	P2	P4	P0	P2	P4
	MTY	100%	82% ± 9%	95% ± 9%	83% ± 7%	29% ± 12%	11% ± 10%
	mty	0	3% ± 1%	2% ± 4%	3% ± 5%	19% ± 10%	22% ± 9%
	mTY	0	10% ± 12%	2% ± 4%	9% ± 5%	13% ± 19%	24% ± 27%
	mtY	0	3% ± 6%	1% ± 2%	5% ± 4%	36% ± 18%	27% ± 16%
	mTy	0	0	0	0	0	0
	Mty	0	0	0	0	0	0
	MtY	0	1% ± 2%	0	0	4% ± 6%	16% ± 22%
	MTy	0	0	0	0	0	0

2.2.4 The ubiquitin proteasome plays an important role in muscle loss

Desmin forms a filamentous network that connects parallel sarcomeres to one another and coordinates myofibril contraction [156–158]. Mutations that cause desminopathies illustrate that Desmin is essential to maintain sarcomere integrity [239]. In mouse models of muscle atrophy triggered by fasting or denervation, phosphorylation of Desmin removes the protein from the sarcomere and targets it for ubiquitination and proteolytic degradation prior to degradation of other sarcomere proteins [240]. The observation that Desmin is the first of an ordered sarcomere disassembly in the jerboa foot may reflect targeted degradation of muscle proteins that is similar to muscle atrophy.

The ubiquitin proteasome system is the main pathway through which cellular proteins are degraded during muscle atrophy, and *MuRF1* E3 ubiquitin ligase and the Cullin-1 linked *Atrogin-1* substrate adaptor are among the ‘atrogenes’ that are highly upregulated [170,171]. To test the hypothesis that muscle loss in the jerboa foot exhibits molecular hallmarks of atrophy, we performed quantitative reverse transcriptase PCR (qRT-PCR) of *MuRF1* and *Atrogin-1* mRNA from intrinsic foot muscles and the *flexor digitorum superficialis* (FDS) of the mouse and jerboa. The FDS, which originates in the autopod during embryogenesis and translocates to the forearm [241], is the most easily dissected of the analogous forelimb muscles and serves as a control for typical muscle maturation in both species. When normalized to expression in the FDS at birth of each species, *Atrogin-1* expression is 3.1-fold higher in the jerboa foot at P3 (Figure 2.15A). *MuRF1* mRNA expression is already significantly elevated at birth and remains elevated at P3 (Figure 2.15B).

The NF-κB pathway can function as an upstream regulator of the ubiquitin proteasome system in skeletal muscle. Muscle-specific transgenic activation of NF-κB causes severe muscle atrophy and increases *MuRF1* expression [193,197]. To lend further support to the hypothesis that jerboa foot muscle loss involves an 'atrophy-like' mechanism, we performed qRT-PCR of *NF-κB2* and its binding partner, *Relb.* We observed that each gene is expressed greater than three-fold higher in jerboa foot at birth and at P3 (Figure 2.15C,D). The progressively disordered ultrastructure of the sarcomere that begins with loss of Desmin localization, the increased expression of multiple atrogenes including *Atrogin-1* and *MuRF1*, and the lack of evidence for cell death or macrophage infiltration are consistent with observations of atrophying muscle in mice and rats [240,178,242,243].

Despite these similarities to muscle atrophy, myofiber loss in the jerboa foot does not seem to be simply explained by an atrophic response to denervation. First, and in contrast to the rapid rate of jerboa foot myofiber loss, chronic denervation in mice (100 days after nerve transection at P14) reduced the size but not the number of individual myofibers [244]. Additionally, we found that the post-synaptic Acetylcholine Receptor (AchR) exclusively coincides with the presynaptic neuronal protein, Synaptophysin, in neonatal jerboa foot muscles (Figure 2.16). In the mouse, AchR clusters are present in a broad domain of fetal muscle prior to innervation and are refined to nerve terminals in response to chemical synapse activity before birth [93]. The refinement of AchR clusters in jerboa foot muscles suggests that the muscles are not only innervated at birth but are also responsive to motor terminals.

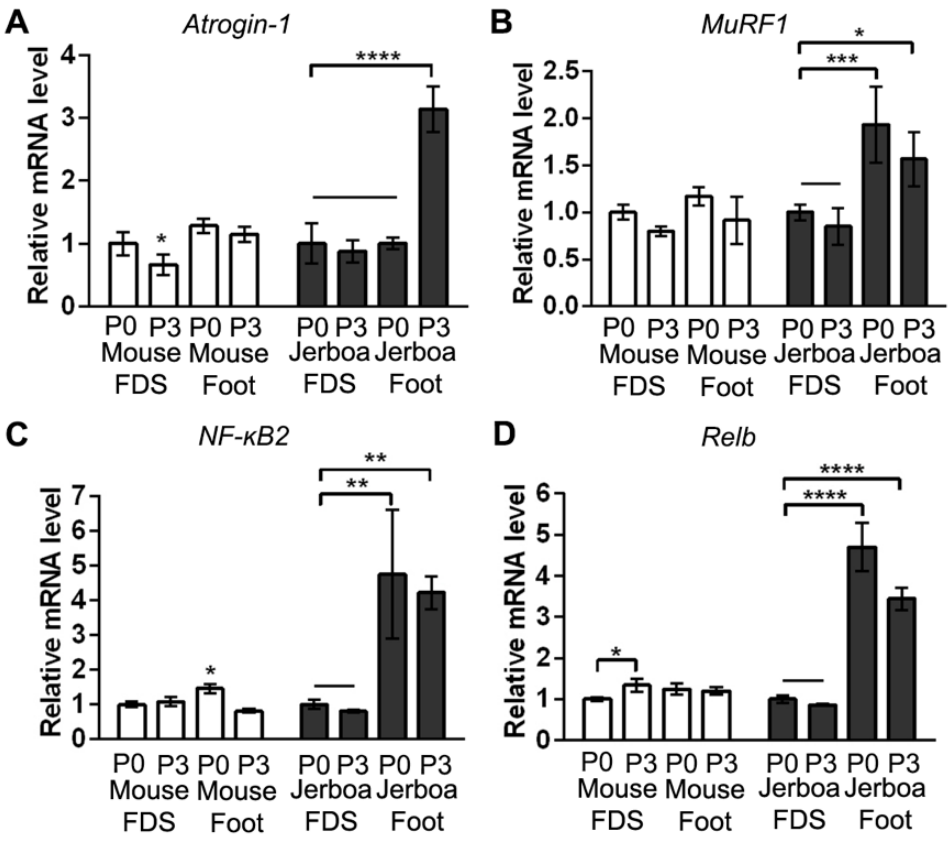

Figure 2.15 – Upregulation of UPS pathway suggests an 'atrophy-like' mechanism of jerboa foot muscle loss

(A and B) RT-qPCR measurements of (A) *Atrogin-1/MAFbx* and (B) *MuRF1* mRNA normalized to *SDHA*. Fold-change and standard deviations are expressed relative to the mean for P0 forearm muscle (FDS) of the same species. Mouse P0 FDS (n=5), foot (n=4); mouse P3 FDS (n=3), foot (n4); jerboa P0 FDS (n=6), foot (n=5); jerboa P3 FDS (n=4), foot (n=6). In A: *p=0.0203, ****p<0.0001. In B: *p=0.0125, ***p=0.0002.

(C and D) RT-qPCR measurements of (C) *NF-κB2* and (D) *Relb* mRNA normalized to *SDHA*. Fold-change and standard deviations are expressed relative to the mean for P0 forearm muscle (FDS) of the same species. Mouse P0 FDS (n=4), foot (n=3); mouse P3 FDS & foot (n=3); jerboa P0 FDS & foot (n=3); jerboa P3 FDS & foot (n=4). In C: *p=0.0112, ****p<0.0001. In D: *p=0.0473, **p=0.0017 & p=0.0032.

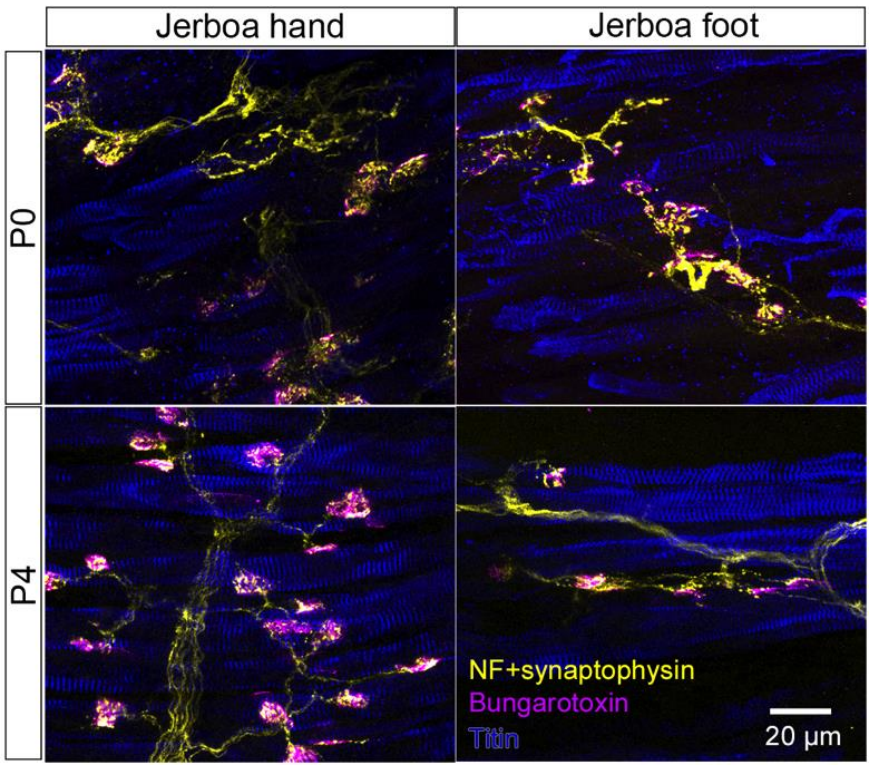

Figure 2.16 – Jerboa foot muscles are innervated
Representative longitudinal multicolor immunofluorescence images of P0 and P4 jerboa hand and foot muscles with correlated expression of the presynaptic neuronal protein, Synaptophysin, and post-synaptic Acetylcholine Receptor (AchR) (P0: n=4 animals, P4: n=5 animals).

2.3 Discussion

The natural process of muscle loss in the jerboa foot is surprising in the context of what is known about muscle development and pathology. Although we found multinucleated myofibers in the feet of neonatal jerboas, all muscle protein expression rapidly disappears from the jerboa foot shortly after birth. We were perplexed to find no evidence of apoptotic or necrotic cell death by a variety of assays and throughout the time when muscle cells are lost, nor did we observe macrophages that are commonly recruited to clear the remains of dying cells. Instead, we saw structural and molecular similarities to muscle atrophy, though atrophy in young mice leads to reduced myofiber size rather than number as in the jerboa [244,245]. The rapid and complete loss of myofibers in the neonatal jerboa foot does not appear to simply reflect a species-level difference in the animal's generalized response to disuse atrophy, since hindlimb denervation and immobilization in adults causes gradual loss of muscle mass, primarily through a significant reduction in the diameter of individual myofibers [246,247]. These observations are very similar to what has been shown in disuse atrophy models in mice and in rats [178,248] and differ from what we see in the neonatal foot.

Why would an embryo expend energy to form muscles that are almost immediately lost? The formation and subsequent loss of intrinsic foot muscles in jerboas, which also occurs in hooved animals [210], may simply reflect a series of chance events in each lineage with no fitness cost, or these similarities in multiple species may reveal true developmental constraints. Muscle is not required for autopod tendon formation or maintenance in mice, but the tendons that develop in a muscle-less or a paralyzed mouse are thinner and less well organized [249]. It is therefore possible

that muscle is initially required in the fetus and neonate for tendons to establish sufficient architecture from origin to insertion so that the tendon, after further growth, can withstand high locomotor forces in the adult [214,215].

Regardless of whether these nascent muscles serve an essential purpose, we are left wondering what is the ultimate fate of jerboa foot myofibers. If these cells do indeed die, perhaps death is too rapid for detection. However, programmed cell death is thought to occur over hours or even days from the initial trigger to the final corpse [250]. Alternatively, death may result from a mechanism that does not proceed through DNA fragmentation, plasma membrane permeability, macrophage recruitment, or stereotyped ultrastructural changes, and yet this would seem to eliminate most known forms of regulated cell death [251].

Alternatively, multinucleated myofibers may transform to another cellular identity after degrading all sarcomere proteins. Although a fate transformation would be surprising, it would not be without precedent. The electric organ of fish that can produce an electric field (e.g. knifefish and elephant fish) is thought to be derived from skeletal muscle. Electrocytes of *Sternopygus macrurus* express skeletal muscle Actin, Desmin, and α-Actinin, and electrocytes of *Paramormyrops kingsleyae* retain sarcomeres that are disarrayed and non-contractile [85,86]. If myofibers in the jerboa foot indeed transdifferentiate, it is possible they transform into the pro-Collagen I positive fibroblasts that are entangled with the filamentous aggregates, though these could also be phagocytic fibroblasts recruited to consume the enucleate detritus without stimulating inflammation [252–255]. Unfortunately, the lineage labeling approaches required to

track the ultimate fate of jerboa myofibers are exceptionally challenging in this non-traditional animal model.

It is clear, however, that regardless of the ultimate fate of jerboa foot myofibers, their path passes through a phase marked by cell biology that is typical of atrophy, including the ordered disassembly of sarcomeres and expression of the E3 ubiquitin ligases, *MuRF1* and *Atrogin-1*. However, skeletal muscle atrophy is typically associated with pathology in the context of disuse, nerve injury, starvation, or disease. In this context, we were struck by a statement in the 1883 anatomical description of the fetal and adult suspensory ligament of four species of hooved mammals: “It is an instance of *pathological* change assisting a *morphological* process” (emphasis his) [210]. Indeed, there are remarkable similarities in the histology of jerboa and horse foot muscle compared to human clinical observations of tissue remodeling that follows rotator cuff tear characterized by muscle atrophy, myofiber loss, and fibrosis [211,256].

Foot muscle atrophy in the jerboa may be one of many cellular responses associated with injury or disease in humans that is utilized in the normal development and physiology of other species. These data suggest that there is less of a clear divide between natural and pathological states than typically thought. Studies of non-traditional species may not only reveal the mechanisms of evolutionary malleability, but may also advance our understanding of fundamental biological processes that are typically associated with pathological conditions.

2.4 Materials and Methods

2.4.1 Animals

Jerboas were housed and reared as previously described [257]. CD1 mice were obtained from Charles River Laboratories (MA, USA), housed in standard conditions, and fed a breeder's diet. All animal care and use protocols for mice and jerboas were approved by the Institutional Animal Care and Use Committee (IACUC) of the University of California, San Diego.

2.4.2 Antibodies

The following primary antibodies and dilutions were used for immunofluorescence of tissue sections: Col1A1 (SP1.D8, 1:20), Dystroglycan (11H6C4, 1:10), Myosin heavy chain (MF20, 1:20), Myomesin (B4, 1:20), Myogenin (F5D, 1:5), Titin (9D10, 1:10), Tropomyosin (CH1, 1:10), Developmental Studies Hybridoma Bank; Desmin (D33, 1:300), α-actinin (EA-53, 1:1000), Sigma Aldrich; Annexin-V (ab14196, 1:100), Desmin (ab8592, 1:500), CD45 (ab10558, 1:200), F4/80 (ab6640, 1:200), Abcam; Cleaved Caspase-3 (Asp175) (#9661, 1:100), Cell Signaling Technologies; Alexa 488 conjugated Wheat Germ Agglutinin (W11261, 1:200), Invitrogen; BrdU (MCA2060, 1:100), Biorad.

Secondary antibodies were obtained from Invitrogen and used at 1:250 dilution: Alexa Fluor 594 conjugated goat anti-mouse IgG2b, Alexa Fluor 488 or 647 conjugated goat anti-mouse IgG1, Alexa Fluor 488 conjugated goat anti-mouse IgM, Alexa Fluor donkey anti-mouse IgG, Alexa Fluor 488 conjugated goat anti-rat IgG, Alexa Fluor 488 or 647 conjugated goat anti-rabbit.

2.4.3 Immunofluorescence and TUNEL

Mouse and jerboa limbs were dissected and fixed in 4% PFA in 1x PBS overnight. Tissues were washed in 1X PBS twice for 20 min and placed in 30% sucrose

in 1x PBS overnight at 4 degrees Celsius. Tissues were then mounted in a cryomold in OCT freezing media, and blocks were frozen and stored at -80°C until cryosectioned. Blocks were sectioned at 12 µm thickness, and sections were transferred to Super-Frost Plus slides (Thermo Fisher). For immunofluorescence, slides were washed for 5 min in 1x PBS and subject to antigen retrieval by incubation in Proteinase K (5 µg/mL) for 10 min followed by 5 min postfix in 4% PFA in PBS and three washes in 1x PBS. Slides were then blocked in a solution of 5% heat inactivated goat serum, 3% Bovine Serum Albumin, 0.1% TritonX-100, 0.02% SDS in PBS. Slides were incubated in the appropriate primary antibody dilution in block overnight at 4°C. On the second day, slides were washed three times for 10 minutes in PBST (1x PBS + 0.1% TritonX-100) and incubated at room temperature in secondary antibodies and 1 µg/ml DAPI for one hour. Slides were then washed three times for 10 minutes in PBST and mounted in Fluoro Gel with DABCO (EMS).

For TUNEL, slides that had been previously processed for MF20 immunofluorescence were placed immediately into the TUNEL reaction mixture following manufacturer's instructions (Roche In Situ Cell Death Detection Kit, TM-Red) for 60 min at 37°C, rinsed three times in 1x PBS, and mounted in Fluoro Gel with DABCO.

Sections were imaged with Olympus compound microscope model BX61, Leica SP5 confocal, or Olympus FV1000 confocal.

2.4.4 Myofiber count

Blocks containing embedded mouse or jerboa feet were cryosectioned at 12µm thickness in transverse orientation onto two serial sets of slides. Slides of the second

series were used as back up in case certain sections of the first series contain folded tissue and thus cannot be used. Slides of the first series were stained with MF20 & WGA and analyzed to locate the proximal and distal ends of the third interosseous muscle. Using this information we estimated the middle area of each muscle and selected 10 sections for subsequent analysis. We analyzed the third interosseous muscle of the hindlimb, spanning approximately 240 μm in muscle length. For each selected section, all cross-sectionally oriented myofibers were manually counted and recorded using the plugin cell counter in ImageJ. The average number of myofibers from 10 sections represents an estimate of the myofiber number for the middle transverse section of the third interosseous muscle. For each developmental stage, data from three animals were collected, and one-way ANOVA with Tukey's multiple comparisons test was performed to determine the statistical significance of mean myofiber number differences between developmental stages in each species.

2.4.5 Myocyte fusion assay

BrdU solution was intraperitoneally injected to achieve 100 μg/g (BrdU/ animal body weight) in P0, P2, and P4 jerboas. Injected animals were sacrificed two days later. The feet and hands of each animal were fixed in 4% PFA/PBS overnight, processed through a sucrose series, and embedded in OCT freezing media. Blocks of embedded tissue were cryosectioned in transverse orientation at 12 μm thickness and placed in serial sets on Superfrost Plus slides. Slides were stained with BrdU and Dystroglycan antibodies as indicated above. As in the methods to count myofibers, we chose ten sections near the midpoint of the interosseous muscle associated with the third metatarsal and counted all BrdU+ nuclei within a Dystroglycan+ myofiber as well as all

myofiber nuclei in each section. Data is represented as the total number of BrdU+ myofiber nuclei divided by the total number of myofiber nuclei, and this ratio was averaged for all 10 sections in each animal. The data was plotted using Prism8 (GraphPad), and the statistical significance between datapoints at each time interval was calculated with one-way ANOVA with Tukey's multiple comparisons test in each of forelimb and hindlimb.

2.4.6 Short-term BrdU labeling

BrdU solution was intraperitoneally injected to achieve 100 μg/g (BrdU/ animal body weight) in P0, P2, and P4 jerboas. Injected animals were sacrificed two hours after injection. The feet and hands of each animal were fixed in 4% PFA/PBS overnight, processed through a sucrose series, and embedded in OCT freezing media. Blocks of embedded tissue were cryosectioned in transverse orientation at 12 μm thickness and placed in serial sets on Superfrost Plus slides. Slides were stained with BrdU and Myosin or BrdU, Laminin, and Dystroglycan antibodies as indicated above for assessment of proliferation in myonuclei. As in the methods of fusion assay, we chose ten sections near the midpoint of the interosseous muscle associated with the third metatarsal and counted all BrdU+ nuclei within a Laminin+ basal lamina and outside Dystroglycan+ myofiber membrane as well as number of Dystroglycan+ myofiber in each section. Data is represented as the total number of BrdU+ myofiber nuclei divided by the total number of myofiber, and this ratio was averaged for all 10 sections in each animal. The data was plotted using Prism8 (GraphPad), and the statistical significance between datapoints at each time interval was calculated with one-way ANOVA with Tukey's multiple comparisons test in each of forelimb and hindlimb.

2.4.7 Muscle stem/progenitor cell culture

Intrinsic foot muscles (*m. flexor digitorum brevis* and *m. interossei*) and lower leg muscles (*tibialis anterior* and *gastrocnemius*) were manually dissected from three animals of P1 jerboas and mice and pooled. After connective tissues were manually removed with forceps, muscle stem/progenitor cells were isolated and cultured as described in [258] Briefly, the tissues were enzymatically with 10 mg/ml Pronase (EMD Millipore) and mechanically dissociated. The cells were plated onto matrigel-coated 8-well chamber slides (Nunc Lab-Tek, Thermo fisher) coated with Matrigel (Corning) at 1×10^4 cells/well. The cells were cultured for 9 days with DMEM (Thermo Fisher), 20% fetal bovine serum (Thermo fisher), 10% horse serum (Thermo Fisher) and 1% chicken embryonic extract (Accurate Chemical). During the culture period, the medium was changed at day 3, 6, and 8. After 6 and 9 days, cells in replicate cultured wells were fixed with 4% PFA/PBS at 4℃ for 15 min and washed with PBS. After permeabilization with 1 % Triton-X 100 in PBS at room temperature for 10 min, the cells were blocked with 5% BSA/PBS for 30 min and stained with BrdU, anti-Myogenin and Myosin antibodies and secondary antibodies. At each time point of each experimental group, the total number of nuclei and nuclei within Myosin+ myofibers were counted in 10 images taken from 8 wells using the Olympus compound microscope at 4x magnification. The numbers in 10 images were averaged and the difference between day 6 and day 9 were statistically analyzed with paired sample t-test in each experimental group.

2.4.8 Evans Blue Dye

We injected Evans Blue Dye as 1% solution by animal body weight (1mg EBD/100µl PBS/10g) 24 hours prior to sample collection [226]. As a positive control for EBD uptake, we create an injured muscle area by inserting a 21-gauge needle 2-3 times into the jerboa gastrocnemius muscle. Samples were fresh frozen in OCT and cryosection at 12 µm thickness. Slides were processed for MF20 fluorescence with primary antibody incubation for 1 hr at RT before secondary antibody incubation. Slides were mounted for analysis: EBD signal is detected using the Cy5 filter and imaged using the Olympus compound microscope or imaged using the Leica SP5 confocal laser 633nm.

2.4.9 Oil red O (ORO) staining

ORO stock solution: 2.5 g of Oil red O to 400 ml of 99% (vol/vol) isopropyl alcohol and mix the solution by magnetic stirring for 2 h at room temperature (RT; 20–25 °C). ORO working solution: 1.5 parts of ORO stock solution to one part of deionized (DI). Cryosections were fixed with 4%PFA in 1x PBS for 5 minutes. Slides were washed with 2x with PBS for 10 minutes each and stained with ORO working solution for 10 minutes followed three 30 second washes with DI water. Slides were then washed in running tap water for 15 minutes followed by three 30 second washes with DI water and mounting in aqueous medium.

2.4.10 Transmission Electron Microscopy (TEM)

Animals were perfused with 2% glutaraldehyde and 2% PFA plus 2mM $CaCl_2$ in 0.15M sodium cacodylate buffer, pH 7.4 @ 35°C for 2-3 minutes. The hands and feet were removed, skinned, and fixed on ice for 2 hours. Samples were then rinsed six times for 5 min in cold 0.15M cacodylate buffer and then post-fixed in 1% OsO4 in

0.15M cacodylate buffer on ice for 1 hour. Samples were then rinsed in cold double distilled water (DDW) six times for 5 min and placed into 1% uranyl acetate in DDW on ice overnight. Fixed tissue was then rinsed in ice cold double distilled water three times for 3 min and dehydrated in an ethanol series (50%, 70%, 90% in DDW) on ice for 5 min each. Samples were further dehydrated into 100% ethanol twice for 5 min at room temperature and then transitioned to 1:1 ethanol:acetone for 5 min followed by two times 5 min in 100% acetone. Dehydrated samples were infiltrated with 1:1 acetone:Durcupan ACM resin for 1 hour at room temperature followed by 100% resin twice for 1 hour and then placed in fresh resin overnight. On the next day, samples were transferred to fresh resin, which was polymerized in a 60°C vacuum oven for 48-72 hours. Resin embedded samples were stored at room temperature until ready for sectioning. Seventy nanometer thick sections were stained in lead solution and image using Tecnai Spirit TEM scope (120 kV).

2.4.11 Lineage labeling

Parent plasmids, gift from Dr. Andrea Simons [259], were modified to contain: in one plasmid, the additional transcription blocker with human skeletal muscle Actin (HSA) promoter driving Flippase; in the other plasmid, FRT-STOP-FRT site. For in vivo electroporation of plasmids into muscles, animals were briefly anesthetized in saran wrap on ice. Using a Hamilton syringe affixed with a 23 gauge need, 1.5 ul of 2 mg/ml hyaluronidase (Sigma-Aldrich, H4272) was subcutaneously injected into the foot. Animals were placed in a warmer for an hour before injection of 1.5 µL of plasmid solution (5 µg DNA per µL 50%PBS solution). Ten minutes following DNA solution injection, we applied an electric current across the injection site using 0.25 mm needle

electrodes coupled to an electroporator (CUY21EDIT, BEX). Settings were 60 V (voltage); 20 ms (duration); 15 pulses (frequency). The conditions were modified based on a previously published protocol in skeletal muscle [260]. Electrical pulses were applied with the electrode needles perpendicular to the muscle fibers. Animals were return to the nest and collected at P4 and P14 for analysis.

2.4.12 Whole-mount in-situ hybridization

Probe generation and whole-mount in-situ hybridization was performed as previously described [261]. The following primers were used for probe cloning: mouseMyoD_F: CGGCTCTCTCTGCTCCTTT; mouseMyoD_R: CATGCCATCAGAGCAGTTGG; jerboaMyoD_F: GATGACCCGTGTTTCGACTC; jerboaMyoD_R: CGAGTCTCCGCTGTAGTGCT.

2.4.13 RNA isolation and quantitative reverse transcriptase polymerase chain reaction (qRT-PCR)

Foot muscles were dissected and stored in RNAlater solution (Thermo Fisher) at -80°C until ready for use. RNA extraction was performed using the PicoPure RNA Isolation Kit (Thermo Fisher) according to the manufacture instructions. RNA was reverse transcribed to generate cDNA using QuantiTect Reverse Transcription Kit. cDNA was used as template for quantitative PCR with PCR amplification detected with Sybr green (SYBR Green Real-time PCR master mixes, Invitrogen). See table 2.7 below for the sequences of primers used to quantify real time amplification. Each quantitative reverse transcriptase PCR experiment was conducted twice with technical triplicates in each experiment. Cq values that are significant outliers were determined using Grubb's test in GraphPad software and eliminated. Expression of

MuRF-1, *Atrogin-1, NF-κB2, and Relb* was normalized to *SDHA,* quantitation of gene expression was determined by the equation $2^{-\Delta\Delta CT}$, and the fold-change of mRNA expression was calculated relative to the mRNA level of P0 FDS samples in each species, which was set to 1. One-way ANOVA with Tukey's multiple comparisons test was performed to determine the statistical significance of fold change differences between samples in each species.

Table 2.7 – Primers used for qPCR

mouseMuRF1_F	TGCCTGGAGATGTTTACCAAGC	[262]
mouseMuRF1_R	AAACGACCTCCAGACATGGACA	[262]
mouseAtrogin_F	TGGGTGTATCGGATGGAGAC	[263]
mouseAtrogin_R	TCAGCCTCTGCATGATGTTC	[263]
jerboaMuRF1_F	CCGCGTGCAGACTATCATCA	
jerboaMuRF1_R	GCAGCTCGCTCTTTTTCTCG	
jerboaAtrogin_F	GCATCGCCCAAAAGAACTTCA	
jerboaAtrogin_R	ACTTGCCGACTCTTTGGACC	
mouseSDHA_F	GGAACACTCCAAAAACAGACCT	[264]
mouseSDHA_R	CCACCACTGGGTATTGAGTAGAA	[264]
jerboaSDHA_F	ACTGGAGGTGGCATTTCTAC	
jerboaSDHA_R	TTTTCTAGCTCGACCACAGATG	
mouseNF-κB2_F	GCCCAGCACAGAGGTGAAAG	
mouseNF-κB2_R	CATTCAGTGCACCTGAGGCT	
mouseRelb_F	TGTCACTAACGGTCTCCAGGAC	
mouseRelb_R	CAGGCGCGGCATCTCACT	
jerboaNF-κB2_F	CTAGCCCACAGACATGGACA	
jerboaNF-κB2_R	TAGGGGCCATCAGCTGTCTC	
jerboaRelb_F	CCTACAATGCTGGCTCTCTGA	
jerboaRelb_R	GTCATAGACAGGCTCGGACA	

2.5 Acknowledgement

I would like to acknowledge V. Fowler, S. Lange, A. Sacco, S. Ward, D. Gokhin and R. Nowak for advice and for sharing reagents. M. Ellisman, Director of the National Center for Microscopy and Imaging Research at UC San Diego (P41 GM103412), T. Deerinck, M. Mackey, and A. Thor provided assistance with transmission electron microscopy. Access to the Olympus FV1000 was provided by the UC San Diego School of Medicine Microsopy Core. H. Grunwald assisted with TUNEL staining. A. Mendelsohn provided advice on the assessment of muscle innervation, and Y. Cho advised us on mouse muscle denervation.

Chapter 2, in full, has been submitted for publication of the material. Tran, Mai P.; Tsutsumi, Rio; Erberich, Joel M.; Chen, Kevin D.; Flores, Michelle D.; and Cooper, Kim L. (2019). “Evolutionary loss of foot muscle during development with characteristics of atrophy and no evidence of cell death.” *Submitted.* The dissertation author was the primary investigator and author of this material.

CHAPTER 3. Transcriptomic characterization of muscle loss in the jerboa foot

3.1 Introduction

Muscle is highly versatile, capable of environmentally-induced changes and extraordinary evolutionary adaptions. Throughout development and growth, muscle is maintained by multiple pathways that regulate anabolic and catabolic processes. A classic hallmark of myopathies is the excessive loss of muscle mass, via muscle cell death and/or cellular shrinkage. While the result – loss of muscle – is the same in various myopathies, cellular characterization showed diseased muscle exhibits diverse pathologic states. The alterations to muscle include muscle fiber necrosis, loss of myofibrillar organization, increased number of central nuclei, fiber splitting, accumulation of fibrillar proteins and/or vacuoles, inflammatory infiltrates, and/or proliferation of fibrous connective tissue [265]. These abnormal cellular characteristics provide important clues about the underlying cause or cellular pathway affected. However, since the morphological abnormalities are diverse, it remains unclear whether seemingly different myopathies share any unifying characteristics and what is the extent of such commonalities.

The advent of genome and gene transcript sequencing revolutionized the field of muscle biology – not only identifying muscle-specific proteins but also redefining muscle disease based on genetics, thus paving the way for new therapeutic development. In addition, genetic analyses allow for assessment of evolutionarily conserved pathways in both muscle development and disease. For example, muscle atrophy is seen in various myopathies and in disorders such as cancer, diabetes, AIDS, disuse, etc. Transcriptomic comparison of normal and atrophic muscle identified muscle-specific E3

ligases, *MuRF1* and the Cullin-1 specific substrate adaptor *Atrogin-1*, as common factors in disparate atrophy conditions including immobilization, denervation, hindlimb unloading, and interleukin-1-induced cachexia [172]. Since then, additional research was undertaken to identify both upstream regulators (FoxO3 and NF-κB) and downstream targets (MyoD and several sarcomeric proteins) of these E3 ligases [193,266]. Such studies provide the basis for comparison of molecular signatures underlying muscle loss in pathological versus natural contexts.

The lesser Egyptian jerboa, *Jaculus jaculus*, is the most derived species of the family Dipodidea. The jerboa has hindlimb morphology adapted for bipedal locomotion in a sparsely vegetated desert environment – loss of intrinsic foot muscles, elongation, and fusion of the metatarsals. Research outlined in Chapter 2 described the cellular characterization of postnatal intrinsic foot muscle loss. I found no evidence of cell death – apoptosis nor necrosis. Instead muscles in the jerboa foot, while initially formed properly, failed to mature. Ultrastructural analysis showed disorganized sarcomeres, a common feature seen in all myopathies, without a distinct cellular phenotype similar to a specific muscle disorder.

Intriguingly, muscle loss in the jerboa foot is a natural process that shares characteristics with human skeletal muscle atrophy: early loss of Desmin followed by orderly loss of sarcomeric proteins and upregulation of the ubiquitin proteasome pathway. Considering the 20 million years of evolution since jerboas diverged from their last ancestor that may have had as many as 16 intrinsic muscles, it is likely that a complex network of genes with functions and interactions that were honed by millions of years of evolution, functions to bring about the disappearance of intrinsic foot muscles.

To identify candidate genes that may be important for initiating and driving the process of muscle loss in jerboa foot, we utilized RNA-sequencing to probe muscle transcriptome dynamics during this developmental period. We investigated the gene expression changes that are associated with the initiation of muscle loss in newborn animals to identify gene candidates that facilitate muscle loss. In addition, we evaluated, genome-wide, shared molecular signatures between disappearing jerboa foot muscles and established models of muscle loss to test the hypothesis that there are broad similarities between natural and pathological muscle loss.

These findings provide a novel platform to identified genes and pathways that reveal the targeted biological and signaling processes underlying the natural process of muscle loss in jerboa. In addition, transcriptomic comparison with established mouse-model of muscle dystrophy/atrophy serves as a useful resource for investigating the evolutionary relationship between processes involved in natural versus pathological muscle loss.

3.2 Results

3.2.1 General information and quality control of the data

Intrinsic foot muscles are absent in the adult jerboa but present at birth and are subsequent lost postnatally. The intrinsic foot muscles are those whose connections are located entirely within the foot and are responsible for movements of individual digits. Unlike the bigger and more easily dissected muscles of the leg (*tibialis anterior* and *gastrocnemius*), intrinsic foot muscles are very small, and there are few at birth, making it extremely difficult to manually collect muscle-enriched tissue for transcriptome

analysis. Thus, laser capture microdissection (LCM) was used to selectively collect the intrinsic foot muscles from newborn mouse and jerboa samples (Figure 3.1A). To identify gene expression differences that are specifically associated with muscle loss in the jerboa foot, the *flexor digitorum superficialis* (FDS) was used as a control for unrelated evolutionary divergence between mouse and jerboa species. The FDS, which originates in the autopod during embryogenesis and translocates to the forearm [267], is the most easily dissected of the analogous forelimb muscles.

Principal component analysis (PCA) and sample-to-sample distance demonstrate good segregation between experimental groups: jerboa hindlimb (JHL), jerboa forelimb (JFL), mouse hindlimb (MHL), mouse forelimb (MFL) (Figure 3.1B). PCA showed that the data is discriminated first by species and then by muscle type (Figure 3.1B). To compare the transcriptome profile of jerboa and mouse directly to one another, we used a 1:1 orthologous transcript annotation set (17,464 transcripts) containing at least one exon with no frameshift, missense, or nonsense mutation (unpublished data). Differentially expressed (DE) genes between different muscles were determined using DESeq2 package with added normalization for transcript length differences between the two species. Statistically significant differential expressed transcripts are defined as those with p-adjusted (padj)-value less than 0.05.

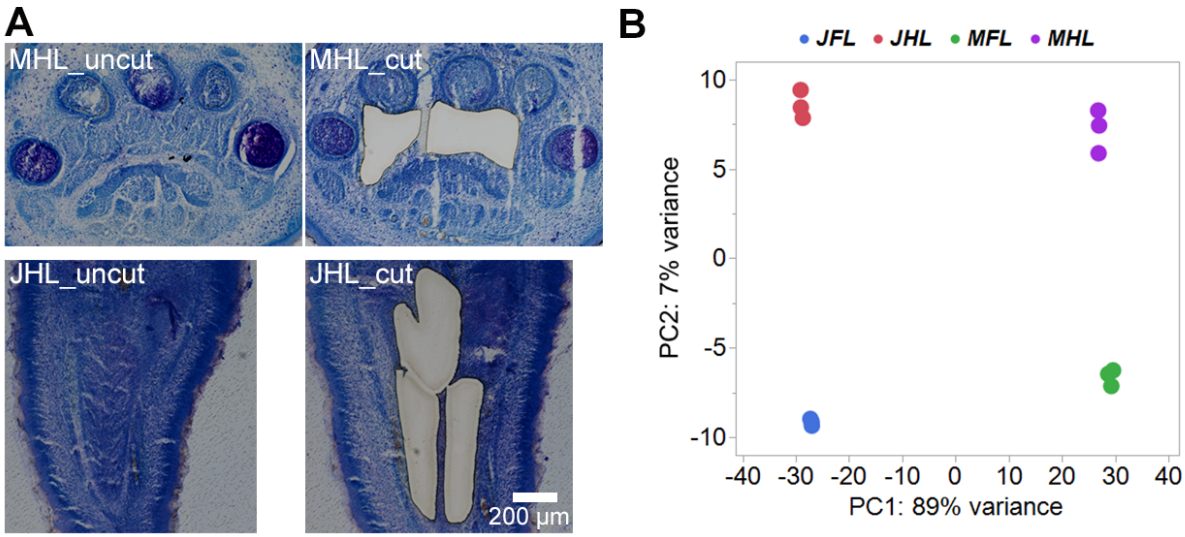

Figure 3.1 – Muscle tissue from LCM generate good quality data for transcriptome analysis

(A) Representative images showing area of tissue captured before and after LCM
(B) PCA analysis of RNA-seq data of new born mouse and jerboa SDF and foot muscles.
Jerboa hindlimb (JHL), jerboa forelimb (JFL), mouse hindlimb (MHL), mouse forelimb (MFL).

3.2.2 Transcriptome changes associated with the initiation of muscle loss

Previous research indicates large transcriptome diversity among skeletal muscle tissues within an individual, and the jerboa and mouse diverged from a common ancestor about 50 million years ago [268]. For these reasons, neither comparison to a different muscle within the same species nor comparison of the same muscle between species are sufficient on their own to identify genes associated with the evolutionary loss of jerboa foot muscle.

We began by identifying differentially expressed genes between homologous muscles (JHL:MHL and JFL:MFL). Of the 10,421 transcripts that differ between foot muscles (59.7% of orthologous genes), 8,661 were also differentially expressed between forelimbs. Given the 55 million years of evolutionary divergence between the two species and the fact that only foot muscles of the jerboa are lost, the 8,661 differentially expressed genes found in both HL and FL comparison most likely reflect the evolutionary divergence unrelated to muscle loss. This leaves 1,760 transcripts that are exclusively differentially expressed between the hindlimb muscles of the two species and not between their forelimb muscles.

We next reasoned that genes that are responsible for the evolutionary loss of foot muscle in the jerboa should also be differentially expressed between foot and forearm muscles within the species. Of the genes that differ between species in the foot, 1,165 transcripts are also found among the 8,273 DE transcripts of the JHL:JFL comparison (Figure 3.2A). We also expected that causative genes should be consistently higher or lower in jerboa foot muscle compared to the typical development of jerboa arm and mouse arm and foot muscle. Of the differentially expressed

transcripts that are common between the JHL:MHL and JHL:JFL analyses, 1,050 transcripts are differentially expressed in the same direction in both comparison – 520 transcripts are higher and 530 are lower (Figure 3.2B-D). These are candidate genes are associated with the initiation of foot muscle loss in the jerboa and were thus selected for further analysis.

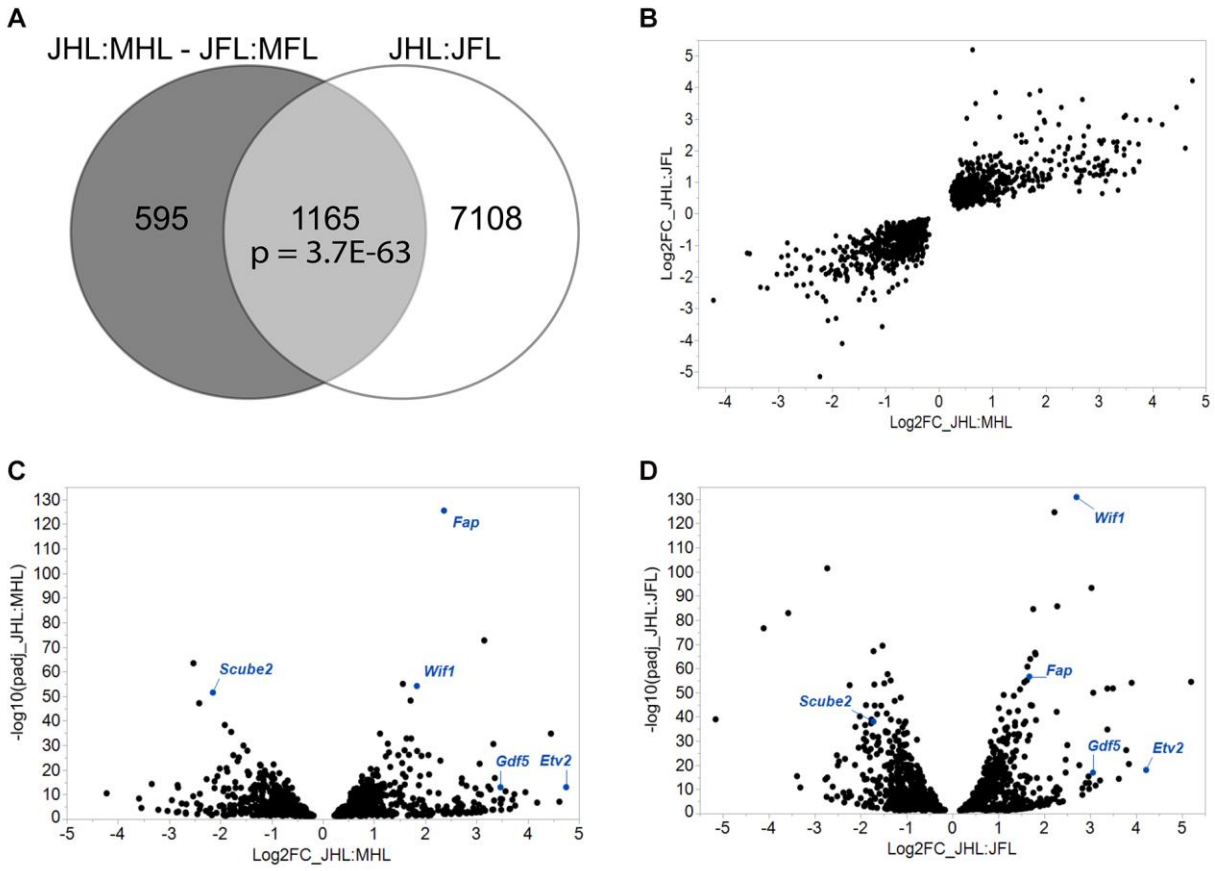

Figure 3.2 – Overview of differential expressed genes in new born jerboa foot muscles

(A) Venn-diagram of overlapped genes between JHL:MHL and JHL:JFL analysis.
(B) Log2 fold change (Log2FC) of the selected 1,050 DE genes from JHL:MHL and JHL:JFL comparison.
Volcano plot showing the Log2 fold change and p-adjusted value from JHL:MHL (C) and JHL:JFL (D) analysis.
Magenta highlight examples of genes with known roles in muscle development and growth or are novel genes of interest in the context of muscle loss.

Characterization of jerboa muscle loss described in Chapter 2 indicates that the atrophy associated muscle-specific ubiquitin ligase, *MuRF1*, was upregulated in newborn jerboa foot compared to 'normal' muscles. Indeed, *MuRF1* is found among the 1,050-transcripts associated with jerboa foot muscle loss. In contrast, consistent with our RT-qPCR analysis, *Atrogin-1* is not yet upregulated in P0.

Curation of genes with elevated expression considering both fold-change and statistical significance highlights genes of particular interest for further investigation (Figure 3.2C,D). Fibroblast activation protein (Fap) is a marker of activated fibroblasts in tissues undergoing remodeling of extracellular matrix, especially due to chronic inflammation, fibrosis or wound healing [269,270]. The role of *Fap* in muscle development and disease is unknown. However, considering the phenotypic changes that occur in the jerboa foot – connective tissue replaces muscle – *Fap* may play a role in promoting such a transition. ETS variant 2 (*etv2*) is a well-known transcription factor that is sufficient to transdifferentiate skeletal muscle to endothelial cells in zebrafish [271]. A similar response to *Etv2* overexpression was shown *in vitro* in cultured mouse muscle cell line, C2C12 but its function in muscle development *in vivo* remains unknown [271]. *Fap* and *Etv2* represent examples of novel gene candidates for which understanding their role in muscle loss in jerboa will expand our fundamental knowledge of muscle development and disease.

The other two genes highlighted here, Wnt inhibitor factor 1 (*Wif1*) and Growth and differentiation factor 5 (*Gdf5*), have been implicated in muscle growth and maintenance. *Wnt* signaling is known to regulate muscle hypertrophy, and WIF1 has been shown to bind multiple Wnts [272–274]. It is possible that *Wif1* plays a similar

function in skeletal muscle and thus contributes to muscle loss in the jerboa foot. *Gdf5* was shown to be important for muscle regeneration. Elevated *Gdf5* expression suppressed muscle satellite cell differentiation and impaired muscle regeneration [275]. Previously, we observed reduced myoblast fusion events in jerboa foot muscle. Perhaps, in conjunction with reduced number of proliferative muscle progenitors (reported in chapter 2), elevated *Gdf5* levels interfere with jerboa foot muscle satellite cell differentiation, which reinforces the muscle loss phenotype.

In contrast to genes with elevated expression, it is difficult to determine if genes with lower expression are required for or simply a consequence of muscle loss though these may provide important information regarding the physiological state of muscle. One of the genes of with significantly lower expression in the jerboa foot compared to other typical developing muscle is *Scube2* (Figure 3.2C,D). In zebrafish, *scube2* has been shown to function in the SHH signaling pathway and when mutated resulted in altered myotomal morphology [276]. In both mammals and fish, SHH is required for maintenance of *MyoD* expression and in fish, SHH is also required for proper specification of slow muscle cell fate [277,278]. It is possible that lower expression of *Scube2* in the jerboa foot indicates failure to maintain proper *MyoD* expression thus contributes to the loss of muscle. *MyoD* itself and other muscle genes such as *Myf5* and Myosin are not found to be associated with jerboa muscle loss (the 1050 gene list). Perhaps this is not too surprising considering that muscles at P0 stage are not morphologically different than other developing muscles. It is likely that a more significant reduction in expression of genes important for muscle identity will be found at later stage, P3, muscle transcriptome.

3.2.3 Pathway analysis of DE genes

To gain broader information about the potential mechanism of jerboa foot muscle cell loss, I used DAVID to determine the enriched biological processes (BP) among Gene Ontology (GO) terms and for pathway analysis using the Kyoto encyclopedia of genes and genomes (KEGG) and Reactome databases. Separately evaluating higher and lower DE genes rather than analyzing all the DE genes together has been shown to be more effective in identifying pertinent candidate pathways [279]. The top 10 most significant biological process GO terms, KEGG, and Reactome pathways associated with upregulated genes are reported in Figure 3.3, and pathways associated with downregulated genes are reported in Figure 3.4. Of note, the Wnt signaling pathway and collagen fibril organization pathways are interesting due to their previously reported roles in muscle development and maintenance. Sixteen genes were found to be associated with the Wnt signaling pathway (fold enrichment of 2.7 and p-value of 8.64E-4). These include Wnt inhibitors such as *Wif1* and *Nkd2*, and transcription factors that are downstream of Wnt activation such as *Lef1* and *Tcf7l1*. Among KEGG pathways, only the ribosome is significant. One Reactome pathway, the TNFR1-induced NF-κB signaling pathway, achieved significance (fold enrichment of 5.6 and p-value of 0.03). The enrichment for TNFR1-induced NF-κB signaling pathway is consistent with data reported in Chapter 2 regarding the presumed involvement of an NF-κB-mediated atrophy-like mechanism in jerboa foot muscle loss.

For genes that are downregulated, many are associated with extracellular matrix organization and include *Col4a1*, *Col4a2*, and *Lamα5* – all highly expressed in skeletal muscle and Collagen 4 has been shown to be essential for maintenance of muscle

structure [280,281]. KEGG pathway analysis showed enrichment of genes involved in focal adhesion are also downregulated (Figure 3.4), further suggesting compromised muscle structure maintenance [282]. Genes involved in Thyroid hormone and Ras signaling pathways (Figure 3.4B), both major muscle-hypertrophy inducing signals, are also downregulated [66,283,284]. Thyroid hormone also plays an important role in the positive regulation of muscle stem cell proliferation [284]. It seems that a big proportion of downregulated genes are important for processes of muscle growth and maintenance, consistent with the observed muscle loss phenotype.

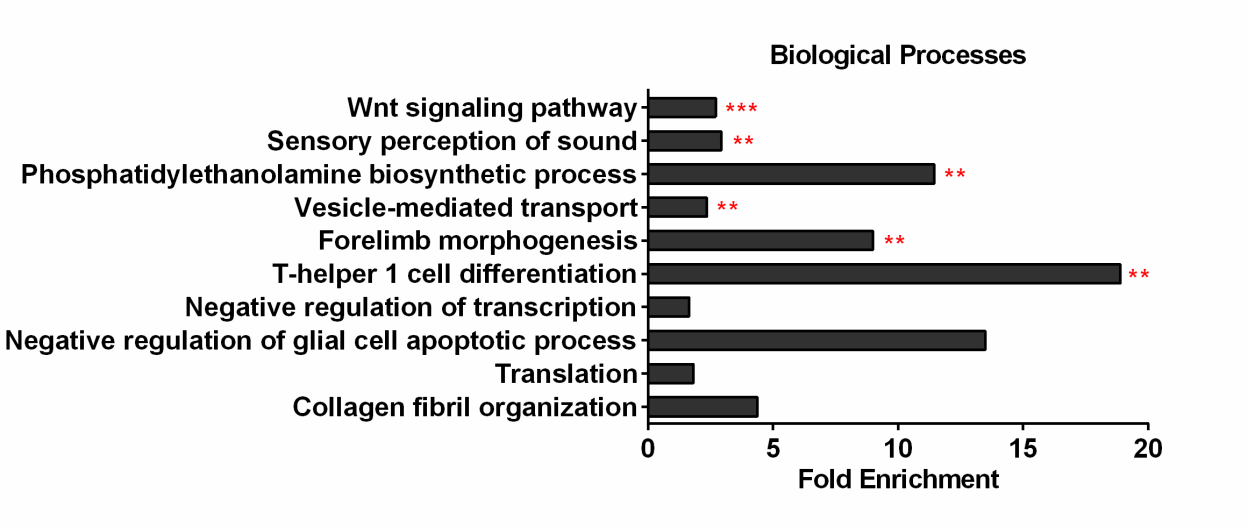

Figure 3.3 – Functional predictions of upregulated DE genes
DAVID analysis was performed to yield functional prediction of upregulated DE genes. Top 10 significant ($p<0.05$) pathways are presented. **$p<0.01$, ***$p<0.001$. From top to bottom: most to least significant.

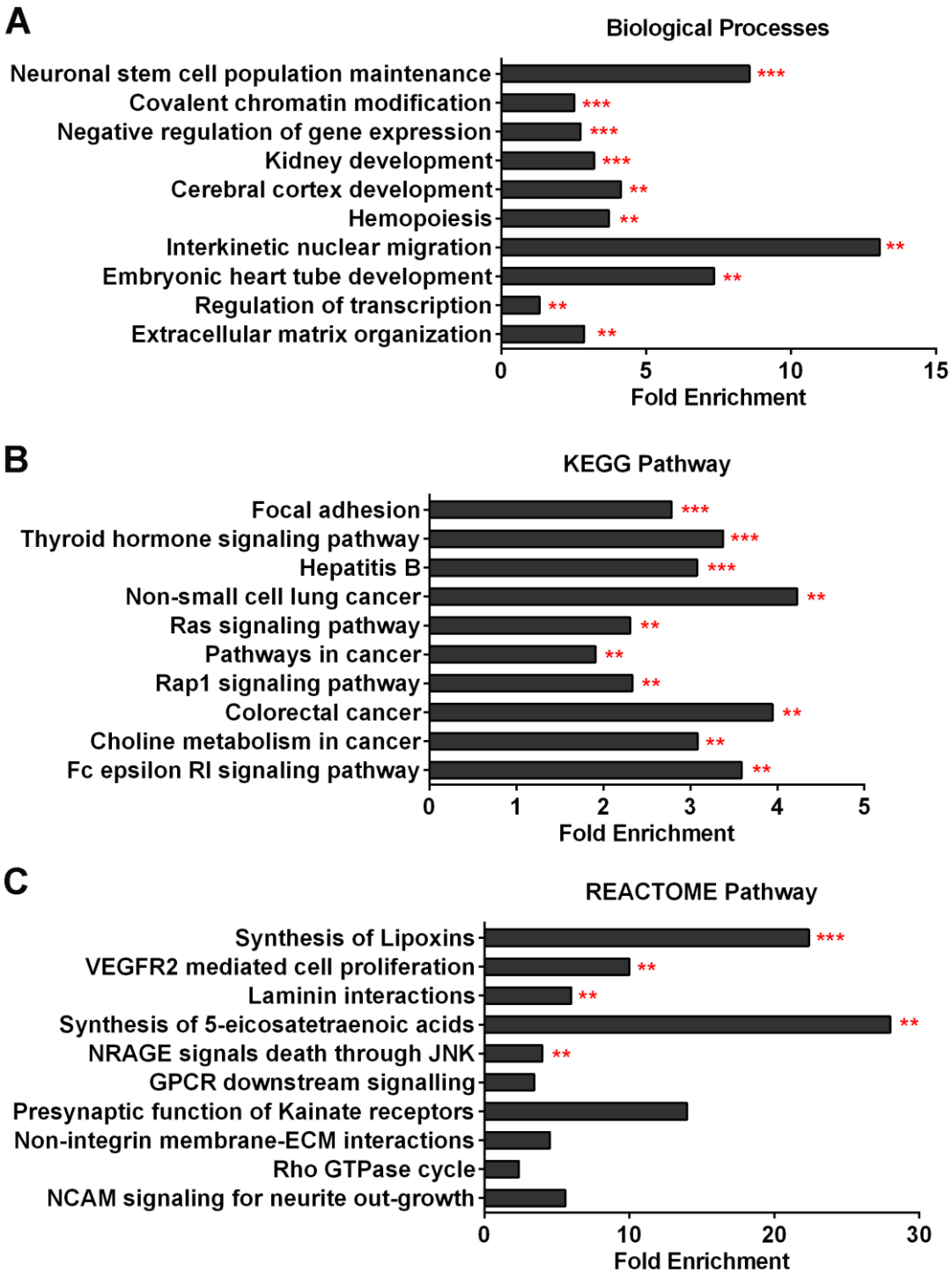

Figure 3.4 – Functional predictions of downregulated DE genes
DAVID analysis was performed to yield functional prediction of upregulated DE genes. Top 10 significant ($p<0.05$) (A) biological processes, (B) KEGG, and (C) REACTOME pathways are presented. **$p<0.01$, ***$p<0.001$. From top to bottom: most to least significant.

3.2.4 Comparison to DE genes of other muscle atrophy models

Muscle loss results from disease-causing mutation or in response to denervation, disuse, cancer, fasting, and aging. Various animal models of muscle loss aid our understanding of disease pathology and the underlying molecular pathways that are affected [285,286]. Thus far, our work suggests that natural foot muscle loss in the jerboa has shared characteristics with muscle atrophy based on upregulation of atrophy-induce ubiquitin ligase genes. To further probe the extent of shared molecular signatures, I intersected the 1,050 DE genes in newborn jerboa to DE genes reported in other animal models of muscle atrophy - cancer-induced muscle loss (i.e. cancer-cachexia), spinal muscular atrophy, and Botolinum toxin (BT)-induced muscle loss, and denervation-induced muscle loss [287–290]. These datasets were chosen based on the accessibility of differential expression datasets.

Cancer-cachexia is a muscle wasting condition that occurs concurrently with cancer and cannot be fully reversed by nutritional interventions [287]. Various methods exist to model cancer-cachexia. In the Blackwell *et al.* study, mice were injected with Lewis Lung carcinoma, and tumors were allowed to develop for one to four weeks [287]. Compare to non-cancer mice, researcher found the most significant differences in transcriptomic data at week four, when mice experienced significant decreased in muscle loss [287]. In contrast, there was less than 100 differentially expressed genes reported in week one and week two following cancer development [287]. Thus, only the dataset for week four was chosen for further comparison with the jerboa muscle loss data.

Spinal muscular atrophy (SMA) is a neuromuscular disease that often results in death in infancy or leads to progressive muscle weakness due to loss of motor neurons [288]. *Doktor et al*. used a SMA model in which mice have lifespan of only 10-11 days after birth [291]. The author evaluated transcriptomic changes at pre-symptomatic (postnatal day 1) and later symptomatic (postnatal day 5) stages of various tissues that included muscle [291]. Both P1 and P5 datasets were chosen since the authors did not comment on the global gene expression changes specifically in muscle over time.

Botulinum toxin-induced muscle loss is the third model of muscle atrophy with an available transcriptome dataset. Injection of BT was used to inhibit motor neuron activity, thus mimicking conditions of muscle inactivity often seen in multiple neuromuscular disorders or bed-ridden patients [289]. *Mukund et al.* reported a long-term study of BT-induced muscle loss from one week to up to a year after BT injection [289]. The authors reported the most dramatic transcriptome changes (1989 genes) happened at one week compared to four weeks (372 genes) and 12 weeks (32 genes) and no biologically significant transcriptional changes at 52 weeks after BT injection [289]. Muscle contraction was already significantly impaired starting at week one [289]. I chose the differentially expressed genes at one, four, and twelve-week after toxin injection for further comparison with the jerboa muscle loss data.

The fourth model of muscle atrophy is denervation-induced muscle loss. Kostrominova *et al.* reported that after two months of denervation, compared with the control muscle, denervated muscle showed substantial myofiber atrophy and increased interstitial connective tissue [290]. The authors identified 128 genes differentially

expressed in the two month-denervated muscle compared to normal innervated muscle [290]. These genes were selected for comparison with the jerboa muscle loss data.

Two studies, BT-induced muscle loss and denervation-induced muscle loss, were done in rat. Since no 1:1 jerboa:rat orthology annotation exist, the following assumption was made: if a gene existed in rat, it would exist in mouse considering that they are closely related, and thus we can use the 1:1 jerboa:mouse orthology annotation. To ensure fair comparison across all dataset, only genes represented in the 1:1 jerboa:mouse othology dataset were used. Table 3.1 reported the number of genes reported in the original dataset and the number of genes represented in the 1:1 jerboa:mouse orthology. Using a Fisher's exact test for enrichment in an intersection of differentially expressed jerboa genes and each of these datasets, I found that there was no significant gene overlap with those reported in spinal muscular atrophy and in denervation-induced muscle loss (Table 3.1). Chapter 2 showed that jerboa foot muscles were innervated so perhaps it was not too surprising that there was no similarly between jerboa muscle loss and denervation-induce muscle loss processes.

The model of cancer-associated muscle loss following four weeks of Lewis lung carcinoma development resulted in transcriptional changes of 3746 genes [287]. Compared to DE genes associated with jerboa foot muscle loss, there was a significant overlap of 285 genes (Figure 3.5A). Reactome pathway analysis of the shared 285 genes revealed significant enrichment in cell-cell (Integrin and Laminin) and membrane-ECM interactions as well as in anchoring fibril formation among the upregulated and downregulated genes (Figure 3.5B).

Table 3.1 – Fisher's exact test result for overlapping genes between jerboa DE and the chosen muscle atrophy model

Dataset	Original DE genes after conversion to MGI_IDs	Represented DE genes in orthology dataset	p-value
Cancer cachexia [287]	4303	3746	5.6E-6
SMA_P1 [291]	712	640	0.92
SMA_P5 [291]	935	850	0.27
BT-induced muscle loss wk1 [289]	1888	1790	0.045
BT-induced muscle loss wk4 [289]	388	363	2.4E-3
Denervation-induced muscle loss [290]	117	106	0.77

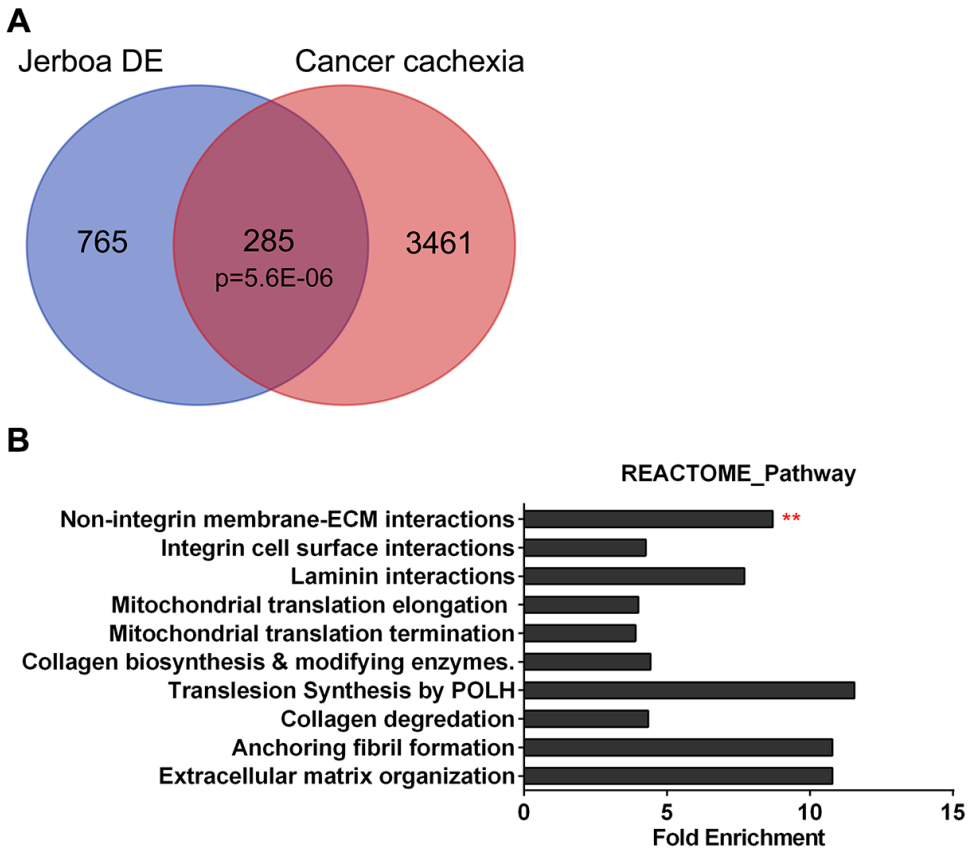

Figure 3.5 – Jerboa foot muscle loss has shared molecular signature with cancer cachexia model
(A) Venn-diagram showing the number of DE genes overlapped with cancer cachexia model of muscle atrophy.
(B) DAVID analysis was performed to yield functional prediction of genes shared between jerboa and cancer cachexia data. Top 10 significant ($p<0.05$) REACTOME pathways are presented. **$p<0.01$. From top to bottom: most to least significant.

In the model of BT-induced muscle loss, the earliest and most extensive transcriptome changes were reported one week after treatment [289]. Compared to DE genes found associated with muscle loss in jerboa, 125 genes were found in common (Figure 3.6A) and Reactome pathway analysis showed only significant enrichment in non-integrin membrane-ECM interactions pathway (fold enrichment of 11.2 and p-value of 0.028). Comparison with differentially expressed genes four weeks after BT injection showed significant overlapped of 36 genes and Reactome pathway analysis of all 36 genes showed significant changes in pathways involved in extracellular matrix organization and interactions (Figure 3.6B,C). There was no significant overlapped between differentially expressed genes 12 week after BT injection and those found in jerboa muscle loss data.

Analysis of common transcriptional changes in cancer cachexia, BT-induced muscle loss at week one and four, and jerboa muscle loss yield changes in 12 genes (Figure 3.7). Reactome pathway analysis of all 12 showed significant enrichment in non-integrin membrane-ECM interactions (fold enrichment of 70.7 and p-value of 0.023). Of the common 12 genes, three genes were found to be significantly elevated in all datasets including the *NF-κB2* gene. Overall, comparison with existing models of muscle loss suggest the common initiation of muscle atrophy via NF-*κB* activation. In addition, there are shared molecular pathways, mainly changes in extracellular matrix organization and membrane-ECM interactions, between natural and pathological muscle loss.

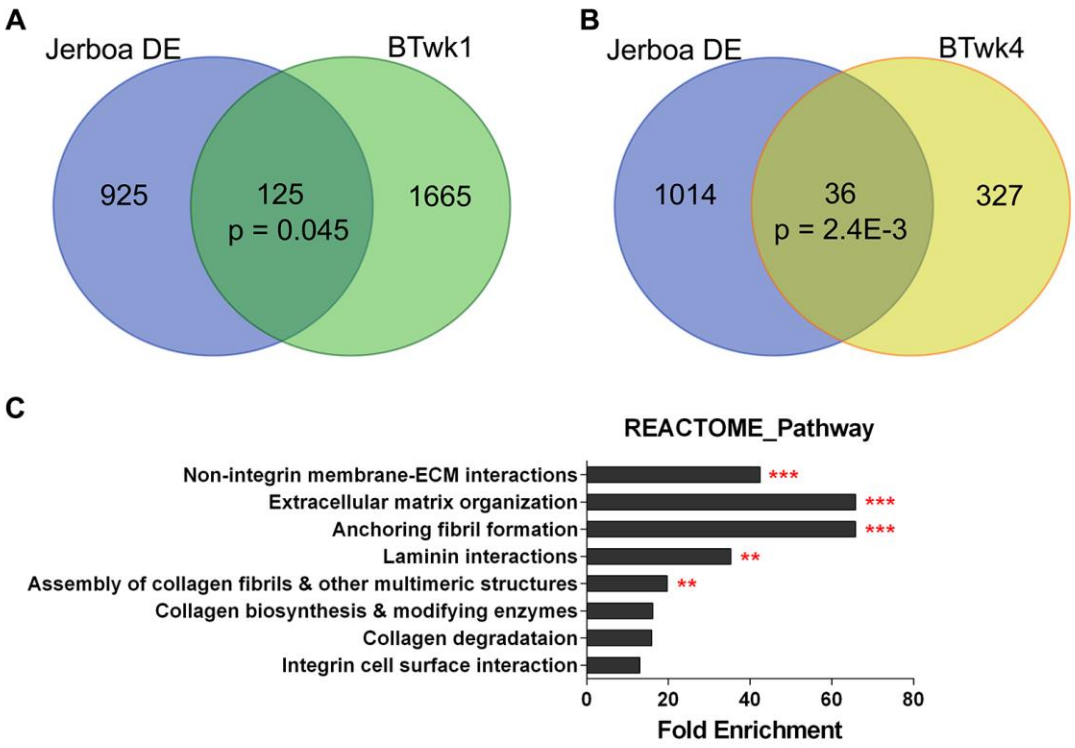

Figure 3.6 – Jerboa foot muscle loss has shared molecular signature with BT-induced muscle loss

Venn-diagram showing the number of DE genes overlapped with BT-induced muscle loss model of muscle atrophy (A) one week and (B) four week after BT injection. (C) DAVID analysis was performed to yield functional prediction of genes shared between jerboa and data from four week after BT injection. Top 10 significant ($p<0.05$) REACTOME pathways are presented. **$p<0.01$, ***$p<0.001$. From top to bottom: most to least significant.

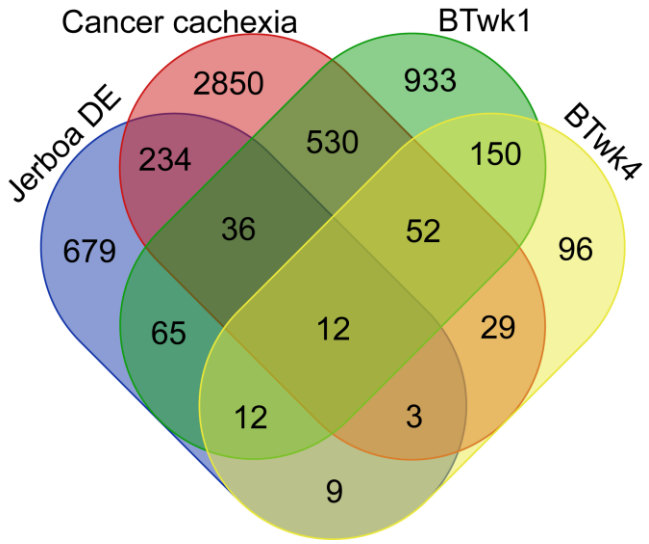

Figure 3.7 – Shared genes between jerboa muscle loss and other models of muscle atrophy
Venn-diagram showing the number of DE genes overlapped with cancer cachexia and BT-induced muscle loss model of muscle atrophy.

To test if the similarity found between the process of jerboa muscle loss and of other muscle atrophy models are likely to reflect true biological similarities or a random probability of intersecting two datasets, I randomly chose six other non-muscle disease datasets for comparison. These include analysis of transcriptional changes in microglia of three Alzheimer models (rTg4510 tau transgenic, APPswe/PS1dE9, and 5xFAD mouse models) [292], in microglia of Fabry lysosomal storage disease [293], in intestinal tissue of dextran sulfate sodium (DSS)-induced colitis model [294], and in lung tissue of IGF1R-driven lung cancer model [295]. Of these six datasets, only one dataset, eight months rTg4510 tau model of Alzheimer disease, showed significant overlap with DE of jerboa muscle loss (Figure 3.8A, Table 3.2). However, functional prediction of the common 121 genes via DAVID showed enrichment in multiple ribosomal processes (Figure 3.8B). It seems that while there is significant overlap with one of six randomly chosen datasets, the overlapped genes, however, did not show obvious meaningful functional predictions in the context of muscle development. This lends support to the interpretation that the similarities between jerboa foot muscle loss and other muscle atrophy models are likely specific and represent common underlying features of natural and pathological muscle loss.

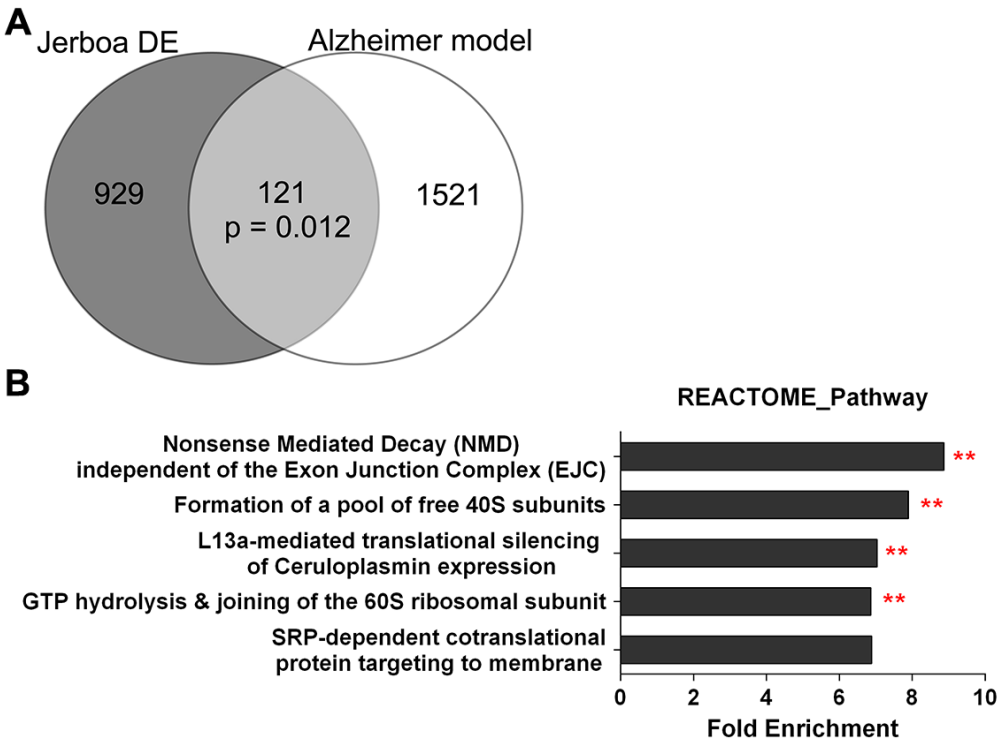

Figure 3.8 – Shared genes between jerboa muscle loss and non-muscle disease models

(A) Venn-diagram showing the number of DE genes overlapped with rTg4510 tau model of Alzheimer disease.

(B) DAVID analysis was performed to yield functional prediction of the 36 shared genes. Top 10 significant ($p<0.05$) REACTOME pathways are presented. **$p<0.01$. From top to bottom: most to least significant.

Table 3.2 – Fisher's exact test result for overlapping genes between jerboa DE and non-muscle disease model

Dataset	Original DE genes after conversion to MGI_IDs	Represented DE genes in orthology dataset	p-value
rTg4510 tau transgenic [292]	2842	1642	0.012
APPswe/PS1dE9 [292]	933	822	0.28
5xFAD [292]	655	553	0.63
Fabry lysosomal storage disease [293]	135	108	0.48
DSS-induced colitis model [294]	1387	1152	0.65
IGF1R-driven lung cancer model [295]	4977	4247	0.59

3.3 Discussion

Since the early discovery of various muscle myopathies, human data and animal models of muscular dystrophy and atrophy have contributed to our understanding of the complex network of cellular and molecular mechanisms that underlie disease pathology and progression. The natural loss of intrinsic foot muscle in the jerboa represents a unique opportunity to complement studies in traditional systems and to expand our understanding of the fundamental mechanisms of muscle development. In this chapter, I report the transcriptomic alterations that coincide with the initiation of muscle loss in newborn jerboa feet. In addition to comparing muscles that are lost in the jerboa foot to homologous muscles that persist in the mouse, comparison to typical developing forearm muscle in each species allows us to distinguish genes associated with muscle loss from the background of evolutionary divergence over time. The strength of our discovery approach lies in the robust phenotype of muscle loss and the relatively close evolutionary divergent, approximately 55 millions years, between the jerboa and mouse.

Some of the genes identified as substantially differentially expressed were previously linked to muscle growth and development but many others have unknown functions in muscle physiology. Enrichment of genes that participate in Wnt signaling indicates Wnt dysregulation occurs in natural muscle loss. Recent work showed that Wnt signaling can regulate the cell growth mTOR/AKT pathway [273]. This suggests misregulation of muscle metabolism and growth. In addition, there is evidence of perturbation in integrin signaling and membrane-ECM interactions. This is consistent with previous data in Chapter 2 suggesting that jerboa muscle loss is a non-cell autonomous process, most likely involved complex signaling interactions between

muscles and the surrounding tissues. In addition, genes with low expression level showed enrichment in focal adhesion pathway, suggesting loss of muscle structure maintenance and altered muscle-muscle interaction.

With the availability of transcriptomic data from various models of myopathies, we found significant overlap of the transcriptomic changes in the natural muscle loss process compared to those reported in various models of muscle atrophy. A common feature found across all datasets with significant similarities is the elevated expression of *NF-κB2*, suggesting a critical role of NF-κB2 – activated proteolytic programs for inducing muscle loss. Interestingly, the overlapped changes are enriched in pathways involving ECM remodeling and muscle-ECM interactions, emphasizing the role of ECM in muscle disease pathology and progression. In addition to the similarities to atrophy demonstrated in chapter 2, global gene expression analysis reveals broader similarities across the transcriptome and identify key pathways critical for muscle maintenance and function.

This is the first study to examine the transcriptome changes associated with the natural process of muscle loss as well as identifying common pathways affected in natural and pathological muscle loss. This serves as a valuable resource to consider in conjunction with histological and morphological data to generate hypothesis testing of specific cellular processes involved. Future work to investigate transcriptomic alterations in a later stage of sarcomere disorganizations – P3 – is required to identify temporally unique cellular processes affected. Such data will also provide insights into how expression of genes in specific pathway changes in the early onset versus later stages of muscle loss in the jerboa.

3.4 Materials and Method

3.4.1 Animals

Jerboas were housed and reared as previously described [257]. CD1 mice were obtained from Charles River Laboratories (MA, USA), housed in standard conditions, and fed a breeder's diet. All animal care and use protocols for mice and jerboas were approved by the Institutional Animal Care and Use Committee (IACUC) of the University of California, San Diego.

3.4.2 Laser capture microdissection

Tissues from six animals (right and left limbs) were pooled per sample, and three samples were used per species (mouse and jerboa). Mouse and jerboa feet were fresh frozen in blocks of OCT freezing media, and blocks were stored at -80°C until cryosectioned. Blocks were sectioned at 30 µm thickness, and sections were transferred to 1.0 PEN (polyethylene naphthalate) MembraneSlides (Zeiss). Sections were stained and dehydrated using the Arcturus HistoGene LCM Frozen Section Staining Kit (ThermoFisher) following manufacturer's protocol with the following modification: prior to 100% EtOH and Xylene dehydration each step was done in 10s rather than 1 minute to ensure high quality RNA. Sections were processed Sections were subjected to laser microdissection using Zeiss PALM MicroBeam microscope with the following setting: 10X objective, cutting speed 30, cut energy 65 with focus 83, LPC energy 80 with focus 90. Tissues were captured into 500µL adhesive cap with cutting time limited to 5 minutes maximum. Immediately after capture, 12.5µL extraction buffer from PicoPure RNA Isolation Kit was added per adhesive tube. Samples were pulled to

reach 50µL total volume and incubated for 30 minutes at 42°C prior to storage at -80°C until RNA isolation.

3.4.3 RNA isolation and sequencing

RNA extraction was performed using the PicoPure RNA Isolation Kit (Thermo Fisher) according to the manufacture instructions. RNA quality and concentration were determined using Agilent TapeStation (Agilent Technologies, Santa Clara, CA). RIN^{e} scores from TapeStation analysis for all samples used were at minimum 7.0. Libraries were prepared using the Illumina TruSeq Stranded mRNA Library Preparation Kit using a polyA-enrichment strategy. Two pools of mouse and jerboa samples were loaded onto Illumina HiSeq 4000 High Output flow cell and sequenced in a 1 × 75 bp single read format. RNA sequencing was completed at the Institute for Genomic Medicine (IGM) Genomics Center at UC San Diego (La Jolla, CA).

3.4.4 Data analysis

Adaptors and low quality bases were trimmed from sequences by using Trimmomatic with default parameters [296]. Quality control of sequences in FASTQ and BAM format was assessed with the FASTQC software (Babraham Bioinfomatics, http://www.bioinformatics.babraham.ac.uk/projects/fastqc/). The STAR software was used to map the reads generated [297]. Mapping was done using a 1:1 jerboa: mouse orthologous gene annotation set (unpublished data). This Orthologous gene annotation set contains syntenic genes with at least one exon with no frameshift, missense, or nonsense mutations [298]. This reference gene set was generated, in collaboration with Dr. Michael Hiller's lab (MGI-CBG, Dresden). Trimmomatic and STAR analysis were done using the 'Comet' Supercomputer at the San Diego Supercomputer

Center (SDSC), UC San Diego (La Jolla, CA). Read counts associated with each specific transcript were employed to carry out analysis of differential expression with DESeq2 [299] with an additional transcript length correction for each species.

3.4.5 Functional enrichment analysis

DAVID was used to identify enrichment of genes (categories: GO_BP_FAT, KEGG_PATHWAYS, and REACTOME_PATHWAYS) [300,301]. Unique MGI_IDs were used as gene identifier input for DAVID. 17379 Unique MGI_IDs of jerboa:mouse orthologous gene annotation set was used as background. DAVID result was graph with GO terms or pathways sorted from top to bottom correlating with smallest to largest p-value. Fold enrichment indicates the ratio of input genes over background genes associated with a particular GO term or pathway.

3.4.6 Data comparison with other muscle atrophy models

The following atrophy model datasets were used for comparison: cancer-cachexia [287], spinal muscular atrophy [288], BT-induce muscle loss [289], and denervation-induce muscle loss [290]. The following non-muscle disease datasets were used: rTg4510 tau transgenic, APPswe/PS1dE9, and 5xFAD models of Alzheimer disease [292], model for Fabry lysosomal storage disease [293], dextran sulfate sodium (DSS)-induced colitis model [294], and IGF1R-driven lung cancer model [295].

Each list of differentially expressed genes were from the original author's DESeq2 or microarray analysis output. Genes selected for further overlap with the jerboa were defined as those with padjusted value (DESeq2) or p-value (microarray) less than 0.05. Gene list was first converted to MGI-ID using the MGI batch query function (http://www.informatics.jax.org/batch). Genes with no associated MGI_IDs and

MGI_IDs not found in jerboa:mouse 1:1 orthology dataset was removed from consideration. Fisher's exact test was performed using GeneOverlap package in R to determine statistical significance of overlapping genes [302]. The 17379 unique MGI_IDs of jerboa:mouse 1:1 orthology dataset was used as reference background for Fisher's exact test. Venn diagram was generated via the online tool 'calculate and draw custom Venn diagrams' (http://bioinformatics.psb.ugent.be/webtools/Venn/).

3.5 Acknowledgement

The author would like to acknowledge Dr. Virag Sharma from the lab of Dr. Michael Hiller for assistance generating the 1:1 jerboa: mouse orthologous gene annotation and Amanda Birmingham at the Center for Computational Biology and Bioinformatics for assistance in modification to DESeq2 R script for gene length normalization. The author would also like to thank the following centers: the Biophotonics Core at Salk Institute for Biological Studies for assistance and usage of the Zeiss PALM MicroBeam microscope; the San Diego Supercomputer Center (SDSC) at UC San Diego for assistance and usage of the supercomputer cluster Comet; and the Center for Computational Biology at UC San Diego for bioinformatic assistance. The author would like to thank Dr. Kavitha Mukund for advice on bioinformatic tools.

Chapter 3, in full, is currently being prepared for submission for publication of the material. Tran, Mai; Saxena, Adytia; Cooper, Kimberly L. The dissertation author was the primary investigator and author of this material.

CHAPTER 4. Summary Discussion

4.1 Thesis summary

Biology is wonderfully diverse with lifeforms colonizing all corners of the Earth: from the invertebrate tube worm living in the harshest deep-sea vent to the monkeys living the prolific rain forest. Animals evolved diverse phenotypes to adapt to their environment. As an example, individual skeletal muscles – the defining factor of movement – were lost and gained throughout the history of animal evolutionary adaption. Take for example the irresistible “puppy dog eyes”. It was recently discovered that facial expression in dogs is possible due to the existence of a muscle responsible for raising the inner eyebrow; the muscle is present in dogs but not in their wolf relatives [303]. On the other hand, rodents living in the desert like the jerboa, have lost the intrinsic foot muscles in the course of their evolution. Interestingly, in the jerboa, foot muscles are lost postnatally, presenting a unique opportunity to trace the cellular processes responsible for the observed morphological change. My thesis sought to investigate the cellular and molecular processes associated with muscle loss in the foot of the three-toed Lesser Egyptian jerboa.

Working backward in time from the adult jerboa phenotype, I found that the intrinsic foot muscles differentiate as multinucleated myofibers that initiate sarcomere assembly, as in other species, but are lost within a few days shortly after birth. Despite the rapid and near complete loss of myofibers, there was no evidence of apoptotic or necrotic cell death, no accumulation of autophagic vesicles, and no macrophage infiltration. Instead, there is evidence of ordered sarcomere disassembly and upregulation of atrophy-associated genes such as the NF-κB transcription factors and

the muscle-specific ubiquitin ligases, *MuRF1* and the Cullin-1 specific substrate adaptor *Atrogin-1*. In addition, transcriptomic changes in newborn jerboa foot muscle showed significant overlap with existing mouse models of muscle atrophy further strengthening the hypothesis that jerboa foot muscles utilize programs similar to atrophy to initiate the process of muscle loss. These data provide evidence for shared molecular pathways between natural and pathological muscle loss. Despite these findings, many questions remain regarding the complex process of muscle loss in jerboa foot, and my work opens exciting new avenues for exploration. Future research focusing on the topics discussed below will not only provide valuable information regarding the modification of conserved developmental pathways to generate morphological diversity but also contribute to our understanding of disease evolution.

4.2 Muscle cell fate maintenance and plasticity

The work described in chapter 2 showed that jerboa foot muscles are lost rapidly within the first week after birth but there was no evidence of cell death. The ultimate fate of these muscles remains unknown. Muscle dedifferentiation has only been observed in newt and salamander [82–84] while transformation of muscle fate has only been reported in electric and deep sea fish [87,304]. Is it possible that muscle of the jerboa foot transdifferentiates to become another cell type? Intriguingly, as muscles disappear, ultrastructural analysis showed fibroblast-like cells surrounding muscle aggregates. Perhaps, these cells were once muscle but now have transformed their identity to be collagen-producing cells. Together with the lack of cell death, this is a plausible hypothesis given the plasticity of muscle cell fate observed in other organisms [79,87].

We have tried multiple approaches to lineage trace muscle cells, but none was successful. There were two technical complications hindering our ability to successfully linage label muscle cell. First, there was a lack of muscle-specific promoter expression. Our lineage labeling strategy utilized the ‘muscle-specific’ promoters previously used for lineage labeling in salamanders [259]. However, in both mice and jerboas, these promoters show expression in non-muscle cells. Perhaps this problem of non-specificity can be circumvented with high number of labeled cells. Unfortunately, our second problem was the lack of sufficient labeled cells. The best methods for expressing foreign DNA in skeletal muscle include virus-mediated deliveries or electroporation [260]. However, these have only been used successfully in adult animals. Foot muscles of newborn mouse and jerboa are too small for successful injection of viruses and the lack of DNA pocket hinder the efficiency of plasmid uptake via electroporation [305].

The advent of single cell sequencing approaches provides an alternative to lineage labeling that may allow us to reconstruct a ‘virtual lineage’ using global similarities in the transcriptome of heterogeneous cell types [306,307]. Commonly, two different approaches can be taken to computationally determine cell grouping. The first approach is discrete grouping via reiterative clustering method in which the initial round of clustering divides cells into the most distinct groups and subsequent clustering within in individual group further defines cells into subtypes [307]. The second approach is continuous grouping via pseudotime analysis where cells are ordered along one dimensional ‘pseudotime’ reflecting progression through a biological process [308]. However, it is often informative to get both a discrete and continuous view of the underlying data. Recent methods were developed to first find discrete clusters and

subsequently infer graph structure connecting the clusters [308]. Our data is expected to contain discrete groups of cells due to their distinct identity, tendon versus muscle cells, and potentially other unknown group of cells that may have biological connection to muscle. Both traditional clustering and pseudotime analysis should be used to fully explore the dataset.

Since muscle is a multinucleated tissue, single nucleus RNA sequencing of muscle and surrounding tissues [309,310] will reveal different cellular developmental trajectories that existed in the jerboa foot as well as jerboa hand, mouse hand and foot muscle. For example, when inferring lineages with pseudotime analysis, muscle satellite cells and differentiated muscles should follow a single trajectory while tenocytes or fibroblasts follow a different trajectory. Identification of cells connecting muscle with another trajectory, a bridge, - that exist exclusively in the jerboa foot and not in normal developing muscle - will suggest that there is fate-switch. However, without true lineage labeling, we cannot be absolutely certain about fate-switching. On the other hand, if muscle cells die via a previously unknown mechanism, the lineage map might reveal only discrete cellular trajectories with no bridging population. If dying cells form a cluster different from either the progenitor or differentiated muscle populations, single cell analysis might reveal the correlating distinguishing gene expressions. Ultimately, single cell analysis is an inferential approach and further *in-vivo* validation via in situ hybridization and functional assays of specific clusters (putatively transdifferentiating or dying cells) are required to confirm their existence and function. Single cell sequencing can provide crucial information regarding the heterogeneity of cell identities in jerboa

foot compared to a typical developing limb and may help us generate hypothesis regarding the fate of the myofibers.

4.3 Similarities and differences between natural and pathological muscle loss

Muscle loss in the jerboa foot is accompanied by massive expansion of fibrous tissue such as the tendon. Similarly, previous investigation in the loss of foot muscles in the horse and ox showed infiltration of fibrous tissue and fat as muscles disappear [212]. These studies suggest striking similarity to the development of fibrosis in muscle pathology. Recent studies reveal the involvement of fibro-adipogenic progenitors (FAPs) in muscle fibrosis development. FAPs are mesodermal-derived mesenchymal cells that reside in the muscle interstitial space [311]. During normal regeneration, FAPs appearance and their timely clearance is important for the muscle regenerative process [312]. However, in pathological conditions of muscle damage, FAPs persist abnormally with associated formation of fibrotic scars and fat deposition, thus impairing muscle regeneration [313]. Interestingly, FAPs have been shown to be a heterogenous population capable of adopting alternative lineages, such as the osteogenic phenotype in response to BMP [311,314]. I hypothesize that, similar to pathological muscle loss, the FAP population is expanded as muscles disappear in the jerboa foot. We have tried to probe for the presence of FAPs via immunostaining for the FAP marker, PDGFRα, but existing antibodies did not show reactivity in jerboa tissue. Future studies employing methods such as in-situ hybridization or RNAScope technology can be used to detect mRNA expression of FAP genes. This will allow us to answer the following questions: are FAPs present in the jerboa foot muscles at the time of muscle loss? If so, how does

the FAP population change as muscle loss progresses? Additionally, single cell sequencing data from jerboa foot muscle and the surrounding tissue will also shed light on the presence and heterogeneity of FAPs.

Although pathological muscle atrophy and natural muscle loss in the jerboa foot share proteolytic programs, jerboa foot muscle loss is different in many ways from a pathological phenotype. For example, muscles disappear in the jerboa foot leaving behind myosin-rich myofilament aggregates yet there was no evidence of immune cell recruitment and inflammation. It is possible that the fibroblast-like cells observed are recruited to phagocytose the aggregates, thus avoiding activation of the inflammatory response [252–255]. Could it be that the immune response is also actively suppressed as muscle disappear? Investigation into the molecular signal involved in fibroblast recruitment and/or signal suppressing immune response could open new therapeutic approaches to treating inflammatory myopathies.

4.4 The role of muscle satellite cells in jerboa foot muscle loss

Muscle satellite cells proliferate, differentiate, and fuse to existing myotubes to aid in muscle growth, and they function to repair damaged myofibers in response to injury [70,71]. Results reported in chapter 2 showed that a decreased number of muscle progenitors precedes muscle loss suggesting an insufficient muscle satellite cell population. In diseases such as DMD, continuous muscle damage leads to a constant demand for reparative myogenic cells and subsequent exhaustion of the satellite cell population [315]. Perhaps, muscle loss in the jerboa foot is simply due to insufficient number of muscle satellite cells. To test this hypothesis, we can isolate muscle

progenitors from the jerboa and graft them back into the foot muscles to increase the pool of muscle satellite cells and assess for delay of muscle loss or rescue of myofiber numbers. One technical challenge of such an experiment includes the cross reactivity of existing antibodies against satellite cell markers in jerboa cells. While the traditional Pax7 antibody did not work in jerboa tissue, there are other combinations of broader markers that we can use. Alternatively, while not ideal due to the requirement for immunosuppression to prevent rejection, engraftment of mouse muscle satellite cells might be possible.

In-vitro culture of jerboa foot muscle progenitors showed normal differentiation suggesting that muscle loss is non-cell autonomous. We also observed reduced fusion events occurring concurrently with muscle loss. Perhaps, there are extrinsic cues that suppress the normal process of muscle regeneration, via impairing muscle proliferation, differentiation, or fusion, thus contributing to muscle loss. It is known that the muscle environment is critical for maintenance of healthy muscle stem cell niche and subsequent stem cell activation and proliferation in response to injury [316]. I hypothesize that foot muscle satellite cells fail to become activated to proceed toward proliferation and differentiation. We can inject different factors, such as nitric oxide or hepatocyte growth factor, known to activate muscle satellite cell activity [53,75], to test whether increased regenerative potential can delay or (partially) rescue muscle loss. A delayed loss or rescue of myofiber number will suggest the involvement of active suppression of muscle satellite cell activity. Future studies of how muscle regeneration is inhibited will shed light on how this process is similar to or different from conditions of impaired muscle-satellite cell response. In addition, transcriptome profiling of P0 jerboa

foot muscles yields *Gdf5* as a potential candidate to cause impaired satellite cell differentiation and future transcriptome study of a later stage of muscle loss (P3) can provide additional information on the expression dynamics of factors regulating muscle satellite cells.

4.5 Muscle interactions with surrounding tissue

Multiple morphological changes occurred in the jerboa foot compared to the ancestral mouse-like limb such as metatarsal elongation, bone fusion, loss of the first and fifth digits, and complete lack of intrinsic foot muscles [317]. Intriguingly, foot muscle loss during the first week after birth in jerboa coincides with the rapid increase in metatarsal length at a rate almost double that in mouse (Figure 4.1). The rapid growth acceleration together with the observation that muscle loss in jerboa foot is a non-autonomous process suggests that muscle loss may be influenced by bone growth. Forcible lengthening in eccentric contractions can result in serious muscle injuries. Signs of muscle damage include regions of unregistered or disorganized sarcomeres and Z-line streaming [67]. Since the intrinsic foot muscles are connected to one or both ends of the metatarsals, it is possible that the rapid rate of bone elongation produces an eccentric contraction-induced muscle injury phenotype that contributes to progressive muscle loss after birth when growth rate accelerates. *In-vivo* inhibition of metatarsal elongation, via growth-plate injury, is one way to test for the requirement of mechanical stretch in muscle loss. If bone elongation is required for foot muscle loss, upon inhibition of bone elongation, I expect to observe higher myofiber number when compare to muscles of untreated foot. Long-term analysis over several developmental stages is

important to determine the extent of the observed muscle rescue. Considering that muscle loss occurs in the jerboa lineage more than 20 million years ago [202,318,319], it is likely that multiple genetic changes contribute to loss of jerboa foot muscle, and bone elongation accelerates rather than acts as the sole cause of muscle loss.

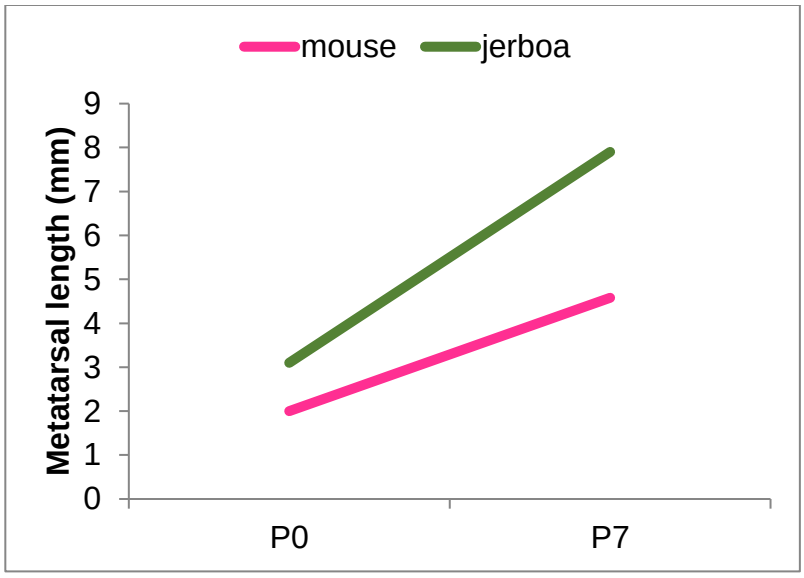

Figure 4.1 – Jerboa metatarsal elongation length within the first week after birth
Metatarsal elongation between P0 and P7 of mouse is 2.53mm and of jerboa is 4.82mm.

In addition to correlated bone elongation, as muscle disappears, it is seamlessly replaced by dense fibrous connective tissue. The correlative phenotypic changes in jerboa hindlimb development are unlikely to be coincidental. The development of tendon, muscle, muscle connective tissue, and bone are known to influence each other to allow for accommodative changes in limb morphology [100,320]. Investigation of signaling pathways known to act as crosstalk-agents between different tissues in the limb will provide information on external cues that are important for not only muscle loss but also the correlative changes in tissue such as the tendon.

For example, TGFβ is a secreted factor with pleiotropic effects on muscle, tendon, and bone development and can act as effector of mechanical strain. TGFβ is a well-known factor in inducing fibroblast proliferation and collagen deposition, thus promoting muscle fibrosis [238,321]. TGFβ is also necessary for the development, growth, and maintenance of tendon [322]. Elevated levels of TGFβ (via exogenous introduction of recombinant TGFβ) or constitutive activation of TGFβ receptor in mouse hindlimb muscle led to muscle atrophy accompanied by increased pro-Collagen I [323,324]. The authors also reported increased *Atrogin-1* expression, likely responsible for the muscle atrophy phenotype while increased Scleraxis, a known tendon and collagen promoting factor, is responsible for increased fibrotic tissue [323]. The transcriptome analysis of jerboa and mouse P0 foot muscle showed that TGFβ is upregulated in jerboa foot muscle compared to mouse, consistent with the jerboa phenotype of muscle loss and tendon expansion. Experimental manipulation of TGFβ signaling *in-vivo,* such as utilizing small molecule inhibitors [325], can dissect the role of TGFβ signaling in jerboa foot muscle loss. For example, if TGFβ facilitates both tendon

proliferation and muscle loss, inhibition of TGFβ signaling will perturb tendon growth while perhaps partially rescuing myofiber numbers.

4.6 Additional remarks

Of the 33 species within the Dipodoidea family, existing morphological data showed varying degree of hindlimb length, metatarsal fusion, and muscle loss [202,203,317]. A meta-analysis of foot morphological data can address question such as does increased hindlimb length correlate with increased muscle loss across the Dipodoidea family? In addition, future studies of morphological data combined with genomic data from different represented hindlimb morphologies in the jerboa family will be valuable for analysis of evolutionary trajectories of developmental genes. We can identify changes in cis-regulatory elements as well as signatures of adaptive evolution within specific genes involved in the development of bone and muscle, the two most modified tissues. Similar studies have been done to understand the evolution of limb loss in snake, a more extreme phenotype loss [326,327]. However, the loss of entire limb element means degeneration of key developmental pathway may be a cause or consequent of limb loss. In contrast, in a less severe phenotype loss, perhaps few genes are affected and thus one can functionally test if specific genetic component can rescue muscle loss. The jerboa, with its varying degree of bone elongation, fusion and muscle loss, provides a model to functionally test hypothesis that complex phenotypes can arise by, or be amplified by, accommodative changes in integrated tissues.

4.7 Concluding statement

Over a century ago, Cunningham observed fat and fibrotic tissue infiltration that replaced the disappearing foot muscles in his examinations of fetal tissue of animals, which lose the intrinsic foot muscles, such horses or deers. He proposed the idea that “it is an instance of *pathological* change assisting a *morphological* process” [210]. Now aided with molecular and genetic tools, we identify that natural muscle loss in jerboa exhibits shared molecular characteristics with diseased atrophic processes. Along with others, my work suggests that evolution and disease are intricately linked and demonstrates that evolution is a powerful tool to inform us about the broader principles of cell biology.

LIST OF REFERENCES

1. Hill Archibald Vivian (1938). The heat of shortening and the dynamic constants of muscle. Proceedings of the Royal Society of London. Series B - Biological Sciences *126*, 136–195.

2. Finanger, E., Vandenborne, K., Finkel, R.S., Lee Sweeney, H., Tennekoon, G., Yum, S., Mancini, M., Bista, P., Nichols, A., Liu, H., *et al.* (2019). Phase 1 Study of Edasalonexent (CAT-1004), an Oral NF-κB Inhibitor, in Pediatric Patients with Duchenne Muscular Dystrophy. J Neuromuscul Dis *6*, 43–54.

3. Evans, D.J.R., and Noden, D.M. (2006). Spatial relations between avian craniofacial neural crest and paraxial mesoderm cells. Dev. Dyn. *235*, 1310–1325.

4. Chevallier, A., Kieny, M., and Mauger, A. (1977). Limb-somite relationship: origin of the limb musculature. Journal of embryology and experimental morphology *41*, 245–58.

5. Hayashi, K., and Ozawa, E. (1991). Vital labelling of somite-derived myogenic cells in the chicken limb bud. Roux's Archives of Developmental Biology *200*, 188–192.

6. Gilbert, S., F. (2014). Developmental Biology 10th ed. (Sunderland, Massachusetts: Sinauer Associates, Incorporated Publishers).

7. Ordahl, C.P., and Le Douarin, N.M. (1992). Two myogenic lineages within the developing somite. Development *114*, 339–353.

8. Brand-Saberi, B., Wilting, J., Ebensperger, C., and Christ, B. (1996). The formation of somite compartments in the avian embryo. Int. J. Dev. Biol. *40*, 411–420.

9. Kato, N., and Aoyama, H. (1998). Dermomyotomal origin of the ribs as revealed by extirpation and transplantation experiments in chick and quail embryos. Development *125*, 3437–3443.

10. Atit, R., Sgaier, S.K., Mohamed, O.A., Taketo, M.M., Dufort, D., Joyner, A.L., Niswander, L., and Conlon, R.A. (2006). Beta-catenin activation is necessary and sufficient to specify the dorsal dermal fate in the mouse. Dev. Biol. *296*, 164–176.

11. Chevallier, A., Kieny, M., and Mauger, A. (1977). Limb-somite relationship: origin of the limb musculature. Journal of embryology and experimental morphology *41*, 245–58.

12. Christ, B., Jacob, H.J., and Jacob, M. (1977). Experimental analysis of the origin of the wing musculature in avian embryos. Anatomy and Embryology *150*, 171–186.

13. Hayashi, K., and Ozawa, E. (1991). Vital labelling of somite-derived myogenic cells in the chicken limb bud. Roux's Archives of Developmental Biology *200*, 188–192.

14. Murphy, M., and Kardon, G. (2011). Origin of vertebrate limb muscle: the role of progenitor and myoblast populations.

15. Kardon, G. (1998). Muscle and tendon morphogenesis in the avian hind limb. Development *125*, 4019–4032.

16. Kardon, G., Harfe, B.D., and Tabin, C.J. (2003). A Tcf4-positive mesodermal population provides a prepattern for vertebrate limb muscle patterning. Dev. Cell *5*, 937–944.

17. Wortham, R.A. (1948). The development of the muscles and tendons in the lower leg and foot of chick embryos. Journal of Morphology *83*, 105–148.

18. Christ, B., Jacob, H.J., and Jacob, M. (1977). Experimental analysis of the origin of the wing musculature in avian embryos. Anatomy and Embryology *150*, 171–186.

19. Tajbakhsh, S., and Spörle, R. (1998). Somite Development: Constructing the Vertebrate Body. Cell *92*, 9–16.

20. Münsterberg, A.E., Kitajewski, J., Bumcrot, D.A., McMahon, A.P., and Lassar, A.B. (1995). Combinatorial signaling by Sonic hedgehog and Wnt family members induces myogenic bHLH gene expression in the somite. Genes Dev. *9*, 2911–2922.

21. Stern, H.M., Brown, A.M., and Hauschka, S.D. (1995). Myogenesis in paraxial mesoderm: preferential induction by dorsal neural tube and by cells expressing Wnt-1. Development *121*, 3675–3686.

22. Borycki, A., Brown, A.M., and Emerson, C.P. (2000). Shh and Wnt signaling pathways converge to control Gli gene activation in avian somites. Development *127*, 2075–2087.

23. Chal, J., and Pourquié, O. (2017). Making muscle: skeletal myogenesis in vivo and in vitro. Development *144*, 2104–2122.

24. Tremblay, P., Dietrich, S., Mericskay, M., Schubert, F.R., Li, Z., and Paulin, D. (1998). A crucial role for Pax3 in the development of the hypaxial musculature and the long-range migration of muscle precursors. Dev. Biol. *203*, 49–61.

25. Daston, G., Lamar, E., Olivier, M., and Goulding, M. (1996). Pax-3 is necessary for migration but not differentiation of limb muscle precursors in the mouse. Development *122*, 1017–1027.

26. Hu, J.K.-H., McGlinn, E., Harfe, B.D., Kardon, G., and Tabin, C.J. (2012). Autonomous and nonautonomous roles of Hedgehog signaling in regulating limb muscle formation. Genes & development *26*, 2088–102.

27. Murphy, M., and Kardon, G. (2011). Origin of vertebrate limb muscle: the role of progenitor and myoblast populations. Available at: http://www.ncbi.nlm.nih.gov/pubmed/21621065.

28. Sartorelli, V., and Juan, A.H. (2011). Chapter three - Sculpting Chromatin Beyond the Double Helix: Epigenetic Control of Skeletal Myogenesis. In Current Topics in Developmental Biology Myogenesis., G. k. Pavlath, ed. (Academic Press), pp. 57–83. Available at: http://www.sciencedirect.com/science/article/pii/B9780123859402000036.

29. Kassar-Duchossoy, L., Gayraud-Morel, B., Gomès, D., Rocancourt, D., Buckingham, M., Shinin, V., and Tajbakhsh, S. (2004). Mrf4 determines skeletal muscle identity in Myf5:Myod double-mutant mice. Nature *431*, 466–471.

30. Hinterberger, T.J., Sassoon, D.A., Rhodes, S.J., and Konieczny, S.F. (1991). Expression of the muscle regulatory factor MRF4 during somite and skeletal myofiber development. Dev. Biol. *147*, 144–156.

31. Rudnicki, M.A., Braun, T., Hinuma, S., and Jaenisch, R. (1992). Inactivation of MyoD in mice leads to up-regulation of the myogenic HLH gene Myf-5 and results in apparently normal muscle development. Cell *71*, 383–390.

32. Braun, T., Rudnicki, M.A., Arnold, H.H., and Jaenisch, R. (1992). Targeted inactivation of the muscle regulatory gene Myf-5 results in abnormal rib development and perinatal death. Cell *71*, 369–382.

33. Rudnicki, M.A., Schnegelsberg, P.N., Stead, R.H., Braun, T., Arnold, H.H., and Jaenisch, R. (1993). MyoD or Myf-5 is required for the formation of skeletal muscle. Cell *75*, 1351–1359.

34. Tapscott, S.J. (2005). The circuitry of a master switch: Myod and the regulation of skeletal muscle gene transcription. Development *132*, 2685–2695.

35. Davis, R.L., Weintraub, H., and Lassar, A.B. (1987). Expression of a single transfected cDNA converts fibroblasts to myoblasts. Cell *51*, 987–1000.

36. Hasty, P., Bradley, A., Morris, J.H., Edmondson, D.G., Venuti, J.M., Olson, E.N., and Klein, W.H. (1993). Muscle deficiency and neonatal death in mice with a targeted mutation in the myogenin gene. Nature *364*, 501–6.

37. Nabeshima, Y., Hanaoka, K., Hayasaka, M., Esumi, E., Li, S., Nonaka, I., and Nabeshima, Y. (1993). Myogenin gene disruption results in perinatal lethality because of severe muscle defect. Nature *364*, 532–5.

38. Resnicow, D.I., Deacon, J.C., Warrick, H.M., Spudich, J.A., and Leinwand, L.A. (2010). Functional diversity among a family of human skeletal muscle myosin motors. PNAS *107*, 1053–1058.

39. Schiaffino, S., Reggiani, C., Acevedo, LM., Rivero, JL., Ackermann, MA., Kontrogianni-Konstantopoulos, A., Adams, GR., Haddad, F., McCue, SA., Bodell, PW., *et al.* (2011). Fiber types in mammalian skeletal muscles. Physiological reviews *91*, 1447–531.

40. Grifone, R., Laclef, C., Spitz, F., Lopez, S., Demignon, J., Guidotti, J.-E., Kawakami, K., Xu, P.-X., Kelly, R., Petrof, B.J., *et al.* (2004). Six1 and Eya1 expression can reprogram adult muscle from the slow-twitch phenotype into the fast-twitch phenotype. Mol. Cell. Biol. *24*, 6253–6267.

41. Richard, A.-F., Demignon, J., Sakakibara, I., Pujol, J., Favier, M., Strochlic, L., Le Grand, F., Sgarioto, N., Guernec, A., Schmitt, A., *et al.* (2011). Genesis of muscle fiber-type diversity during mouse embryogenesis relies on Six1 and Six4 gene expression. Developmental Biology *359*, 303–320.

42. Kelly, R.G., Zammit, P.S., Schneider, A., Alonso, S., Biben, C., and Buckingham, M.E. (1997). Embryonic and fetal myogenic programs act through separate enhancers at the MLC1F/3F locus. Dev. Biol. *187*, 183–199.

43. Biressi, S., Tagliafico, E., Lamorte, G., Monteverde, S., Tenedini, E., Roncaglia, E., Ferrari, S., Ferrari, S., Cusella-De Angelis, M.G., Tajbakhsh, S., *et al.* (2007). Intrinsic phenotypic diversity of embryonic and fetal myoblasts is revealed by genome-wide gene expression analysis on purified cells. Dev. Biol. *304*, 633–651.

44. Stockdale, F.E. (1992). Myogenic cell lineages. Dev. Biol. *154*, 284–298.

45. Biressi, S., Molinaro, M., and Cossu, G. (2007). Cellular heterogeneity during vertebrate skeletal muscle development. Developmental Biology *308*, 281–293.

46. Ross, J., Duxson, M., and Harris, A. (1987). Formation of primary and secondary myotubes in rat lumbrical muscles. Development *100*, 383–394.

47. Kassar-Duchossoy, L., Giacone, E., Gayraud-Morel, B., Jory, A., Gomès, D., and Tajbakhsh, S. (2005). Pax3/Pax7 mark a novel population of primitive myogenic cells during development. Genes Dev. *19*, 1426–1431.

48. Gros, J., Manceau, M., Thomé, V., and Marcelle, C. (2005). A common somitic origin for embryonic muscle progenitors and satellite cells. Nature *435*, 954–958.

49. Zammit, P.S., Relaix, F., Nagata, Y., Ruiz, A.P., Collins, C.A., Partridge, T.A., Beauchamp, J.R., Virtanen, K.A., Nuutila, P., and Schaart, G. (2006). Pax7 and myogenic progression in skeletal muscle satellite cells. Journal of cell science *119*, 1824–32.

50. Mauro, A. (1961). Satellite cell of skeletal muscle fibers. J Biophys Biochem Cytol *9*, 493–495.

51. Frontera, W.R., and Ochala, J. (2015). Skeletal muscle: a brief review of structure and function. Calcified tissue international *96*, 183–195.

52. Irintchev, A., Zeschnigk, M., Starzinski-Powitz, A., and Wernig, A. (1994). Expression pattern of M-cadherin in normal, denervated, and regenerating mouse muscles. Dev. Dyn. *199*, 326–337.

53. Allen, R.E., Sheehan, S.M., Taylor, R.G., Kendall, T.L., and Rice, G.M. (1995). Hepatocyte growth factor activates quiescent skeletal muscle satellite cells in vitro. J. Cell. Physiol. *165*, 307–312.

54. Burkin, D.J., and Kaufman, S.J. (1999). The alpha7beta1 integrin in muscle development and disease. Cell Tissue Res. *296*, 183–190.

55. Beauchamp, J.R., Heslop, L., Yu, D.S., Tajbakhsh, S., Kelly, R.G., Wernig, A., Buckingham, M.E., Partridge, T.A., and Zammit, P.S. (2000). Expression of CD34 and Myf5 defines the majority of quiescent adult skeletal muscle satellite cells. J. Cell Biol. *151*, 1221–1234.

56. Cornelison, D.D., Filla, M.S., Stanley, H.M., Rapraeger, A.C., and Olwin, B.B. (2001). Syndecan-3 and syndecan-4 specifically mark skeletal muscle satellite cells and are implicated in satellite cell maintenance and muscle regeneration. Dev. Biol. *239*, 79–94.

57. White, R.B., Biérinx, A.-S., Gnocchi, V.F., and Zammit, P.S. (2010). Dynamics of muscle fibre growth during postnatal mouse development. BMC developmental biology *10*, 21.

58. Chiakulas, J.J., and Pauly, J.E. (1965). A study of postnatal growth of skeletal muscle in the rat. The Anatomical record *152*, 55–61.

59. Gokhin, D.S., Ward, S.R., Bremner, S.N., and Lieber, R.L. (2008). Quantitative analysis of neonatal skeletal muscle functional improvement in the mouse. J. Exp. Biol. *211*, 837–843.

60. White, R.B., Biérinx, A.-S., Gnocchi, V.F., and Zammit, P.S. (2010). Dynamics of muscle fibre growth during postnatal mouse development. BMC developmental biology *10*, 21.

61. Hellmuth, A.E., and Allbrook, D.B. (1971). Muscle satellite cell numbers during the postnatal period. J. Anat. *110*, 503.

62. Allbrook, D.B., Han, M.F., and Hellmuth, A.E. (1971). Population of muscle satellite cells in relation to age and mitotic activity. Pathology *3*, 223–243.

63. Schmalbruch, H., and Hellhammer, U. (1976). The number of satellite cells in normal human muscle. Anat. Rec. *185*, 279–287.

64. Liu, N., Garry, G.A., Li, S., Bezprozvannaya, S., Sanchez-Ortiz, E., Chen, B., Shelton, J.M., Jaichander, P., Bassel-Duby, R., and Olson, E.N. (2017). A Twist2-Dependent Progenitor Cell Contributes to Adult Skeletal Muscle. Nat Cell Biol *19*, 202–213.

65. Morkin, E. (1970). Postnatal muscle fiber assembly: localization of newly synthesized myofibrillar proteins. Science *167*, 1499–1501.

66. Bodine, S.C., Stitt, T.N., Gonzalez, M., Kline, W.O., Stover, G.L., Bauerlein, R., Zlotchenko, E., Scrimgeour, A., Lawrence, J.C., Glass, D.J., *et al.* (2001). Akt/mTOR pathway is a crucial regulator of skeletal muscle hypertrophy and can prevent muscle atrophy in vivo. Nature Cell Biology *3*, 1014.

67. Tidball, J.G. (2011). Mechanisms of muscle injury, repair, and regeneration. Compr Physiol *1*, 2029–2062.

68. McPherron, A.C., Lawler, A.M., and Lee, S.J. (1997). Regulation of skeletal muscle mass in mice by a new TGF-beta superfamily member. Nature *387*, 83–90.

69. McPherron, A.C., and Lee, S.J. (1997). Double muscling in cattle due to mutations in the myostatin gene. Proc. Natl. Acad. Sci. U.S.A. *94*, 12457–12461.

70. Wang, Y.X., and Rudnicki, M.A. (2012). Satellite cells, the engines of muscle repair. Nature Reviews Molecular Cell Biology *13*, 127–133.

71. Rudnicki, M.A., Grand, F.L., McKinnell, I., and Kuang, S. (2008). The Molecular Regulation of Muscle Stem Cell Function. Cold Spring Harb Symp Quant Biol *73*, 323–331.

72. Fukada, S., Yamaguchi, M., Kokubo, H., Ogawa, R., Uezumi, A., Yoneda, T., Matev, M.M., Motohashi, N., Ito, T., Zolkiewska, A., *et al.* (2011). Hesr1 and Hesr3 are essential to generate undifferentiated quiescent satellite cells and to maintain satellite cell numbers. Development *138*, 4609–4619.

73. Mourikis, P., Sambasivan, R., Castel, D., Rocheteau, P., Bizzarro, V., and Tajbakhsh, S. (2012). A Critical Requirement for Notch Signaling in Maintenance of the Quiescent Skeletal Muscle Stem Cell State. STEM CELLS *30*, 243–252.

74. Bjornson, C.R.R., Cheung, T.H., Liu, L., Tripathi, P.V., Steeper, K.M., and Rando, T.A. (2012). Notch signaling is necessary to maintain quiescence in adult muscle stem cells. Stem Cells *30*, 232–242.

75. Tatsumi, R., Liu, X., Pulido, A., Morales, M., Sakata, T., Dial, S., Hattori, A., Ikeuchi, Y., and Allen, R.E. (2006). Satellite cell activation in stretched skeletal muscle and the role of nitric oxide and hepatocyte growth factor. Am. J. Physiol., Cell Physiol. *290*, C1487-1494.

76. Brack, A.S., Conboy, I.M., Conboy, M.J., Shen, J., and Rando, T.A. (2008). A temporal switch from notch to Wnt signaling in muscle stem cells is necessary for normal adult myogenesis. Cell Stem Cell *2*, 50–59.

77. Mathew, S.J., Hansen, J.M., Merrell, A.J., Murphy, M.M., Lawson, J. a, Hutcheson, D. a, Hansen, M.S., Angus-Hill, M., and Kardon, G. (2011). Connective tissue fibroblasts and Tcf4 regulate myogenesis. Development (Cambridge, England) *138*, 371–84.

78. Palacios, D., Mozzetta, C., Consalvi, S., Caretti, G., Saccone, V., Proserpio, V., Marquez, V.E., Valente, S., Mai, A., Forcales, S.V., *et al.* (2010). TNF/p38α/polycomb signaling to Pax7 locus in satellite cells links inflammation to the epigenetic control of muscle regeneration. Cell Stem Cell *7*, 455–469.

79. Frasch, M. (2016). Dedifferentiation, Redifferentiation, and Transdifferentiation of Striated Muscles During Regeneration and Development. Current Topics in Developmental Biology *116*, 331–355.

80. Tabebordbar, M., Wang, E.T., and Wagers, A.J. (2013). Skeletal muscle degenerative diseases and strategies for therapeutic muscle repair. Annual review of pathology *8*, 441–75.

81. Goebel, H.H., Sewry, C., and Weller, R. eds. (2013). Muscle Disease (Oxford, UK: John Wiley & Sons, Ltd) Available at: http://doi.wiley.com/10.1002/9781118635469.

82. Hay, E.D. (1959). Electron microscopic observations of muscle dedifferentiation in regenerating Amblystoma limbs. Developmental Biology *1*, 555–585.

83. Tanaka, E.M., Gann, A.A.F., Gates, P.B., and Brockes, J.P. (1997). Newt Myotubes Reenter the Cell Cycle by Phosphorylation of the Retinoblastoma Protein. The Journal of Cell Biology *136*, 155–165.

84. Kumar, A., Velloso, C.P., Imokawa, Y., and Brockes, J.P. (2000). Plasticity of Retrovirus-Labelled Myotubes in the Newt Limb Regeneration Blastema. Developmental Biology *218*, 125–136.

85. Gallant, J.R., Traeger, L.L., Volkening, J.D., Moffett, H., Chen, P.-H., Novina, C.D., Phillips, G.N., Anand, R., Wells, G.B., Pinch, M., *et al.* (2014). Nonhuman genetics. Genomic basis for the convergent evolution of electric organs. Science (New York, N.Y.) *344*, 1522–5.

86. Unguez, G.A., and Zakon, H.H. (1998). Reexpression of myogenic proteins in mature electric organ after removal of neural input. The Journal of neuroscience : the official journal of the Society for Neuroscience *18*, 9924–35.

87. Johnston, I.A., and Herring, P.J. (1985). The Transformation of Muscle into Bioluminescent Tissue in the Fish Benthalbella infans Zagmayer. Proceedings of the Royal Society of London. Series B, Biological Sciences *225*, 213–218.

88. Sohal, G.S., and Holt, R.K. (1980). Role of innervation on the embryonic development of skeletal muscle. Cell Tissue Res. *210*, 383–393.

89. Wilson, S.J., and Harris, A.J. (1993). Formation of Myotubes in Aneural Rat Muscles. Developmental Biology *156*, 509–518.

90. Ashby, P.R., Wilson, S.J., and Harris, A.J. (1993). Formation of primary and secondary myotubes in aneural muscles in the mouse mutant peroneal muscular atrophy. Developmental biology *156*, 519–28.

91. Purves, D., and Lichtman, J.W. (1980). Elimination of synapses in the developing nervous system. Science *210*, 153–157.

92. Colman, H., Nabekura, J., and Lichtman, J.W. (1997). Alterations in synaptic strength preceding axon withdrawal. Science *275*, 356–361.

93. Yang, X., Arber, S., William, C., Li, L., Tanabe, Y., Jessell, T.M., Birchmeier, C., and Burden, S.J. (2001). Patterning of muscle acetylcholine receptor gene expression in the absence of motor innervation. Neuron *30*, 399–410.

94. Buller, A.J., Eccles, J.C., and Eccles, R.M. (1960). Interactions between motoneurones and muscles in respect of the characteristic speeds of their responses. J Physiol *150*, 417–439.

95. Buller, A.J., and Pope, R. (1977). Plasticity in mammalian skeletal muscle. Philos. Trans. R. Soc. Lond., B, Biol. Sci. *278*, 295–305.

96. Robbins, N., Karpati, G., and Engel, W.K. (1969). Histochemical and contractile properties in the cross-innervated guinea pig soleus muscle. Arch. Neurol. *20*, 318–329.

97. Christ, B., and Brand-Saberi, B. (2002). Limb muscle development. The International journal of developmental biology *914*, 905–914.

98. Kardon, G. (1998). Muscle and tendon morphogenesis in the avian hind limb. Development (Cambridge, England) *125*, 4019–32.

99. Crawford, G.N.C. (1954). An experimental study of muscle growth in the rabbit. Bone & Joint Journal *36-B*.

100. Tsutsumi, R., Tran, M.P., and Cooper, K.L. (2017). Changing While Staying the Same: Preservation of Structural Continuity During Limb Evolution by Developmental Integration. Integrative and Comparative Biology *57*, 1269–1280.

101. Gordon, A.M., Huxley, A.F., and Julian, F.J. (1966). The variation in isometric tension with sarcomere length in vertebrate muscle fibres. J. Physiol. (Lond.) *184*, 170–192.

102. Julian, F.J., and Morgan, D.L. (1979). Intersarcomere dynamics during fixed-end tetanic contractions of frog muscle fibres. J. Physiol. (Lond.) *293*, 365–378.

103. Hill, A.V. (1953). The mechanics of active muscle. Proc. R. Soc. Lond., B, Biol. Sci. *141*, 104–117.

104. Burkholder, T.J., and Lieber, R.L. (2001). Sarcomere length operating range of vertebrate muscles during movement. The Journal of experimental biology *204*, 1529–36.

105. Williams, P.E., and Goldspink, G. (1978). Changes in sarcomere length and physiological properties in immobilized muscle. J Anat *127*, 459–468.

106. Rhee, D., Sanger, J.M., and Sanger, J.W. (1994). The premyofibril: evidence for its role in myofibrillogenesis. Cell motility and the cytoskeleton *28*, 1–24.

107. Sanger, J.M., and Sanger, J.W. (2008). The dynamic Z bands of striated muscle cells. Science signaling *1*, pe37.

108. Sanger, J.W., Chowrashi, P., Shaner, N.C., Spalthoff, S., Wang, J., Freeman, N.L., and Sanger, J.M. (2002). Myofibrillogenesis in skeletal muscle cells. Clinical orthopaedics and related research, S153-62.

109. Ono, S. (2010). Dynamic regulation of sarcomeric actin filaments in striated muscle. Cytoskeleton (Hoboken, N.J.) *67*, 677–92.

110. Furst, D.O., Fürst, D.O., Osborn, M., and Weber, K. (1989). Myogenesis in the mouse embryo: differential onset of expression of myogenic proteins and the involvement of titin in myofibril assembly. The Journal of cell biology *109*, 517–27.

111. Sanger, J.W., Wang, J., Fan, Y., White, J., and Sanger, J.M. (2010). Assembly and dynamics of myofibrils. Journal of biomedicine & biotechnology *2010*, 858606.

112. van der Ven, P.F., and Fürst, D.O. (1997). Assembly of titin, myomesin and M-protein into the sarcomeric M band in differentiating human skeletal muscle cells in vitro. Cell structure and function *22*, 163–171.

113. Ehler, E., and Gautel, M. (2008). The Sarcomere and Sarcomerogenesis. In The Sarcomere and Skeletal Muscle Disease Advances in Experimental Medicine and Biology., N. G. Laing, ed. (New York, NY: Springer New York), pp. 1–14.

114. Ono, S. (2010). Dynamic regulation of sarcomeric actin filaments in striated muscle. Cytoskeleton (Hoboken, N.J.) *67*, 677–92.

115. Huxley, H.E. (1957). The double array of filaments in cross-striated muscle. J Biophys Biochem Cytol *3*, 631–648.

116. Schultheiss, T., Lin, Z.X., Lu, M.H., Murray, J., Fischman, D.A., Weber, K., Masaki, T., Imamura, M., and Holtzer, H. (1990). Differential distribution of subsets of myofibrillar proteins in cardiac nonstriated and striated myofibrils. J. Cell Biol. *110*, 1159–1172.

117. Holtzer, H., Hijikata, T., Lin, Z.X., Zhang, Z.Q., Holtzer, S., Protasi, F., Franzini-Armstrong, C., and Sweeney, H.L. (1997). Independent assembly of 1.6 microns long bipolar MHC filaments and I-Z-I bodies. Cell Struct. Funct. *22*, 83–93.

118. Casella, J.F., Craig, S.W., Maack, D.J., and Brown, A.E. (1987). Cap Z(36/32), a barbed end actin-capping protein, is a component of the Z-line of skeletal muscle. J. Cell Biol. *105*, 371–379.

119. Fowler, V.M., Sussmann, M.A., Miller, P.G., Flucher, B.E., and Daniels, M.P. (1993). Tropomodulin is associated with the free (pointed) ends of the thin filaments in rat skeletal muscle. J. Cell Biol. *120*, 411–420.

120. Littlefield, R., Almenar-Queralt, A., and Fowler, V.M. (2001). Actin dynamics at pointed ends regulates thin filament length in striated muscle. Nat. Cell Biol. *3*, 544–551.

121. Nagaoka, R., Kusano, K., Abe, H., and Obinata, T. (1995). Effects of cofilin on actin filamentous structures in cultured muscle cells. Intracellular regulation of cofilin action. J. Cell. Sci. *108 (Pt 2)*, 581–593.

122. Agrawal, P.B., Greenleaf, R.S., Tomczak, K.K., Lehtokari, V.-L., Wallgren-Pettersson, C., Wallefeld, W., Laing, N.G., Darras, B.T., Maciver, S.K., Dormitzer, P.R., *et al.* (2007). Nemaline myopathy with minicores caused by mutation of the CFL2 gene encoding the skeletal muscle actin-binding protein, cofilin-2. Am. J. Hum. Genet. *80*, 162–167.

123. Zak, R., Martin, A.F., Prior, G., and Rabinowitz, M. (1977). Comparison of Turnover of Several Myofibrillar Proteins and Critical Evaluation of Double Isotope Method*. The Journal of Biological Chemistry *252*, 3430–3435.

124. Bönnemann, C.G., and Laing, N.G. (2004). Myopathies resulting from mutations in sarcomeric proteins. Current opinion in neurology *17*, 529–37.

125. Laing, N.G., and Nowak, K.J. (2005). When contractile proteins go bad: the sarcomere and skeletal muscle disease. BioEssays : news and reviews in molecular, cellular and developmental biology *27*, 809–22.

126. Morita, H., Seidman, J., and Seidman, C.E. (2005). Genetic causes of human heart failure. The Journal of clinical investigation *115*, 518–26.

127. Rhee, D., Sanger, J.M., and Sanger, J.W. (1994). The premyofibril: evidence for its role in myofibrillogenesis. Cell motility and the cytoskeleton *28*, 1–24.

128. Whalen, R.G., Sell, S.M., Butler-Browne, G.S., Schwartz, K., Bouveret, P., and Pinset-Härström, I. (1981). Three myosin heavy-chain isozymes appear sequentially in rat muscle development. Nature *292*, 805–809.

129. HILL, A.V. (1950). THE DIMENSIONS OF ANIMALS AND THEIR MUSCULAR DYNAMICS. Science Progress (1933-) *38*, 209–230.

130. Pellegrino, M.A., Canepari, M., Rossi, R., D'Antona, G., Reggiani, C., and Bottinelli, R. (2003). Orthologous myosin isoforms and scaling of shortening velocity with body size in mouse, rat, rabbit and human muscles. J. Physiol. (Lond.) *546*, 677–689.

131. Perry, S.V. (2001). Vertebrate tropomyosin: distribution, properties and function. Journal of Muscle Research and Cell Motility *22*, 5–49.

132. Thierfelder, L., Watkins, H., MacRae, C., Lamas, R., McKenna, W., Vosberg, H.P., Seidman, J.G., and Seidman, C.E. (1994). Alpha-tropomyosin and cardiac troponin T mutations cause familial hypertrophic cardiomyopathy: a disease of the sarcomere. Cell *77*, 701–712.

133. Broschat, K.O., Weber, A., and Burgess, D.R. (1989). Tropomyosin stabilizes the pointed end of actin filaments by slowing depolymerization. Biochemistry *28*, 8501–8506.

134. Wegner, A. (1982). Kinetic analysis of actin assembly suggests that tropomyosin inhibits spontaneous fragmentation of actin filaments. Journal of Molecular Biology *161*, 217–227.

135. Ono, S., and Ono, K. (2002). Tropomyosin inhibits ADF/cofilin-dependent actin filament dynamics. J Cell Biol *156*, 1065–1076.

136. Cooper, J.A. (2002). Actin dynamics: tropomyosin provides stability. Curr. Biol. *12*, R523-525.

137. Schachat, F.H., Canine, A.C., Briggs, M.M., and Reedy, M.C. (1985). The presence of two skeletal muscle alpha-actinins correlates with troponin-tropomyosin expression and Z-line width. J. Cell Biol. *101*, 1001–1008.

138. MacArthur, D.G., and North, K.N. (2004). A gene for speed? The evolution and function of α-actinin-3. BioEssays *26*, 786–795.

139. MacArthur, D.G., Seto, J.T., Raftery, J.M., Quinlan, K.G., Huttley, G.A., Hook, J.W., Lemckert, F.A., Kee, A.J., Edwards, M.R., Berman, Y., *et al.* (2007). Loss of ACTN3 gene function alters mouse muscle metabolism and shows evidence of positive selection in humans. Nat. Genet. *39*, 1261–1265.

140. Gupta, V., Discenza, M., Guyon, J.R., Kunkel, L.M., and Beggs, A.H. (2012). α-Actinin-2 deficiency results in sarcomeric defects in zebrafish that cannot be

rescued by α-actinin-3 revealing functional differences between sarcomeric isoforms. FASEB J *26*, 1892–1908.

141. Labeit, S., and Kolmerer, B. (1995). Titins: giant proteins in charge of muscle ultrastructure and elasticity. Science *270*, 293–296.

142. Sanger, J.W., Chowrashi, P., Shaner, N.C., Spalthoff, S., Wang, J., Freeman, N.L., and Sanger, J.M. (2002). Myofibrillogenesis in skeletal muscle cells. Clinical orthopaedics and related research, S153-62.

143. Sanger, J.W., Kang, S., Siebrands, C.C., Freeman, N., Du, A., Wang, J., Stout, A.L., and Sanger, J.M. (2006). How to build a myofibril. Journal of Muscle Research and Cell Motility *26*, 343–354.

144. Van der Ven, P.F., Ehler, E., Perriard, J.C., and Fürst, D.O. (1999). Thick filament assembly occurs after the formation of a cytoskeletal scaffold. J. Muscle Res. Cell. Motil. *20*, 569–579.

145. van der Loop, F.T., van der Ven, P.F., Fürst, D.O., Gautel, M., van Eys, G.J., and Ramaekers, F.C. (1996). Integration of titin into the sarcomeres of cultured differentiating human skeletal muscle cells. European journal of cell biology *69*, 301–7.

146. van der Ven, P.F., and Fürst, D.O. (1997). Assembly of titin, myomesin and M-protein into the sarcomeric M band in differentiating human skeletal muscle cells in vitro. Cell structure and function *22*, 163–171.

147. Fulton, A.B., and L'Ecuyer, T. (1993). Cotranslational assembly of some cytoskeletal proteins: implications and prospects. J. Cell. Sci. *105 (Pt 4)*, 867–871.

148. van der Ven, P.F., Bartsch, J.W., Gautel, M., Jockusch, H., and Furst, D.O. (2000). A functional knock-out of titin results in defective myofibril assembly. Journal of Cell Science *113*. Available at: http://jcs.biologists.org/content/113/8/1405.long [Accessed May 6, 2017].

149. Gotthardt, M., Hammer, R.E., Hübner, N., Monti, J., Witt, C.C., McNabb, M., Richardson, J.A., Granzier, H., Labeit, S., and Herz, J. (2003). Conditional expression of mutant M-line titins results in cardiomyopathy with altered sarcomere structure. J. Biol. Chem. *278*, 6059–6065.

150. Peng, J., Raddatz, K., Labeit, S., Granzier, H., and Gotthardt, M. (2005). Muscle atrophy in titin M-line deficient mice. Journal of muscle research and cell motility *26*, 381–8.

151. Agarkova, I., Schoenauer, R., Ehler, E., Carlsson, L., Carlsson, E., Thornell, L.-E., and Perriard, J.-C. (2004). The molecular composition of the sarcomeric M-band correlates with muscle fiber type. Eur. J. Cell Biol. *83*, 193–204.

152. Schoenauer, R., Lange, S., Hirschy, A., Ehler, E., Perriard, J.-C., and Agarkova, I. (2008). Myomesin 3, a novel structural component of the M-band in striated muscle. J. Mol. Biol. *376*, 338–351.

153. Obermann, W.M. (1996). The structure of the sarcomeric M band: localization of defined domains of myomesin, M-protein, and the 250-kD carboxy-terminal region of titin by immunoelectron microscopy. The Journal of Cell Biology *134*, 1441–1453.

154. Fürst, D.O., Obermann, W.M., and van der Ven, P.F. (1999). Structure and assembly of the sarcomeric M band. Rev. Physiol. Biochem. Pharmacol. *138*, 163–202.

155. Fukuzawa, A., Lange, S., Holt, M., Vihola, A., Carmignac, V., Ferreiro, A., Udd, B., and Gautel, M. (2008). Interactions with titin and myomesin target obscurin and obscurin-like 1 to the M-band – implications for hereditary myopathies. Journal of Cell Science *121*, 1841–1851.

156. Bär, H., Strelkov, S. V, Sjöberg, G., Aebi, U., and Herrmann, H. (2004). The biology of desmin filaments: how do mutations affect their structure, assembly, and organisation? Journal of structural biology *148*, 137–52.

157. Goldfarb, L.G., Olive, M., Vicart, P., and Goebel, H.H. (2008). Intermediate filament diseases: desminopathy. In The sarcomere and skeletal muscle disease, N. G. Laing, ed. (New York, NY: Landes Biosciences and Springer Science+Business Media, LLC), pp. 131–160.

158. Capetanaki, Y., Papathanasiou, S., Diokmetzidou, A., Vatsellas, G., and Tsikitis, M. (2015). Desmin related disease: A matter of cell survival failure. Current Opinion in Cell Biology *32*, 113–120.

159. Li, Z., Colucci-Guyon, E., Pinçon-Raymond, M., Mericskay, M., Pournin, S., Paulin, D., and Babinet, C. (1996). Cardiovascular lesions and skeletal myopathy in mice lacking desmin. Dev. Biol. *175*, 362–366.

160. Milner, D.J., Weitzer, G., Tran, D., Bradley, A., and Capetanaki, Y. (1996). Disruption of muscle architecture and myocardial degeneration in mice lacking desmin. J. Cell Biol. *134*, 1255–1270.

161. Capetanaki, Y., Papathanasiou, S., Diokmetzidou, A., Vatsellas, G., and Tsikitis, M. (2015). Desmin related disease: A matter of cell survival failure. Current Opinion in Cell Biology *32*, 113–120.

162. Clemen, C.S., Herrmann, H., Strelkov, S.V., and Schröder, R. (2013). Desminopathies: pathology and mechanisms. Acta Neuropathol *125*, 47–75.

163. Schröder, R., and Clemen, C.S. (2013). Desminopathies. In Muscle Disease (Oxford, UK: John Wiley & Sons, Ltd), pp. 178–184. Available at: http://doi.wiley.com/10.1002/9781118635469.ch20 [Accessed May 6, 2017].

164. Carmeli, E., Aizenbud, D., and Rom, O. (2015). How Do Skeletal Muscles Die? An Overview. In Advances in experimental medicine and biology, pp. 99–111. Available at: http://www.ncbi.nlm.nih.gov/pubmed/26017731 [Accessed April 30, 2017].

165. Elmore, S. (2007). Apoptosis: a review of programmed cell death. Toxicologic pathology *35*, 495–516.

166. Krysko, D.V., Vanden Berghe, T., Parthoens, E., D'Herde, K., and Vandenabeele, P. (2008). Methods for distinguishing apoptotic from necrotic cells and measuring their clearance. Methods in enzymology *442*, 307–41.

167. Dupont-Versteegden, E.E. (2006). Apoptosis in skeletal muscle and its relevance to atrophy. World journal of gastroenterology *12*, 7463–6.

168. Berghe, T. Vanden, Linkermann, A., Jouan-Lanhouet, S., Walczak, H., Vandenabeele, P., Vanden Berghe, T., Linkermann, A., Jouan-Lanhouet, S., Walczak, H., and Vandenabeele, P. (2014). Regulated necrosis: the expanding network of non-apoptotic cell death pathways. Nature Reviews Molecular Cell Biology *15*, 135–47.

169. Leist, M., Single, B., Castoldi, A.F., Kühnle, S., and Nicotera, P. (1997). Intracellular adenosine triphosphate (ATP) concentration: a switch in the decision between apoptosis and necrosis. J. Exp. Med. *185*, 1481–1486.

170. Schiaffino, S., Dyar, K.A., Ciciliot, S., Blaauw, B., and Sandri, M. (2013). Mechanisms regulating skeletal muscle growth and atrophy. FEBS Journal *280*, 4294–4314.

171. Bodine, S.C., and Baehr, L.M. (2014). Skeletal muscle atrophy and the E3 ubiquitin ligases MuRF1 and MAFbx/atrogin-1. American journal of physiology. Endocrinology and metabolism *307*, E469-84.

172. Bodine, S.C., Latres, E., Baumhueter, S., Lai, V.K., Nunez, L., Clarke, B.A., Poueymirou, W.T., Panaro, F.J., Na, E., Dharmarajan, K., *et al.* (2001). Identification of ubiquitin ligases required for skeletal muscle atrophy. Science (New York, N.Y.) *294*, 1704–8.

173. Cong, H., Sun, L., Liu, C., and Tien, P. (2011). Inhibition of atrogin-1/MAFbx expression by adenovirus-delivered small hairpin RNAs attenuates muscle atrophy in fasting mice. Hum. Gene Ther. *22*, 313–324.

174. Tintignac, L.A., Lagirand, J., Batonnet, S., Sirri, V., Leibovitch, M.P., and Leibovitch, S.A. (2005). Degradation of MyoD mediated by the SCF (MAFbx) ubiquitin ligase. J. Biol. Chem. *280*, 2847–2856.

175. Csibi, A., Cornille, K., Leibovitch, M.-P., Poupon, A., Tintignac, L.A., Sanchez, A.M.J., and Leibovitch, S.A. (2010). The translation regulatory subunit eIF3f controls the kinase-dependent mTOR signaling required for muscle differentiation and hypertrophy in mouse. PLoS ONE *5*, e8994.

176. Cohen, S., Zhai, B., Gygi, S.P., and Goldberg, A.L. (2012). Ubiquitylation by Trim32 causes coupled loss of desmin, Z-bands, and thin filaments in muscle atrophy. The Journal of Cell Biology *198*, 575–589.

177. Paul, P.K., Gupta, S.K., Bhatnagar, S., Panguluri, S.K., Darnay, B.G., Choi, Y., and Kumar, A. (2010). Targeted ablation of TRAF6 inhibits skeletal muscle wasting in mice. J Cell Biol *191*, 1395–1411.

178. Bonaldo, P., and Sandri, M. (2013). Cellular and molecular mechanisms of muscle atrophy. Disease Models & Mechanisms *6*, 25–39.

179. Sandri, M., Sandri, C., Gilbert, A., Skurk, C., Calabria, E., Picard, A., Walsh, K., Schiaffino, S., Lecker, S.H., and Goldberg, A.L. (2004). Foxo Transcription Factors Induce the Atrophy-Related Ubiquitin Ligase Atrogin-1 and Cause Skeletal Muscle Atrophy. Cell *117*, 399–412.

180. Reed, S.A., Sandesara, P.B., Senf, S.M., and Judge, A.R. (2012). Inhibition of FoxO transcriptional activity prevents muscle fiber atrophy during cachexia and induces hypertrophy. FASEB J. *26*, 987–1000.

181. Sanchez, A.M.J., Candau, R.B., and Bernardi, H. (2014). FoxO transcription factors: Their roles in the maintenance of skeletal muscle homeostasis. Cellular and Molecular Life Sciences *71*.

182. Milan, G., Romanello, V., Pescatore, F., Armani, A., Paik, J.-H., Frasson, L., Seydel, A., Zhao, J., Abraham, R., Goldberg, A.L., *et al.* (2015). Regulation of autophagy and the ubiquitin–proteasome system by the FoxO transcriptional network during muscle atrophy. Nature Communications *6*, 6670.

183. Ravikumar, B., Sarkar, S., Davies, J.E., Futter, M., Garcia-Arencibia, M., Green-Thompson, Z.W., Jimenez-Sanchez, M., Korolchuk, V.I., Lichtenberg, M., Luo, S., *et al.* (2010). Regulation of mammalian autophagy in physiology and pathophysiology. Physiological reviews *90*, 1383–435.

184. Grumati, P., and Bonaldo, P. (2012). Autophagy in skeletal muscle homeostasis and in muscular dystrophies. Cells *1*, 325–45.

185. Penna, F., Costamagna, D., Pin, F., Camperi, A., Fanzani, A., Chiarpotto, E.M., Cavallini, G., Bonelli, G., Baccino, F.M., and Costelli, P. (2013). Autophagic

degradation contributes to muscle wasting in cancer cachexia. Am. J. Pathol. *182*, 1367–1378.

186. Grumati, P., and Bonaldo, P. (2012). Autophagy in skeletal muscle homeostasis and in muscular dystrophies. Cells *1*, 325–45.

187. Mammucari, C., Milan, G., Romanello, V., Masiero, E., Rudolf, R., Del Piccolo, P., Burden, S.J., Di Lisi, R., Sandri, C., Zhao, J., *et al.* (2007). FoxO3 controls autophagy in skeletal muscle in vivo. Cell Metab. *6*, 458–471.

188. Zhao, J., Brault, J.J., Schild, A., Cao, P., Sandri, M., Schiaffino, S., Lecker, S.H., and Goldberg, A.L. (2007). FoxO3 coordinately activates protein degradation by the autophagic/lysosomal and proteasomal pathways in atrophying muscle cells. Cell Metab. *6*, 472–483.

189. Mizushima, N. (2007). Autophagy: process and function. Genes Dev. *21*, 2861–2873.

190. Kroemer, G., and Levine, B. (2008). Autophagic cell death: the story of a misnomer. Nat Rev Mol Cell Biol *9*, 1004–1010.

191. Denton, D., and Kumar, S. (2019). Autophagy-dependent cell death. Cell Death & Differentiation *26*, 605.

192. Peterson, J.M., Bakkar, N., and Guttridge, D.C. (2011). Chapter four - NF-κB Signaling in Skeletal Muscle Health and Disease. In Current Topics in Developmental Biology Myogenesis., G. k. Pavlath, ed. (Academic Press), pp. 85–119. Available at: http://www.sciencedirect.com/science/article/pii/B9780123859402000048.

193. Li, H., Malhotra, S., and Kumar, A. (2008). Nuclear Factor-kappa B Signaling in Skeletal Muscle Atrophy. J Mol Med (Berl) *86*, 1113–1126.

194. Hunter, R.B., and Kandarian, S.C. (2004). Disruption of either the Nfkb1 or the Bcl3 gene inhibits skeletal muscle atrophy. J. Clin. Invest. *114*, 1504–1511.

195. Judge, A.R., Koncarevic, A., Hunter, R.B., Liou, H.-C., Jackman, R.W., and Kandarian, S.C. (2007). Role for IkappaBalpha, but not c-Rel, in skeletal muscle atrophy. Am. J. Physiol., Cell Physiol. *292*, C372-382.

196. Van Gammeren, D., Damrauer, J.S., Jackman, R.W., and Kandarian, S.C. (2009). The IkappaB kinases IKKalpha and IKKbeta are necessary and sufficient for skeletal muscle atrophy. FASEB J. *23*, 362–370.

197. Cai, D., Frantz, J.D., Tawa, N.E., Melendez, P.A., Oh, B.-C., Lidov, H.G.W., Hasselgren, P.-O., Frontera, W.R., Lee, J., Glass, D.J., *et al.* (2004). IKKbeta/NF-kappaB activation causes severe muscle wasting in mice. Cell *119*, 285–98.

198. Diogo, R., Ziermann, J.M., Molnar, J., Siomava, N., Abdala, V., Ziermann, J.M., Molnar, J., Siomava, N., and Abdala, V. (2018). Muscles of Chordates : Development, Homologies, and Evolution (CRC Press) Available at: https://www.taylorfrancis.com/books/9780203702987.

199. Moro, S., and Abdala, V. (2004). Análisis descriptivo de la miología flexora y extensora del miembro anterior de Polychrus acutirostris (Squamata, Polychrotidae). Papéis Avulsos de Zoologia *44*, 81–89.

200. Young, R.W. (2003). Evolution of the human hand: the role of throwing and clubbing. J Anat *202*, 165–174.

201. Molnar, J.L., Diaz, R.E., Skorka, T., Dagliyan, G., and Diogo, R. (2017). Comparative musculoskeletal anatomy of chameleon limbs, with implications for the evolution of arboreal locomotion in lizards and for teratology. Journal of Morphology *278*, 1241–1261.

202. Berman, S.L. (1985). Convergent evolution in the hindlimb of bipedal rodents. Journal of Zoological Systematics and Evolutionary Research *23*, 59–77.

203. Moore, T.Y., Organ, C.L., Edwards, S.V., Biewener, A.A., Tabin, C.J., Jenkins, F.A., and Cooper, K.L. (2015). Multiple phylogenetically distinct events shaped the evolution of limb skeletal morphologies associated with bipedalism in the jerboas. Current Biology *25*, 2785–2794.

204. Hudson, G.E. (1937). Studies on the Muscles of the Pelvic Appendage in Birds. The American Midland Naturalist *18*, 1–108.

205. Raikow, R.J. (1987). Hindlimb Myology and Evolution of the Old World Suboscine Passerine Birds (Acanthisittidae, Pittidae, Philepittidae, Eurylaimidae). Ornithological Monographs, iii–81.

206. Pavaux, C., and Lignereux, Y. (1995). Une dissection myologique de la Jambe et du Pied de l'Autruche (Struthio camelus)*. Anatomia, Histologia, Embryologia *24*, 127–131.

207. Botelho, J.F., Smith-Paredes, D., Nuñez-Leon, D., Soto-Acuña, S., and Vargas, A.O. (2014). The developmental origin of zygodactyl feet and its possible loss in the evolution of Passeriformes. Proc Biol Sci *281*. Available at: https://www.ncbi.nlm.nih.gov/pmc/articles/PMC4083792/ [Accessed January 8, 2019].

208. Abdala, V., Grizante, M.B., Diogo, R., Molnar, J., and Kohlsdorf, T. (2015). Musculoskeletal anatomical changes that accompany limb reduction in lizards. Journal of Morphology *276*, 1290–1310.

209. Berman, S.L. (1985). Convergent evolution in the hindlimb of bipedal rodents. Journal of Zoological Systematics and Evolutionary Research *23*, 59–77.

210. Cunningham, D.J. (1883). The Development of the Suspensory Ligament of the Fetlock in the Foetal Horse, Ox, Roe-Deer, and Sambre-Deer. Journal of anatomy and physiology *18*, i1-12.

211. Souza, M.V., Van Weeren, P.R., Van Schie, H.T.M., and Van De Lest, C.H.A. (2010). Regional differences in biochemical, biomechanical and histomorphological characteristics of the equine suspensory ligament. Equine Veterinary Journal *42*, 611–620.

212. Cunningham, D.J. (1883). The Development of the Suspensory Ligament of the Fetlock in the Foetal Horse, Ox, Roe-Deer, and Sambre-Deer. Journal of anatomy and physiology *18*, i1-12.

213. Lieber, R.L., and Ward, S.R. (2013). Cellular Mechanisms of Tissue Fibrosis. 4. Structural and functional consequences of skeletal muscle fibrosis. American Journal of Physiology-Cell Physiology *305*, C241–C252.

214. Lochner, F.K., Milne, D.W., Mills, E.J., and Groom, J.J. (1980). In vivo and in vitro measurement of tendon strain in the horse. Am. J. Vet. Res. *41*, 1929–1937.

215. Moore, T.Y., Rivera, A.M., and Biewener, A.A. (2017). Vertical leaping mechanics of the Lesser Egyptian Jerboa reveal specialization for maneuverability rather than elastic energy storage. Frontiers in Zoology *14*, 32.

216. Stein, B.R. (1990). Limb myology and phylogenetic relationships in the superfamily Dipodoidea (birch mice, jumping mice, and jerboas). Journal of Zoological Systematics and Evolutionary Research *28*, 299–314.

217. Wu, S., Wu, W., Zhang, F., Ye, J., Ni, X., Sun, J., Edwards, S.V., Meng, J., and Organ, C.L. (2012). Molecular and Paleontological Evidence for a Post-Cretaceous Origin of Rodents. PLoS ONE *7*, e46445.

218. Pisano, J., Condamine, F.L., Lebedev, V., Bannikova, A., Quere, J.-P., Shenbrot, G.I., Pages, M., and Michaux, J.R. (2015). Out of Himalaya: the impact of past Asian environmental changes on the evolutionary and biogeographical history of Dipodoidea (Rodentia). J. Biogeogr. *42*, 856–870.

219. Kelly, A.M., and Zacks, S.I. (1969). The histogenesis of rat intercostal muscle. The Journal of cell biology *42*, 135–53.

220. Abmayr, S.M., and Pavlath, G.K. (2012). Myoblast fusion: lessons from flies and mice. Development *139*, 641–656.

221. Danoviz, M.E., and Yablonka-Reuveni, Z. (2012). Skeletal Muscle Satellite Cells: Background and Methods for Isolation and Analysis in a Primary Culture System. In Myogenesis: Methods and Protocols Methods in Molecular Biology., J. X. DiMario, ed. (Totowa, NJ: Humana Press), pp. 21–52. Available at: https://doi.org/10.1007/978-1-61779-343-1_2.

222. Fernández-Terán, M. a, Hinchliffe, J.R., and Ros, M. a (2006). Birth and death of cells in limb development: a mapping study. Developmental dynamics : an official publication of the American Association of Anatomists *235*, 2521–37.

223. Brill, A., Torchinsky, A., Carp, H., and Toder, V. (1999). The Role of Apoptosis in Normal and Abnormal Embryonic Development. J Assist Reprod Genet *16*, 512–519.

224. Elmore, S. (2007). Apoptosis: a review of programmed cell death. Toxicologic pathology *35*, 495–516.

225. Magerl, M., Tobin, D.J., Müller-Röver, S., Hagen, E., Lindner, G., McKay, I.A., and Paus, R. (2001). Patterns of Proliferation and Apoptosis during Murine Hair Follicle Morphogenesis. Journal of Investigative Dermatology *116*, 947–955.

226. Hamer, P.W., McGeachie, J.M., Davies, M.J., and Grounds, M.D. (2002). Evans Blue Dye as an in vivo marker of myofibre damage: optimising parameters for detecting initial myofibre membrane permeability. Journal of Anatomy *200*, 69–79.

227. Matsuda, R., Nishikawa, A., and Tanaka, H. (1995). Visualization of dystrophic muscle fibers in mdx mouse by vital staining with Evans blue: evidence of apoptosis in dystrophin-deficient muscle. Journal of biochemistry *118*, 959–64.

228. Arnold, L., Henry, A., Poron, F., Baba-Amer, Y., van Rooijen, N., Plonquet, A., Gherardi, R.K., and Chazaud, B. (2007). Inflammatory monocytes recruited after skeletal muscle injury switch into antiinflammatory macrophages to support myogenesis. The Journal of experimental medicine *204*, 1057–69.

229. Londhe, P., and Guttridge, D.C. (2015). Inflammation induced loss of skeletal muscle. Bone *80*, 131–42.

230. Tidball, J.G., and Wehling-Henricks, M. (2007). Macrophages promote muscle membrane repair and muscle fibre growth and regeneration during modified muscle loading in mice in vivo. The Journal of physiology *578*, 327–36.

231. Dymecki, S.M., Ray, R.S., and Kim, J.C. (2010). Mapping Cell Fate and Function Using Recombinase-Based Intersectional Strategies 2nd ed. (Elsevier Inc.).

232. Jaynes, J.B., Johnson, J.E., Buskin, J.N., Gartside, C.L., and Hauschka, S.D. (1988). The muscle creatine kinase gene is regulated by multiple upstream elements, including a muscle-specific enhancer. Molecular and cellular biology *8*, 62–70.

233. Fazeli, S. (1996). Altered secondary myogenesis in transgenic animals expressing the neural cell adhesion molecule under the control of a skeletal muscle alpha-actin promoter. The Journal of Cell Biology *135*, 241–251.

234. Sandoval-Guzmán, T., Wang, H., Khattak, S., Schuez, M., Roensch, K., Nacu, E., Tazaki, A., Joven, A., Tanaka, E.M., and Simon, A. (2014). Fundamental Differences in Dedifferentiation and Stem Cell Recruitment during Skeletal Muscle Regeneration in Two Salamander Species. Cell Stem Cell *14*, 174–187.

235. Borisov, A.B., Martynova, M.G., and Russell, M.W. (2008). Early incorporation of obscurin into nascent sarcomeres: implication for myofibril assembly during cardiac myogenesis. Histochemistry and cell biology *129*, 463–78.

236. Raeker, M.Ö., Shavit, J.A., Dowling, J.J., Michele, D.E., and Russell, M.W. (2014). Membrane-myofibril cross-talk in myofibrillogenesis and in muscular dystrophy pathogenesis: lessons from the zebrafish. Frontiers in Physiology *5*, 14.

237. Sanger, J.W., Kang, S., Siebrands, C.C., Freeman, N., Du, A., Wang, J., Stout, A.L., and Sanger, J.M. (2006). How to build a myofibril. Journal of Muscle Research and Cell Motility *26*, 343–354.

238. Mann, C.J., Perdiguero, E., Kharraz, Y., Aguilar, S., Pessina, P., Serrano, A.L., and Muñoz-Cánoves, P. (2011). Aberrant repair and fibrosis development in skeletal muscle. Skelet Muscle *1*, 21.

239. Clemen, C.S., Herrmann, H., Strelkov, S.V., and Schröder, R. (2013). Desminopathies: pathology and mechanisms. Acta Neuropathol. *125*, 47–75.

240. Volodin, A., Kosti, I., Goldberg, A.L., and Cohen, S. (2017). Myofibril breakdown during atrophy is a delayed response requiring the transcription factor PAX4 and desmin depolymerization. Proceedings of the National Academy of Sciences *114*, E1375–E1384.

241. Huang, A.H., Riordan, T.J., Wang, L., Eyal, S., Zelzer, E., Brigande, J.V., and Schweitzer, R. (2013). Repositioning forelimb superficialis muscles: tendon attachment and muscle activity enable active relocation of functional myofibers. Developmental cell *26*, 544–51.

242. Sakuma, K., Aoi, W., and Yamaguchi, A. (2015). Current understanding of sarcopenia: possible candidates modulating muscle mass. Pflügers Archiv - European Journal of Physiology *467*, 213–229.

243. von Haehling, S., Morley, J.E., and Anker, S.D. (2010). An overview of sarcopenia: facts and numbers on prevalence and clinical impact. J Cachexia Sarcopenia Muscle *1*, 129–133.

244. Moschella, M.C., and Ontell, M. (1987). Transient and chronic neonatal denervation of murine muscle: a procedure to modify the phenotypic expression of muscular dystrophy. Journal of Neuroscience *7*, 2145–2152.

245. Bruusgaard, J.C., and Gundersen, K. (2008). In vivo time-lapse microscopy reveals no loss of murine myonuclei during weeks of muscle atrophy. J. Clin. Invest. *118*, 1450–1457.

246. AlWohaib, M.A., and Alnaqeeb, M.A. (1997). The effect of denervation and immobilization on the hindlimb muscles of the jerboa (Jaculus jaculus). Kuwait J. Sci. Eng. *24*, 309–323.

247. Aryan, F.A., and Alnaqeeb, M.A. (2002). Effect of immobilization and under-load on skeletal muscle in the Hindlimb of the Jerboa. Kuwait J. Sci. Eng. *29*, 83–97.

248. Moschella, M.C., and Ontell, M. (1987). Transient and chronic neonatal denervation of murine muscle: a procedure to modify the phenotypic expression of muscular dystrophy. J. Neurosci. *7*, 2145–2152.

249. Huang, A.H., Riordan, T.J., Pryce, B., Weibel, J.L., Watson, S.S., Long, F., Lefebvre, V., Harfe, B.D., Stadler, H.S., Akiyama, H., *et al.* (2015). Musculoskeletal integration at the wrist underlies the modular development of limb tendons. Development *142*, 2431–2441.

250. Green, D.R. (2005). Apoptotic Pathways: Ten Minutes to Dead. Cell *121*, 671–674.

251. Galluzzi, L., Maiuri, M.C., Vitale, I., Zischka, H., Castedo, M., Zitvogel, L., and Kroemer, G. (2007). Cell death modalities: classification and pathophysiological implications. Cell Death and Differentiation *14*, 1237–1243.

252. Heredia, J.E., Mukundan, L., Chen, F.M., Mueller, A.A., Deo, R.C., Locksley, R.M., Rando, T.A., and Chawla, A. (2013). Type 2 innate signals stimulate fibro/adipogenic progenitors to facilitate muscle regeneration. Cell *153*, 376–388.

253. Joe, A.W.B., Yi, L., Natarajan, A., Le Grand, F., So, L., Wang, J., Rudnicki, M.A., and Rossi, F.M. V. (2010). Muscle injury activates resident fibro/adipogenic progenitors that facilitate myogenesis. Nature Cell Biology *12*, 153–163.

254. Monks, J., Rosner, D., Jon Geske, F., Lehman, L., Hanson, L., Neville, M.C., and Fadok, V.A. (2005). Epithelial cells as phagocytes: apoptotic epithelial cells are engulfed by mammary alveolar epithelial cells and repress inflammatory mediator release. Cell Death Differ *12*, 107–114.

255. Schwegler, M., Wirsing, A.M., Dollinger, A.J., Abendroth, B., Putz, F., Fietkau, R., and Distel, L.V. (2015). Clearance of primary necrotic cells by non-professional phagocytes. Biol. Cell *107*, 372–387.

256. Gibbons, M.C., Singh, A., Anakwenze, O., Cheng, T., Pomerantz, M., Schenk, S., Engler, A.J., and Ward, S.R. (2017). Histological Evidence of Muscle Degeneration in Advanced Human Rotator Cuff Disease. J Bone Joint Surg Am *99*, 190–199.

257. Jordan, B., Vercammen, P., and Cooper, K.L. (2011). Husbandry and breeding of the lesser Egyptian Jerboa, Jaculus jaculus. Cold Spring Harbor protocols *2011*, 1457–61.

258. Danoviz, M.E., and Yablonka-Reuveni, Z. (2012). Skeletal muscle satellite cells: background and methods for isolation and analysis in a primary culture system. Methods Mol. Biol. *798*, 21–52.

259. Sandoval-Guzmán, T., Wang, H., Khattak, S., Schuez, M., Roensch, K., Nacu, E., Tazaki, A., Joven, A., Tanaka, E.M., and Simon, A. (2014). Fundamental Differences in Dedifferentiation and Stem Cell Recruitment during Skeletal Muscle Regeneration in Two Salamander Species. Cell Stem Cell *14*, 174–187.

260. Schertzer, J.D., Plant, D.R., Lynch, G.S., Beitzel, F., Stupka, N., and Lynch, G.S. (2006). Optimizing plasmid-based gene transfer for investigating skeletal muscle structure and function. Molecular therapy : the journal of the American Society of Gene Therapy *13*, 795–803.

261. Cooper, K.L., Sears, K.E., Uygur, A., Maier, J., Baczkowski, K.-S., Brosnahan, M., Antczak, D., Skidmore, J.A., and Tabin, C.J. (2014). Patterning and post-patterning modes of evolutionary digit loss in mammals. Nature *511*, 41–5.

262. Dogra, C., Changotra, H., Wedhas, N., Qin, X., Wergedal, J.E., and Kumar, A. (2007). TNF-related weak inducer of apoptosis (TWEAK) is a potent skeletal muscle-wasting cytokine. FASEB journal : official publication of the Federation of American Societies for Experimental Biology *21*, 1857–69.

263. Files, D.C., D'Alessio, F.R., Johnston, L.F., Kesari, P., Aggarwal, N.R., Garibaldi, B.T., Mock, J.R., Simmers, J.L., DeGorordo, A., Murdoch, J., *et al.* (2012). A Critical Role for Muscle Ring Finger-1 in Acute Lung Injury–associated Skeletal Muscle Wasting. American Journal of Respiratory and Critical Care Medicine *185*, 825–834.

264. Xu, P., Oosterveer, M.H., Stein, S., Demagny, H., Ryu, D., Moullan, N., Wang, X., Can, E., Zamboni, N., Comment, A., *et al.* (2016). LRH-1-dependent programming of mitochondrial glutamine processing drives liver cancer. Genes & development *30*, 1255–60.

265. Engel, A. (2004). Myology 3 edition. (New York: McGraw-Hill Professional).

266. Bonaldo, P., Sandri, M., Allen, D.L., Unterman, T.G., Amirouche, A., Durieux, A.C., Banzet, S., Koulmann, N., Bonnefoy, R., Mouret, C., *et al.* (2013). Cellular and molecular mechanisms of muscle atrophy. Disease models & mechanisms *6*, 25–39.

267. Huang, A.H., Riordan, T.J., Wang, L., Eyal, S., Zelzer, E., Brigande, J.V., and Schweitzer, R. (2013). Re-positioning forelimb superficialis muscles: tendon

attachment and muscle activity enable active relocation of functional myofibers. Dev Cell *26*, 544–551.

268. Terry, E.E., Zhang, X., Hoffmann, C., Hughes, L.D., Lewis, S.A., Li, J., Wallace, M.J., Riley, L.A., Douglas, C.M., Gutierrez-Monreal, M.A., *et al.* (2018). Transcriptional profiling reveals extraordinary diversity among skeletal muscle tissues. eLife *7*, e34613.

269. Jacob, M., Chang, L., and Puré, E. (2012). Fibroblast activation protein in remodeling tissues. Curr. Mol. Med. *12*, 1220–1243.

270. Lee, H.-O., Mullins, S.R., Franco-Barraza, J., Valianou, M., Cukierman, E., and Cheng, J.D. (2011). FAP-overexpressing fibroblasts produce an extracellular matrix that enhances invasive velocity and directionality of pancreatic cancer cells. BMC Cancer *11*, 245.

271. Veldman, M.B., Zhao, C., Gomez, G. a, Lindgren, A.G., Huang, H., Yang, H., Yao, S., Martin, B.L., Kimelman, D., and Lin, S. (2013). Transdifferentiation of fast skeletal muscle into functional endothelium in vivo by transcription factor Etv2. PLoS biology *11*, e1001590.

272. von Maltzahn, J., Bentzinger, C.F., and Rudnicki, M.A. (2012). Wnt7a–Fzd7 signalling directly activates the Akt/mTOR anabolic growth pathway in skeletal muscle. Nature Cell Biology *14*, 186–191.

273. von Maltzahn, J., Chang, N.C., Bentzinger, C.F., and Rudnicki, M.A. (2012). Wnt Signaling in Myogenesis. Trends Cell Biol *22*, 602–609.

274. Cruciat, C.-M., and Niehrs, C. (2013). Secreted and Transmembrane Wnt Inhibitors and Activators. Cold Spring Harb Perspect Biol *5*, a015081.

275. Hatazawa, Y., Ono, Y., Hirose, Y., Kanai, S., Fujii, N.L., Machida, S., Nishino, I., Shimizu, T., Okano, M., Kamei, Y., *et al.* (2018). Reduced Dnmt3a increases Gdf5 expression with suppressed satellite cell differentiation and impaired skeletal muscle regeneration. FASEB J. *32*, 1452–1467.

276. Hollway, G.E., Maule, J., Gautier, P., Evans, T.M., Keenan, D.G., Lohs, C., Fischer, D., Wicking, C., and Currie, P.D. (2006). Scube2 mediates Hedgehog signalling in the zebrafish embryo. Developmental Biology *294*, 104–118.

277. Voronova, A., Coyne, E., Madhoun, A.A., Fair, J.V., Bosiljcic, N., St-Louis, C., Li, G., Thurig, S., Wallace, V.A., Wiper-Bergeron, N., *et al.* (2013). Hedgehog Signaling Regulates MyoD Expression and Activity. J. Biol. Chem. *288*, 4389–4404.

278. Hirsinger, E., Stellabotte, F., Devoto, S.H., and Westerfield, M. (2004). Hedgehog signaling is required for commitment but not initial induction of slow muscle precursors. Dev. Biol. *275*, 143–157.

279. Hong, G., Zhang, W., Li, H., Shen, X., and Guo, Z. (2014). Separate enrichment analysis of pathways for up- and downregulated genes. J R Soc Interface *11*. Available at: https://www.ncbi.nlm.nih.gov/pmc/articles/PMC3899863/.

280. Pöschl, E., Schlötzer-Schrehardt, U., Brachvogel, B., Saito, K., Ninomiya, Y., and Mayer, U. (2004). Collagen IV is essential for basement membrane stability but dispensable for initiation of its assembly during early development. Development *131*, 1619–1628.

281. Patton, B.L. (2000). Laminins of the neuromuscular system. Microsc. Res. Tech. *51*, 247–261.

282. Graham, Z.A., Gallagher, P.M., and Cardozo, C.P. (2015). Focal adhesion kinase and its role in skeletal muscle. J. Muscle Res. Cell. Motil. *36*, 305–315.

283. Bikle, D.D., Tahimic, C., Chang, W., Wang, Y., Philippou, A., and Barton, E.R. (2015). Role of IGF-I signaling in muscle bone interactions. Bone *80*, 79–88.

284. Salvatore, D., Simonides, W.S., Dentice, M., Zavacki, A.M., and Larsen, P.R. (2014). Thyroid hormones and skeletal muscle — new insights and potential implications. Nat Rev Endocrinol *10*, 206–214.

285. Romanick, M., Thompson, L.V., and Brown-Borg, H.M. (2013). Murine models of atrophy, cachexia, and sarcopenia in skeletal muscle. Biochimica et Biophysica Acta (BBA) - Molecular Basis of Disease *1832*, 1410–1420.

286. McGreevy, J.W., Hakim, C.H., McIntosh, M.A., and Duan, D. (2015). Animal models of Duchenne muscular dystrophy: from basic mechanisms to gene therapy. Disease models & mechanisms *8*, 195–213.

287. Blackwell, T.A., Cervenka, I., Khatri, B., Brown, J.L., Rosa-Caldwell, M.E., Lee, D.E., Perry, R.A., Brown, L.A., Haynie, W.S., Wiggs, M.P., *et al.* (2018). Transcriptomic analysis of the development of skeletal muscle atrophy in cancer-cachexia in tumor-bearing mice. Physiol. Genomics *50*, 1071–1082.

288. Doktor, T.K., Hua, Y., Andersen, H.S., Brøner, S., Liu, Y.H., Wieckowska, A., Dembic, M., Bruun, G.H., Krainer, A.R., and Andresen, B.S. (2017). RNA-sequencing of a mouse-model of spinal muscular atrophy reveals tissue-wide changes in splicing of U12-dependent introns. Nucleic Acids Res *45*, 395–416.

289. Mukund, K., Mathewson, M., Minamoto, V., Ward, S.R., Subramaniam, S., and Lieber, R.L. (2014). Systems analysis of transcriptional data provides insights into muscle's biological response to botulinum toxin. Muscle & Nerve *50*, 744–758.

290. Kostrominova, T.Y., Dow, D.E., Dennis, R.G., Miller, R.A., and Faulkner, J.A. (2005). Comparison of gene expression of 2-mo denervated, 2-mo stimulated-denervated, and control rat skeletal muscles. Physiological Genomics *22*. Available

at: http://physiolgenomics.physiology.org/content/22/2/227 [Accessed June 12, 2017].

291. Hua, Y., Sahashi, K., Rigo, F., Hung, G., Horev, G., Bennett, C.F., and Krainer, A.R. (2011). Peripheral SMN restoration is essential for long-term rescue of a severe spinal muscular atrophy mouse model. Nature *478*, 123–126.

292. Wang, H., Li, Y., Ryder, J.W., Hole, J.T., Ebert, P.J., Airey, D.C., Qian, H.-R., Logsdon, B., Fisher, A., Ahmed, Z., *et al.* (2018). Genome-wide RNAseq study of the molecular mechanisms underlying microglia activation in response to pathological tau perturbation in the rTg4510 tau transgenic animal model. Molecular Neurodegeneration *13*, 65.

293. GEO Accession viewer Available at: https://www.ncbi.nlm.nih.gov/geo/query/acc.cgi?acc=GSE112895 [Accessed August 26, 2019].

294. Chen, M., Li, Q., Cao, N., Deng, Y., Li, L., Zhao, Q., Wu, M., and Ye, M. (2019). Profiling of histone 3 lysine 27 acetylation reveals its role in a chronic DSS-induced colitis mouse model. Mol. Omics *15*, 296–307.

295. Jones, R.A., Franks, S.E., and Moorehead, R.A. (2018). Comparative mRNA and miRNA transcriptome analysis of a mouse model of IGFIR-driven lung cancer. PLoS One *13*. Available at: https://www.ncbi.nlm.nih.gov/pmc/articles/PMC6226179/ [Accessed August 26, 2019].

296. Bolger, A.M., Lohse, M., and Usadel, B. (2014). Trimmomatic: a flexible trimmer for Illumina sequence data. Bioinformatics *30*, 2114–2120.

297. Dobin, A., Davis, C.A., Schlesinger, F., Drenkow, J., Zaleski, C., Jha, S., Batut, P., Chaisson, M., and Gingeras, T.R. (2013). STAR: ultrafast universal RNA-seq aligner. Bioinformatics *29*, 15–21.

298. Sharma, V., Elghafari, A., and Hiller, M. (2016). Coding exon-structure aware realigner (CESAR) utilizes genome alignments for accurate comparative gene annotation. Nucleic Acids Research *44*, e103–e103.

299. Love, M.I., Huber, W., and Anders, S. (2014). Moderated estimation of fold change and dispersion for RNA-seq data with DESeq2. Genome Biol. *15*, 550.

300. Huang, D.W., Sherman, B.T., and Lempicki, R.A. (2009). Bioinformatics enrichment tools: paths toward the comprehensive functional analysis of large gene lists. Nucleic Acids Res. *37*, 1–13.

301. Huang, D.W., Sherman, B.T., and Lempicki, R.A. (2009). Systematic and integrative analysis of large gene lists using DAVID bioinformatics resources. Nat Protoc *4*, 44–57.

302. Shen, L. GeneOverlap: Test and visualize gene overlaps. R package version 1.20.0. Available at: http://shenlab-sinai.github.io/shenlab-sinai/.

303. Kaminski, J., Waller, B.M., Diogo, R., Hartstone-Rose, A., and Burrows, A.M. (2019). Evolution of facial muscle anatomy in dogs. Proc. Natl. Acad. Sci. U.S.A. *116*, 14677–14681.

304. Unguez, G.A., and Zakon, H.H. (1998). Reexpression of myogenic proteins in mature electric organ after removal of neural input. The Journal of neuroscience : the official journal of the Society for Neuroscience *18*, 9924–35.

305. Krull, C.E. (2004). A primer on using in ovo electroporation to analyze gene function. Developmental Dynamics *229*, 433–439.

306. Trapnell, C. (2015). Defining cell types and states with single-cell genomics. Genome Res. *25*, 1491–1498.

307. Potter, S.S. (2018). Single-cell RNA sequencing for the study of development, physiology and disease. Nat Rev Nephrol *14*, 479–492.

308. Kiselev, V.Y., Andrews, T.S., and Hemberg, M. (2019). Challenges in unsupervised clustering of single-cell RNA-seq data. Nat Rev Genet *20*, 273–282.

309. Habib, N., Avraham-Davidi, I., Basu, A., Burks, T., Shekhar, K., Hofree, M., Choudhury, S.R., Aguet, F., Gelfand, E., Ardlie, K., *et al.* (2017). Massively parallel single-nucleus RNA-seq with DroNc-seq. Nature Methods *14*, 955–958.

310. Zeng, W., Jiang, S., Kong, X., El-Ali, N., Ball, A.R., Ma, C.I.-H., Hashimoto, N., Yokomori, K., and Mortazavi, A. (2016). Single-nucleus RNA-seq of differentiating human myoblasts reveals the extent of fate heterogeneity. Nucleic Acids Res. *44*, e158.

311. Malecova, B., Gatto, S., Etxaniz, U., Passafaro, M., Cortez, A., Nicoletti, C., Giordani, L., Torcinaro, A., Bardi, M.D., Bicciato, S., *et al.* (2018). Dynamics of cellular states of fibro-adipogenic progenitors during myogenesis and muscular dystrophy. Nat Commun *9*, 1–12.

312. Lemos, D.R., Babaeijandaghi, F., Low, M., Chang, C.-K., Lee, S.T., Fiore, D., Zhang, R.-H., Natarajan, A., Nedospasov, S.A., and Rossi, F.M.V. (2015). Nilotinib reduces muscle fibrosis in chronic muscle injury by promoting TNF-mediated apoptosis of fibro/adipogenic progenitors. Nat. Med. *21*, 786–794.

313. Uezumi, A., Fukada, S., Yamamoto, N., Ikemoto-Uezumi, M., Nakatani, M., Morita, M., Yamaguchi, A., Yamada, H., Nishino, I., Hamada, Y., *et al.* (2014). Identification and characterization of PDGFRα+ mesenchymal progenitors in human skeletal muscle. Cell Death Dis *5*, e1186.

314. Gatto, S., Puri, P.L., and Malecova, B. (2017). Single Cell Gene Expression Profiling of Skeletal Muscle-Derived Cells. Methods Mol. Biol. *1556*, 191–219.

315. Blau, H.M., Webster, C., and Pavlath, G.K. (1983). Defective myoblasts identified in Duchenne muscular dystrophy. Proc. Natl. Acad. Sci. U.S.A. *80*, 4856–4860.

316. Jejurikar, S.S., and Kuzon, W.M. (2003). Satellite cell depletion in degenerative skeletal muscle. Apoptosis *8*, 573–578.

317. Cooper, K.L. (2011). The lesser egyptian jerboa, jaculus jaculus: A unique rodent model for evolution and development. Cold Spring Harbor Protocols *6*, 1451–1456.

318. Wu, S., Wu, W., Zhang, F., Ye, J., Ni, X., Sun, J., Edwards, S.V., Meng, J., and Organ, C.L. (2012). Molecular and paleontological evidence for a post-Cretaceous origin of rodents. PloS one *7*, e46445.

319. Stein, B.R. (1990). Limb myology and phylogenetic relationships in the superfamily Dipodoidea (birch mice, jumping mice, and jerboas). Journal of Zoological Systematics and Evolutionary Research *28*, 299–314.

320. West-Eberhard, M.J. (2003). Developmental Plasticity and Evolution (Oxford ; New York: Oxford University Press, U.S.A.).

321. MacDonald, E.M., and Cohn, R.D. (2012). TGFβ signaling: its role in fibrosis formation and m. Current Opinion in Rheumatology *24*, 628–634.

322. Pryce, B.A., Watson, S.S., Murchison, N.D., Staverosky, J.A., Dünker, N., and Schweitzer, R. (2009). Recruitment and maintenance of tendon progenitors by TGF β signaling are essential for tendon formation. *1361*, 1351–1361.

323. Mendias, C.L., Gumucio, J.P., Davis, M.E., Bromley, C.W., Davis, C.S., and Brooks, S.V. (2012). Transforming growth factor-beta induces skeletal muscle atrophy and fibrosis through the induction of atrogin-1 and scleraxis. Muscle Nerve *45*, 55–59.

324. Sartori, R., Milan, G., Patron, M., Mammucari, C., Blaauw, B., Abraham, R., and Sandri, M. (2009). Smad2 and 3 transcription factors control muscle mass in adulthood. Am. J. Physiol., Cell Physiol. *296*, C1248-1257.

325. Yanagita, M. (2012). Inhibitors/antagonists of TGF-β system in kidney fibrosis. Nephrol Dial Transplant *27*, 3686–3691.

326. Roscito, J.G., Sameith, K., Parra, G., Langer, B.E., Petzold, A., Moebius, C., Bickle, M., Rodrigues, M.T., and Hiller, M. (2018). Phenotype loss is associated with widespread divergence of the gene regulatory landscape in evolution. Nat Commun *9*, 1–15.

327. Yin, W., Wang, Z., Li, Q., Lian, J., Zhou, Y., Lu, B., Jin, L., Qiu, P., Zhang, P., Zhu, W., *et al.* (2016). Evolutionary trajectories of snake genes and genomes revealed by comparative analyses of five-pacer viper. Nat Commun *7*. Available at: https://www.ncbi.nlm.nih.gov/pmc/articles/PMC5059746/.